1996

Bryostatin downregulates protein kinase C by production of incompetent enzyme and degradation by the ubiquitin-proteasome pathway.

Hyeon-Woo Lee
University of Alabama at Birmingham

INFORMATION TO USERS

This manuscript has been reproduced from the microfilm master. UMI films the text directly from the original or copy submitted. Thus, some thesis and dissertation copies are in typewriter face, while others may be from any type of computer printer.

The quality of this reproduction is dependent upon the quality of the copy submitted. Broken or indistinct print, colored or poor quality illustrations and photographs, print bleedthrough, substandard margins, and improper alignment can adversely affect reproduction.

In the unlikely event that the author did not send UMI a complete manuscript and there are missing pages, these will be noted. Also, if unauthorized copyright material had to be removed, a note will indicate the deletion.

Oversize materials (e.g., maps, drawings, charts) are reproduced by sectioning the original, beginning at the upper left-hand corner and continuing from left to right in equal sections with small overlaps. Each original is also photographed in one exposure and is included in reduced form at the back of the book.

Photographs included in the original manuscript have been reproduced xerographically in this copy. Higher quality 6" x 9" black and white photographic prints are available for any photographs or illustrations appearing in this copy for an additional charge. Contact UMI directly to order.

UMI

A Bell & Howell Information Company
300 North Zeeb Road, Ann Arbor MI 48106-1346 USA
313/761-4700 800/521-0600

BRYOSTATIN DOWNREGULATES PROTEIN KINASE C BY PRODUCTION OF INCOMPETENT ENZYME AND DEGRADATION BY THE UBIQUITIN-PROTEASOME PATHWAY

by

HYEON-WOO LEE

A DISSERTATION

Submitted in partial fulfillment of the requirements of the degree of Doctor of Philosophy in the Department of Pharmacology and Toxicology in the Graduate School, The University of Alabama at Birmingham

BIRMINGHAM, ALABAMA

1996

ABSTRACT OF DISSERTATION
GRADUATE SCHOOL, UNIVERSITY OF ALABAMA AT BIRMINGHAM

Degree Ph.D. Major Subject Pharmacology

Name of Candidate Hyeon-Woo Lee

Title Bryostatin Downregulates Protein Kinase C by Production of Incompetent Enzyme and Degradation by the Ubiquitin-Proteasome Pathway.

We show that treatment of human fibroblasts or renal epithelial cells with bryostatin 1 (Bryo) or phorbol myristate acetate (PMA) induced autophosphorylation of 80 kDa PKC-α, which was accompanied by production of dephosphorylated 76 kDa PKC-α and degradation by the proteasome. Bryo concomitantly increased the ^{32}P labeling of 80 kDa PKC-α by autophosphorylation and produced a 76 kDa form that lacked detectable ^{32}P. The 76 kDa form was in the particulate fraction, suggesting that it was produced from activated kinase. Alkaline phosphatase treatment of immunoprecipitated PKC-α converted the 80 kDa form to 76 kDa but had no effect on the mobility of the 76 kDa form. Pulse-chase labeling of PKC-α suggested that there is a precursor-product relationship between the 80 and 76 kDa forms, respectively. Inhibition of protein synthesis had no effect on the production of 76 kDa PKC-α by Bryo. Incubation with

phosphatase inhibitors prevented 80 kDa PKC-α from Byro-evoked degradation and concomitantly blocked formation of the 76 kDa form. The 76 kDa form is inactive and incompetent because it lacked detectable ^{32}P. Lactacystin or a peptidyl aldehyde, selective proteasome inhibitors, antagonized Bryo or PMA-induced PKC-α degradation. In vitro assays of PKC activity showed that cells treated with lactacystin plus Bryo or PMA retained more PKC activity than those treated with Bryo or PMA alone. Incubation with lactacystin prevented Bryo-induced autophosphorylated PKC-α. Incubation with Bryo and lactacystin produced a ladder of >80 kDa ubiquitinated PKC-α bands. The most abundant ubiquitinated PKC-α band lacked detectable ^{32}P, suggesting that ubiquitinated PKC-α may be derived from the dephosphorylated 76 kDa form. We suggest that dephosphorylation predisposes PKC to ubiquitin-proteasome mediated proteolysis. Prolonged incubation with PMA but not Bryo changed cell morphology from flat to round. Bryo prevented PMA from rounding the cells. Proteasome inhibitors converted Bryo from a PKC antagonist to an agonist with respect to the shape change. These findings support the idea that Bryo antagonizes PMA by producing more efficient proteolysis of PKC than PMA.

Abstract Approved by: **Committee Chairman** Stephen Barnes

Program Director

Date 7/24/96 **Dean of Graduate School**

DEDICATION

I dedicate this dissertation to my wife, Eun-Joo, and my daughters, Jee-Hae and Jee-Eun.

ACKNOWLEDGEMENTS

I express my deep appreciation to Dr. Jeffrey B. Smith, my dissertation advisor, who provided excellent guidance and intellectual challenges along the way. He has been a true teacher during the pursuit of my degree.

I would like to thank Cindy Smith for her selfless help and encouragement.

I would also like to thank the members of my Ph.D. committee, Drs. Joseph Messina, Gail Johnson, Charles Falany, and Stephen Barnes, for their helpful suggestions and for taking time out of their busy schedules to serve on my committee.

TABLE OF CONTENTS

Page

ABSTRACT ii

DEDICATION iv

ACKNOWLEDGEMENTS v

LIST OF TABLES.....viii

LIST OF FIGURES ix

LIST OF DIAGRAMS.....xiii

LIST OF ABBREVIATIONS xiv

INTRODUCTION 1

METHODS AND MATERIALS 22

Cell Culture.....22
NCX mRNA, Protein and Activity.....22
PKC-α Translocation.....23
Western Analysis of PKC-α.....24
Extraction of Total Cellular PKC-α by SDS.....25
PKC-α Immunoprecipitation.....26
Western Analysis of Ubiquitinated PKC-α.....26
^{32}P-PKC-α Labeling.....27
Pulse-Chase PKC-α Labeling.....28
Dephosphorylation of PKC-α by Alkaline Phosphatase....28
PKC Activity.....29
Cell Morphology.....30
Materials.....30

RESULTS 32

Bryo Antagonizes Phorbol Ester-Evoked Responses of LLC-MK$_2$ Renal Epithelial Cells.....32

Dephosphorylation of Activated PKC-α Contributes to Downregulation By Bryo or PMA in LLC-MK$_2$ Renal Epithelial Cells 33

TABLE OF CONTENTS (Continued)

Bryo- or PMA-Induced PKC-α Downregulation by the Production of Incompetent, Nonphosphorylated Enzyme from Activated, Autophosphorylated Form and Degradation by the Ubiquitin-Proteasome Pathway in Human Fibroblasts.....42

Lactacystin Preserves Activated PKC-α and Proteasome Inhibitors Convert Bryo from a PKC Antagonist to an Agonist by Preventing Downregulation by Ubiquitin-Proteasome Pathway in LLC-MK_2 Renal Epithelial Cells.....49

DISCUSSION 55

LIST OF REFERENCES.....97

APPENDIX

ACTIVATION OF PROTEIN KINASES BY CADMIUM: ROLE OF A PUTATIVE ORPHAN RECEPTOR IN HUMAN DERMAL FIBROBLASTS.....108

LIST OF TABLES

Table — Page

1. Half-life of 80 kDa PKC-α in renal epithelial cells treated with 0.1 or 1 μM Bryo or PMA.....35

2. Amount of protein (mg) extracted by TX-100 and eluted by NaCl from DEAE column.....37

3. Ca^{2+} and lipid-dependent PKC activity of renal epithelial cells treated with Bryo or PMA for 4 or 8 h.....37

APPENDIX

1. Densitometric analysis of ^{32}P-labeled proteins from Figure 1.....146

2. Densitometric analysis of ^{32}P-labeled proteins from Figures 2 and 3.....147

LIST OF FIGURES

Figure — Page

1. Bryo prevents PMA from decreasing NCX mRNA, [^{3}H]MAb binding, and activity.....66

2. PKC-α translocation and downregulation by Bryo, PMA, or both in renal epithelial cells.....68

3. Effect of Bryo, PMA, or both on depletion of 80 kDa PKC-α and production of the 76 kDa form in renal epithelial cells.....69

4. Pulse-chase labeling of PKC-α with ^{35}S-Met/Cys in renal epithelial cells.....70

5. Autophosphorylation of PKC-α by Bryo and PMA and lack of ^{32}P in the 76 kDa form in renal epithelial cells.....71

6. Production of 76 kDa PKC-α is independent of protein synthesis in renal epithelial cells.....72

7. Effect of alkaline phosphatase on the electrophoretic mobility of PKC-α immunoprecipitated from renal epithelial cells treated with Bryo.....73

8. Production of the 76 kDa PKC-α and depletion of 80 kDa form by Bryo or PMA in human fibroblasts.....74

9. Effect of orthovanadate on Bryo-induced depletion of 80 kDa PKC-α and production of the 76 kDa form in human fibroblasts.....75

10. Effect of okadeic acid on Bryo-induced depletion of 80 kDa PKC-α and production of the 76 kDa form in human fibroblasts.....76

11. In vivo protection of PKC-α from degradation by proteasome inhibitors but not by a calpain inhibitor in human fibroblasts.....77

12. Effect of Lacta on Bryo-induced PKC-α degradation in human fibroblasts.....78

LIST OF FIGURES (Continued)

Figure — Page

13. Concentration dependence of Lacta for the preservation of PKC-α in human fibroblasts.....79

14. Effect of BzGLAL-al or BzGLAL-ol on Bryo-induced PKC-α degradation in human fibroblasts.....80

15. Inhibition of Bryo- or PMA-induced PKC-α degradation by Lacta in human fibroblasts.....81

16. Ubiquitination of >80 kDa PKC-α immunoprecipitated from human fibroblasts treated with Bryo plus Lacta.....82

17. Localization of 76 kDa and >80 kDa PKC-α in the particulate fraction from human fibroblasts.....83

18. Preservation of Bryo-evoked ^{32}P-labeled PKC-α by Lacta in human fibroblasts.....84

19. Lack of detectable ^{32}P in monoubiquitinated PKC-α from human fibroblasts.....85

20. Lack of detectable ^{32}P in 76 kDa PKC-α produced by PMA or Bryo in the presence or absence of cycloheximide or bisindolylmaleimide in human fibroblasts.....86

21. Effect of alkaline phosphatase on the electrophoretic mobility of PKC-α immunoprecipitated from human fibroblasts treated with Bryo.....87

22. Lacta protects PKC-α protein and PKC activity from degradation evoked by Bryo or PMA in human fibroblasts.....88

23. BzGLAL-al protects PKC-α protein and PKC activity from Bryo- or PMA-induced degradation in human fibroblasts.....89

24. Preservation of Bryo-evoked ^{32}P-labeled PKC-α by Lacta in renal epithelial cells.....90

25. Demonstration of ubiquitinated PKC-α in renal epithelial cells treated with Bryo plus Lacta.....91

26. Lack of detectable ^{32}P in monoubiquitinated PKC-α in renal epithelial cells.....92

LIST OF FIGURES (Continued)

Figure Page

27. In vivo protection of PKC-α from degradation by proteasome inhibitors in renal epithelial cells.....93

28. Lacta preserves PKC activity and PKC-α protein in renal epithelial cells treated with Bryo or PMA.....94

29. Effects of Bryo, PMA, Lacta, BzGLAL-al, and BzGLAL-ol on the morphology of renal epithelial cells.....96

APPENDIX

1. Effect of Cd^{2+}, Fe^{2+} and bradykinin on in vivo phosphorylation of fibroblast proteins.....148

2. Effect of Cd^{2+}, forskolin and PMA on in vivo phosphorylation of fibroblast proteins.....150

3. Effect of forskolin, dd-forskolin, and ionomycin on in vivo phosphorylation of fibroblast proteins.....152

4. Effect of Cd^{2+}, angiotensin II, and ionomycin on in vivo protein phosphorylation in rat aortic myocytes.....154

5. Activation of ERK2 by Cd^{2+} and antagonism by Zn^{2+} 156

6. Activation of ERK2 by EGF, Cd^{2+}, bradykinin, and PMA....157

7. Zn^{2+} blocks Cd^{2+}-evoked ERK2 activation without affecting the response to bradykinin.....158

8. Activation of ERK2 by Cd^{2+} and PMA but not by calcium ionophores or forskolin.....159

9. PKC-α translocation and downregulation 160

10. Downregulation of PKC abolishes ERK2 activation by Cd^{2+} and PMA but not EGF.....161

11. Cd^{2+} increases MARCKS phosphorylation and Zn^{2+} blocks Cd^{2+}-evoked MARCKS phosphorylation without affecting the response to bradykinin 162

12. In vivo phosphorylation of MARCKS by Ni^{2+}, Co^{2+} (A), and Fe^{2+} (B).....164

LIST OF FIGURES (Continued)

Figure Page

13. In vivo phosphorylation of MARCKS by metals and antagonism of Zn^{2+}.....166

14. Downregulation of PKC has no effect on MARCKS phosphorylation evoked by Cd^{2+} or bradykinin in vivo ..167

15. Herbimycin A has no effect on MARCKS phosphorylation evoked by Cd^{2+} and PMA.....168

16. Herbimycin A abolishes ERK2 activation evoked by EGF, Cd^{2+}, and PMA in vivo.....169

LIST OF DIAGRAMS

Diagram Page

1. Primary structure of conventional, novel, and atypical protein kinase Cs 2

2. Model of cPKC activation by Ca^{2+} and membrane lipids.....5

3. Structural comparison of Bryo, PMA, and DAG 10

4. Ubiquitin-proteasome pathway of protein degradation 12

5. Conjugation and degradation of proteins via the ubiquitin system 15

6. Structure and absolute configuration of lactacystin.....20

7. Hypothetical pathway of PKC synthesis, activation, dephosphorylation, and degradation by Bryo 58

APPENDIX

Diagram of transmembrane-signaling events and protooncogene induction via the orphan receptor triggered by cadmium 144

LIST OF ABBREVIATIONS

Bryo	bryostatin 1
BSA	bovine serum albumin
CHX	cycloheximide
DMEM	Dulbecco's modified Eagle's medium
FBS	fetal bovine serum
EGTA	[ethylenebis(oxyethylenenitrilo)] tetraacetic acid
HEPES	4-(2-hydroxyethyl)-1-piperazineethanesulfonic acid
Lacta	lactacystin
MAb	monoclonal antibody
NCX	Na^+-Ca^{2+} exchanger
PAGE	polyacrylamide gel electrophoresis
PSS	physiological salt solution
PBS	phosphate buffered saline
BCA	bicinchoninic acid
PKC	protein kinase C
PMA	phorbol 12-myristate 13-acetate
DAG	diacylglycerol
PDBu	phorbol 12, 13-dibutyrate
PS	phosphatidylserine
SDS	sodium dodecyl sulfate

LIST OF ABBREVIATIONS (Continued)

Tris	tris(hydroxymethyl)aminomethane
BzGLAL-al	Benzyloxycarbonyl-Gly-Leu-Ala-leucinal
BzGLAL-ol	Benzyloxycarbonyl-Gly-Leu-Ala-leucinol

INTRODUCTION

Protein kinase C (PKC) is a family of Ser/Thr kinase that was originally discovered as a histone protein kinase that was activated in vitro by limited proteolysis, Ca^{2+}, phospholipids, or phorbol esters/diacylglycerol (DAG) (Inoue et al., 1977; Takai et al., 1979; Castagua et al., 1982). Members of the PKC family transduce a variety of stimuli, which may originate from G protein-coupled receptors, receptor tyrosine kinases, or non-receptor tyrosine kinases, leading to DAG formation by phospholipase Cs or phospholipase D (Asaka et al., 1992; Nishizuka, 1992, 1995). In addition, *cis*-unsaturated fatty acids such as arachidonic acid, linoleic acid, and oleic acid can modulate PKC activity (Nishizuka, 1995; McPhail et al., 1984; Murakami et al., 1986). PKC activation is a convergent point for multiple receptor pathways producing membrane phospholipid hydrolysis products. PKC modulates gene expression to regulate proliferation and differentiation of eukaryotic cells via protein kinases and phosphatases (Nishizuka, 1995; Hug and Sarre, 1993).

To date, the mammalian PKC family (Diagram 1) is composed of eleven isoforms, which fall into three groups on

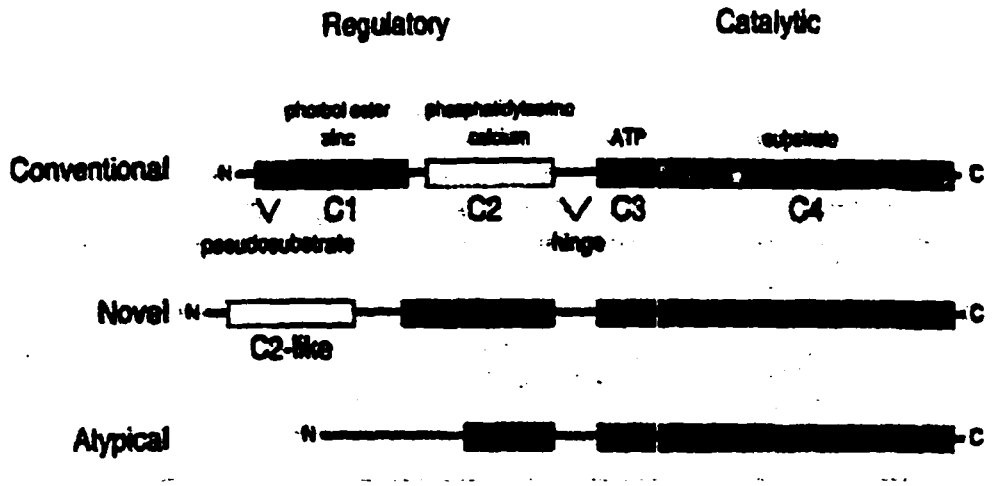

Diagram 1. Primary structure of conventional, novel, and atypical protein kinase Cs (Newton, A. C. J. Biol. Chem. 48, 28495, 1995).

the basis of structure and cofactor regulation (Nishizuka, 1995; Newton, 1995a): conventional PKC ($\alpha, \beta I, \beta II, \gamma$), novel PKC ($\delta, \varepsilon, \eta, \theta, \mu$), and atypical PKC ($\xi, \lambda$). Conventional PKCs (cPKC) consist of a single polypeptide containing four conserved regions (C1-4) and five variable regions (V1-5) (Newton, 1995a). The N-terminal regulatory domain contains Ca^{2+}, phospholipids (C2), and DAG/phorbol ester (C1) binding sites, and the C-terminal catalytic domain contains ATP (C3) and substrate (C4) binding sites (Bell and Burns, 1991; Newton, 1995b; Tayer and Radzio-Andzelm, 1994). The regulatory and catalytic regions are separated by a hinge region that is susceptible to proteolysis in vitro (Newton, 1993). Novel PKCs (nPKCs) have a similar structure to cPKCs, except that these isoforms are insensitive to Ca^{2+}, although the Ca^{2+} binding site has many residues in common with that in cPKCs (Newton, 1995a; Sossin and Schwartz, 1993). Atypical PKCs (aPKCs) are the least understood. These isoforms have a significantly different structure from cPKCs and nPKCs: The DAG/phorbol ester binding site contains only one Cys-rich motif instead of two, and the Ca^{2+}, phospholipid binding site is absent (Nishizuka, 1992; Newton, 1995a). aPKC isoforms are not responsive to phorbol esters (Nishizuka, 1995). There is an autoinhibitory pseudosubstrate sequence N-terminal to C1 in all known PKC isoforms (House and Kemp, 1987). Basic residues of the pseudosubstrate segment pair with acidic residues of substrate binding cavity, which maintains the

enzyme in an inactive configuration in the absence of PKC activators (House et al., 1989; Pears et al., 1990). *n*-Chimaerin, a GTPase activating protein, and *Caenorhabdtis elegans* unc-13 gene product are known to bind phorbol 12,13-dibutyrate (PDBu) with high affinity (Kd ~0.2 nM for *n*-Chimaerin and 67 nM for Unc-13) (Ahmed et al., 1992; Areces et al., 1994). These proteins are expressed only in the nervous system and testis (Ahmed et al., 1992; Areces et al., 1994).

Bell and co-workers (1986) have proposed a model for PKC activation. The model (Diagram 2) has been extensively studied with cPKCs (Bell, 1986; Hannun and Bell, 1986; Orr and Newton, 1992). In the resting state, most PKC appears to be cytoplasmic. At 0.2-0.7 μM concentration, Ca^{2+} increases the affinity of PKC for negatively charged membrane lipids which interact with the C2 site. Consequently, PKC translocates to the membrane. In the initial membrane-associated state, PKC remains inactive, although a conformational change occurs upon binding to the negative charged head groups of membrane lipids (Nelsestuen and Bassi, 1991; Bosca and Moran, 1993). The juxtaposition of C1 site with the inner leaflet of the plasma membrane would facilitate its subsequent interaction with DAG. DAG strikingly and selectively increases the affinity of PKC for phosphatidylserine (PS), membrane phospholipid, by binding

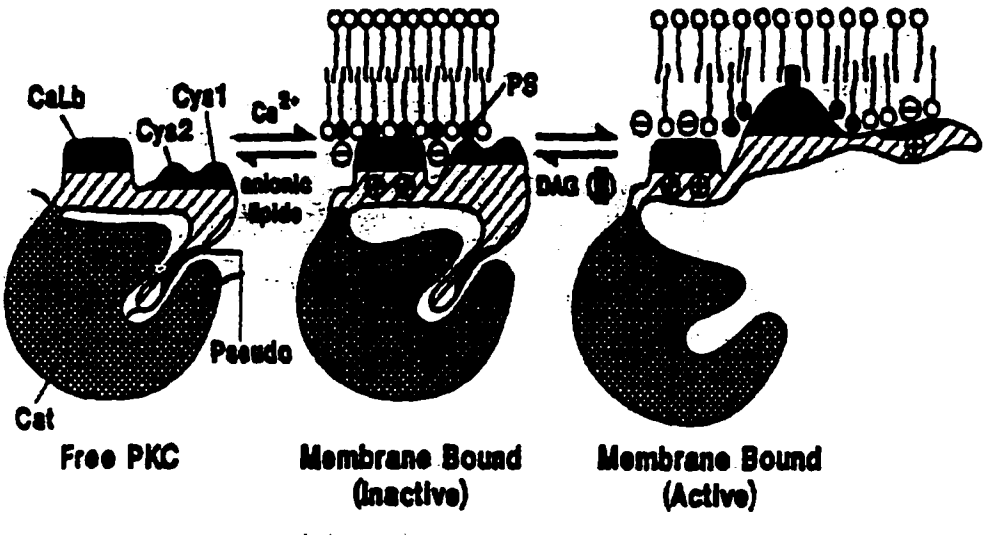

Diagram 2. Model of cPKC activation by Ca^{2+} and membrane lipids (In Protein Kinase C, edited by Kuo, J. F., New York: Oxford University Press, p.70, 1994). Lipid interaction sites in the regulatory domain are represented as dark shaded areas: pseudo, pseudosubstrate motif in V1 region; Cys1, Cys2, cysteine-rich motifs in C1 region; CaLB, calcium-dependent lipid-binding site in C2 region. Cat indicates catalytic domain.

within C1 site, and produces additional conformational changes which release the pseudosubstrate segment from the substrate binding cavity and activate the kinase (Newton, 1995a; Quest and Bell, 1994; Lester et al., 1990). Phorbol esters, which are potent tumor promotors, activate PKC in the same fashion as DAG (Asaka et al., 1992; Nishizuka, 1992, 1995). Unlike DAG, phorbol esters such as phorbol 12-myristate 13-acetate (PMA) are not readily metabolized and, consequently, produce a sustained activation of PKC in contrast to stimuli that evoke DAG production (Newton, 1995a). Since nPKCs are insensitive to a Ca^{2+}, these isoforms may already be located close to the membrane, making translocation unnecessary, or the extended V1 region could mediate initial translocation in Ca^{2+} insensitive manner (Quest and Bell, 1994). It has been suggested that RACKs (Receptor for Activated C Kinase) have specificity for PKC isoforms and, thus, contribute to the subcellular localization of PKC isoforms (Ron et al., 1995; Mochly-Rosen et al., 1991).

Phosphorylation of PKC occurs by two distinct mechanisms, transphosphorylation by an unidentified "PKC kinase" and intramolecular autophosphorylation, which accompanies activation (Borner et al., 1989; Cazaubon and Parker, 1993; Dutil et al., 1994; Flint et al., 1990; Huang et al., 1986; Orr and Newton, 1994; Pears et al., 1992; Zhang et al., 1993, 1994). Transphosphorylation of newly

synthesized PKC makes it catalytically competent (Borner et al., 1989; Cazaubon and Parker, 1993; Dutil et al., 1994; Orr and Newton, 1994; Pears et al., 1992; Zhang et al., 1993, 1994; Cazaubon et al., 1994). Parker and co-workers (Cazaubon and Parker, 1993; Cazaubon et al., 1994) have identified Thr^{497} and possibly Thr^{495} of PKC-α as the critical residue(s) for permissive activation by "PKC kinase." PKC activation by lipids and Ca^{2+} requires negative charge in the "activation loop" which is provided by phospho-Thr^{497} or -Thr^{500} in the α or βII isoforms, respectively (Orr and Newton, 1994; Cazaubon et al., 1994). The autophosphorylation sites of PKC-α appear to be limited to the C-terminal portion (Thr^{631} and Thr^{638}) in contrast to the β isoform, which has N-terminal and hinge autophosphorylation sites in addition to the C-terminal sites (Dutil et al., 1994; Flint et al., 1990; Orr and Newton, 1994; Pears et al., 1992; Zhang et al., 1993, 1994; Cazaubon et al., 1994). In the presence of PKC activators, autophosphorylation may induce a conformational change that removes the autoinhibitory pseudosubstrate segment from the active site and unmasks the segments that bind PS and DAG. Thus activated PKC becomes firmly bound to the plasma membrane via the C1 site that binds DAG and the C2 site that binds PS and Ca^{2+} (Bazzi and Nelsestuen, 1989). The conformational change also may predispose PKC to proteolysis (Quest and Bell, 1994). This possibility provides an explanation for PKC downregulation, a common response on

chronic exposure to phorbol esters. Supportive evidence was provided by Ohno and co-workers (1990) that PKC-α with a point mutation in the catalytic domain was not downregulated on phorbol ester treatment, although it translocated to the membrane. In addition, a recent study by Parker and others (Goode et al., 1995) found that a truncated, catalytically inactive PKC-δ mutant failed to downregulate in response to PMA unless it was coexpressed with wild type PKC-δ or γ, suggesting downregulation by PMA depends on the kinase function of PKC. PKC downregulation is generally attributed to dramatically accelerated proteolysis with no significant change in its rate of synthesis (Mahoney and Huang, 1994; Young et al., 1987). Although PKC can be proteolyzed by trypsin or calpain in vitro, the in vivo pathway for PKC degradation remains unclear.

The bryostatins consist of 17 related macrocyclic lactones that were isolated from marine bryozoans by Pettit and co-workers (1970, 1982, 1991). Bryostatin 1 (Bryo) was shown to have antineoplastic activity against murine P388 leukemia cells and murine M5076 reticulum cell sarcoma (Pettit et al., 1970, 1982; Schuchter et al., 1991). In 1985, Smith and co-workers identified PKC as the cellular receptor of the bryostatins (Smith et al., 1985; Tallant et al., 1987; Kraft et al., 1986). Addition of Bryo to mammalian cells induces translocation, activation, autophosphorylation, and downregulation of PKC similarly to phorbol esters or DAG (Kazanietz et al., 1994; Huwiler et al., 1994; Isakov et al.,

1993; Jalava et al., 1993). Bryo has similar pharmacophoric groups as PMA and DAG, which are responsible for high affinity association with PKC (Diagram 3 and Wender et al., 1988). An in vitro binding study showed that Bryo has a ~10- to 25-fold higher affinity for C1 site of cPKC isoforms and a much slower rate of release than phorbol esters (Kazanietz et al., 1994; de Vries et al., 1988). Kd for Bryo is 2-5 nM, whereas that for PDBu is 0.2-0.3 nM (Kazanietz et al., 1994). Interestingly, Bryo elicits a subset of cellular responses evoked by PMA and antagonizes those PMA-induced responses that it does not produce (Huwiler et al., 1994; Hennings et al., 1987; Kraft et al., 1986; Smith et al., 1985). For example, Bryo inhibits phorbol ester-stimulated phospholipase A2, transglutaminase activity, and ornithine decarboxylase (ODC) induction in keratinocytes (Hennings et al., 1987). Bryo also blocks phorbol ester-induced differentiation of HL 60 cells (Kraft, et al., 1986). In the LLC-MK_2 line of renal epithelial cells, PMA downregulates expression of Na^{2+}-Ca^{2+} exchanger (NCX) mRNA, protein, and activity (Smith et al., 1995). Bryo alone has no effect on NCX expression but completely blocks the effect of PMA on NCX expression (this dissertation). Previous studies have suggested that more efficient downregulation of PKC by Bryo compared to PMA contributes to PKC antagonism by Bryo (Kazanietz et al., 1994; Huwiler et al., 1994; Isakov et al., 1993; Jalava et al., 1993).

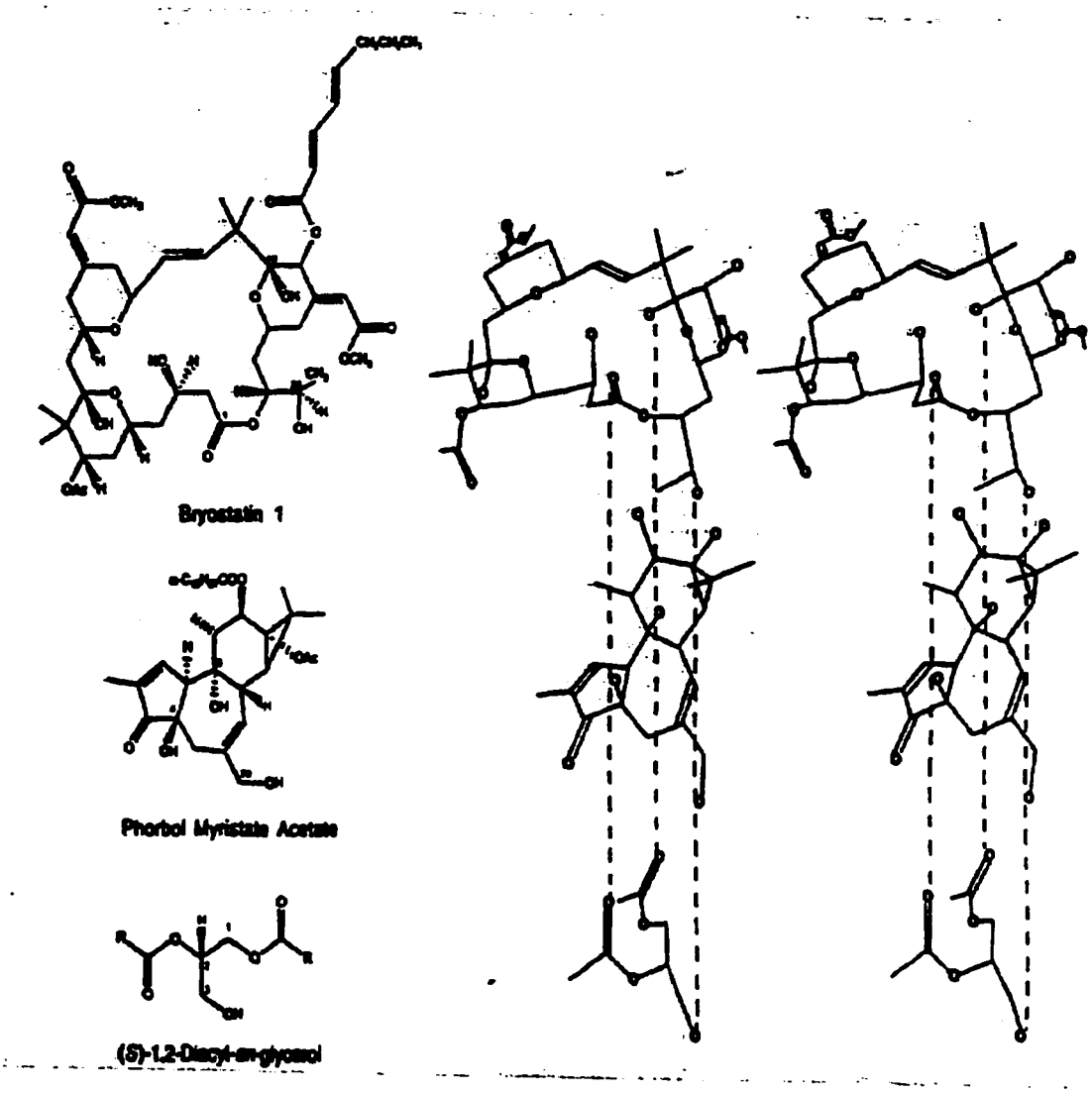

Diagram 3. Structural comparison of Bryo, PMA, and DAG (Wender et al. PNAS 85, 7197, 1988).

The 26S proteasome complex (Diagram 4) is the non-lysosomal proteolytic pathway that requires ATP and ubiquitination of the substrate (Ciechanover, 1994; Rechsteiner et al., 1993). Ubiquitination occurs outside the proteasome complex (Ciechanover, 1994; Rechsteiner et al., 1993). One protein, ODC, has been shown to be degraded by the 26S proteasome without ubiquitination (Murakami et al., 1992). The ubiquitin-proteasome system rapidly eliminates highly abnormal proteins produced by mutation or posttranslational damage, as well as many critical regulatory proteins (Ciechanover, 1994; Goldberg, 1995).

Ubiquitin has 76 amino acids, and its primary sequence is highly conserved. Only three amino acids of the human sequence differ from that of yeast and plants (Jentsch, 1992). The X-ray structure of ubiquitin shows a compact globular structure with the C-terminal Arg-Gly-Gly extended into the solvent (Vijay-Kumar et al., 1985; Rechsteiner, 1987). The molecule contains four strands of β-sheet plus a single α-helix with 3.5 turns; all sequence differences are located on a small portion of ubiquitin's surface (Vijay-Kumar et al., 1985; Rechsteiner, 1987). It remains folded at pH values from 1 to 13 and temperatures below 80°C (Cary et al., 1980). The X-ray structure of tetraubiquitin reveals an asymmetric, extremely compact structure having some different β-strands and loops from native ubiquitin that generally reflect movement to accommodate close contacts between adjacent ubiquitin molecules in tetraubiquitin (Cook et al.,

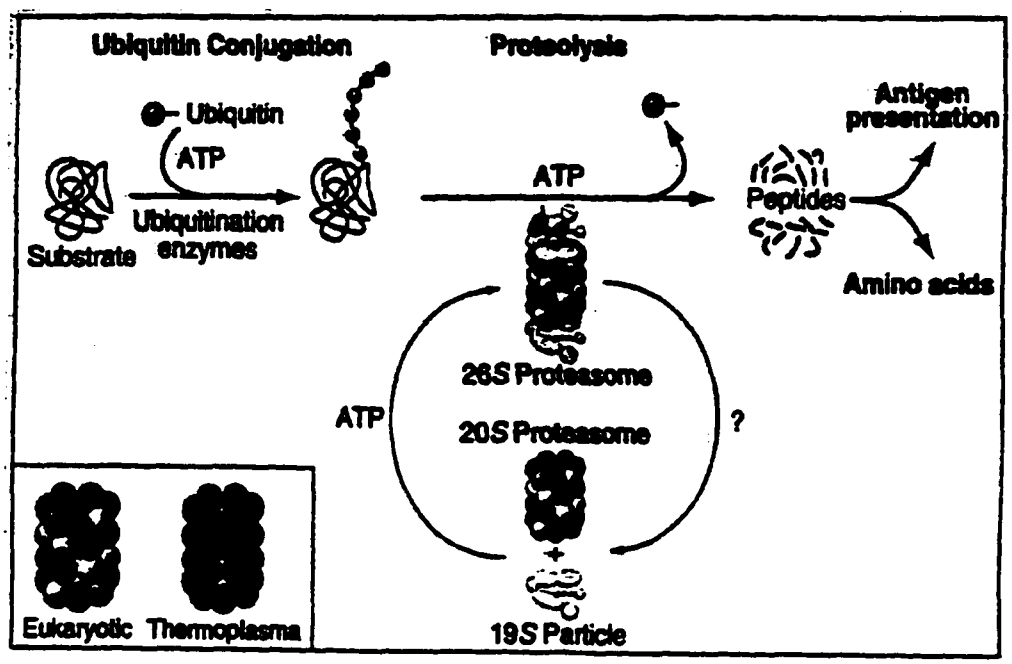

Diagram 4. Ubiquitin-proteasome pathway of protein degradation (Goldberg, A. L. Science, 268, 522, 1995).

1994). Tetraubiquitin has no large hydrophobic, basic, or acidic surface (Cook et al., 1994). The isopeptide bonds in tetraubiquitin are formed between residues Gly^{76} and Lys^{148}, Gly^{176} and Lys^{248}, and Gly^{276} and Lys^{348} (Cook et al., 1994). The presence of ubiquitin on histones and the lymphocyte homing receptor suggests that ubiquitination does not serve exclusively to target proteins to the proteasome. Ubiquitin appears to be a multifunctional protein that affects chromatin structure, cell-cell interactions, the stress response, and intracellular proteolysis (Rechsteiner, 1987; Jentsch, 1992).

Conjugation of ubiquitin to protein substrates destined for proteolytic degradation occurs by three enzymes called ubiquitin activating enzyme (E1), ubiquitin conjugating enzyme (E2), and ubiquitin protein ligase (E3) (Hass et al., 1988; Cook et al., 1992). Initially, the C-terminal Gly^{76} of ubiquitin is activated by ATP to a high energy thiol ester intermediate by E1. E2 transfers activated ubiquitin from E1 to the protein substrate, which is usually bound to E3, and forms an isopeptide bond between activated C-terminal Gly^{76} of ubiquitin and an ε-NH_2 group of Lys of the protein substrate. Substrates may be either mono-ubiquitinated or multiubiquitinated by attachment of ubiquitin chains or trees as depicted in diagram 5 (Ciechanover, 1994; Coris et al., 1995). Genes encoding E1 enzyme (~110 kDa) have been identified from various organisms, including human A1S9, *S.*

cerevisiae UBA1, *E. coli* chlN, and wheat UBA1 (McGrath et al., 1991). E1 enzymes, which appear to be homodimers, form complexes with individual E2 enzyme. In yeast twelve genes encoding different E2 enzymes have been identified (Ciechanover, 1994). In mammalian systems, at least six E2 enzymes have been identified: Ubc2 (Rad6), Ubc3 (Cdc34), Ubc4, Ubc8, epidermal Ubc (Ubc-epi), and Ubc9 (Pagano et al., 1995). The family of E2s differ in amino acid sequence, molecular mass (14-32 kDa), and target specificity. All contain a conserved domain of about 150 amino acids that include the active site cysteine (Gosink and Vierstra, 1995). It has been suggested that association of a limited set of E2 enzymes into multiple hetero-oligomeric complexes expands the repertoire of substrate specificities in the ubiquitin conjugating system (Hochstrasser, 1995). Moreover, this expansion of specificity may be extended by formation of E2-E3 ubiquitin protein ligase complex. Only two genes encoding E3 enzymes (~180 kDa) have been identified so far. These are UBR1 of *S. cerevisiae* and human E6-associated protein (E6-AP) (Ciechanover, 1994). E6-AP is involved in the degradation of p53, a negative regulator of the cell cycle, as well as other protein substrates (Ciechanover, 1994). For many proteins, conjugation to ubiquitin requires a specific E3 enzyme (Ciechanover, 1994). In several proteins such as IκB-α, cyclin, RAG-2, and the cFos-cJun heterodimer, phosphorylation makes these proteins become substrates for ubiquitination enzymes and the proteasome (Lahav-Baratz et al., 1995; Brown et al.,

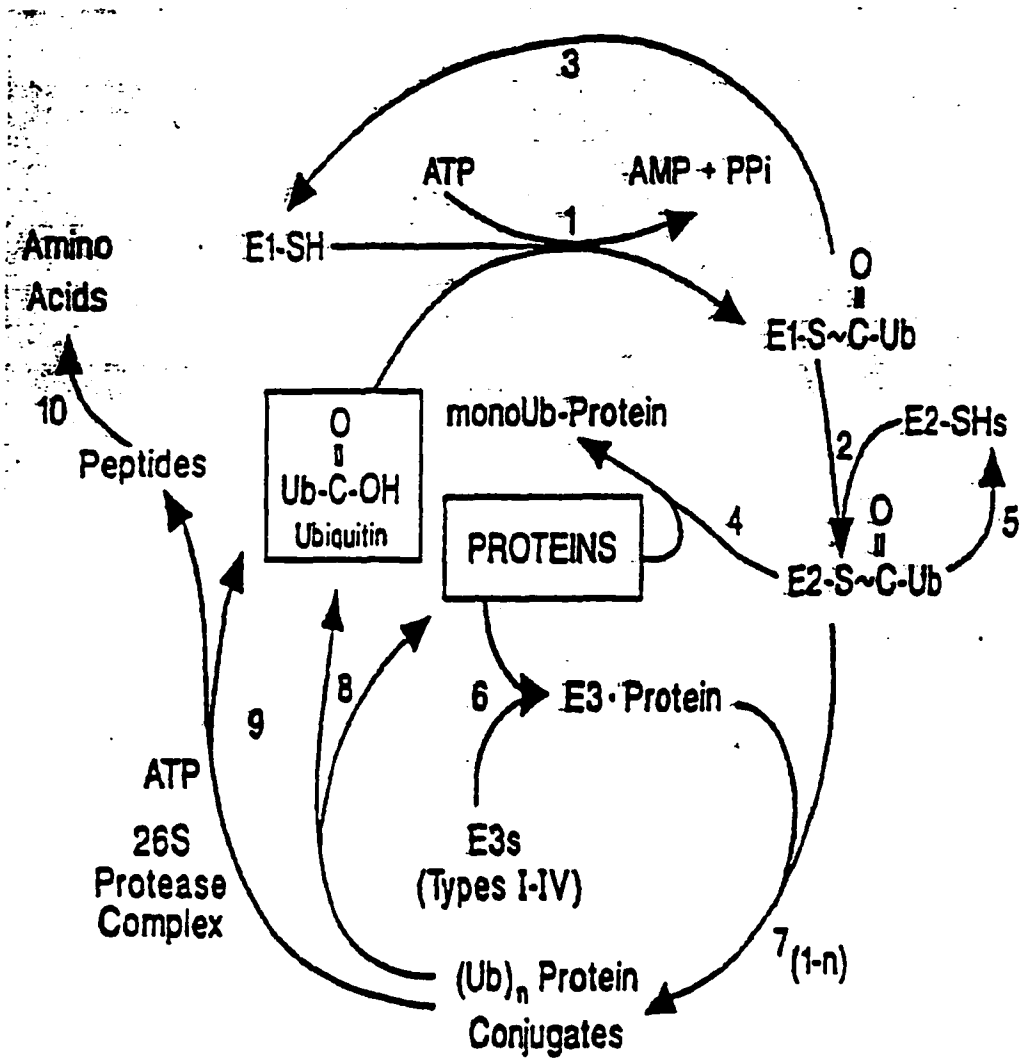

Diagram 5. Conjugation and degradation of proteins via the ubiquitin system (Ciechanover et al. TIBS 14,483, 1989). (1) Activation of ubiquitin by E1. (2) Transfer of ubiquitin-E1 intermediate to E2. (3) Recycling of E1. (4) Conjugation of protein to ubiquitin by E2. (5) Recycling of E2. (6) Formation of protein-E3 complex. (7) Conjugation of multi-ubiquitin to the protein substrate. (8) Recycling of an intact substrate and ubiquitin. (9) ATP-dependent degradation of conjugates into peptides by the 26S proteasome complex. (10) Release of amino acids from peptides.

1995; Lin and Desiderio, 1993; Papavassilion et al., 1992), whereas dephosphorylation of Ser^3 residue is required for ubiquitin-mediated degradation of Mos (Nishizawa et al., 1993). In addition, E3 enzymes appear to be regulated by phosphorylation, as has been suggested for the cyclin-ubiquitin ligase (Lahav-Baratz et al., 1995).

Removal of ubiquitin from protein substrates apparently plays as important a role in the regulation of ubiquitin-proteasome-mediated proteolysis as ubiquitination (Ciechanover, 1994; Hochstrasser, 1995). The removal of ubiquitin from protein substrates by ubiquitin hydrolases produces intact ubiquitin and the protein substrate (Diagram 5). Intact ubiquitin is also released from isopeptide linkage with a Lys residue of the substrate at the final stages of the proteolytic process and is usually recycled rather than degraded by the proteasome. This deubiquitination is carried out by ubiquitin C-terminal hydrolases (isopeptidases or deubiquitinating enzymes) (Ciechanover, 1994; Hochstrasser, 1995; Coris et al., 1995). The family of ubiquitin-specific processing proteases (Ubp), one class of deubiquitinating enzymes, is extremely diverse, which leads to the possibility that the proteolysis of specific protein could be regulated by deubiquitinating enzymes (Hochstrasser and Papa, 1993; Coris et al., 1995).

Following ubiquitination of a protein substrate, it is selectively degraded by a 26S proteasome complex, which requires ATP. The 26S proteasome complex is composed of a key

proteolytic component known as 20S proteasome and a pair of regulatory multisubunit proteins called the 19S particle or PA700 (700 kDa proteasome activator) (Ma et al., 1994; Peters et al., 1994). At least four subunits of PA700 were identified as a novel ATPase (Rechsteiner et al., 1993), and an additional subunit was shown to bind to multiubiquitinated proteins (Deverany et al., 1994). The PA700 complex may contribute to unfolding ubiquitinated proteins and feeding them into the central cavity of the 20S proteasome (Hochstrasser, 1995; Goldberg, 1995). X-ray crystallographic analysis of archaebacterium *Thermoplasma acidophilium* 20S proteasome showed that it has four stacked rings, each consisting of seven subunits, as depicted in diagram 5 (Rechsteiner et al., 1993; Goldberg 1995; Senfert et al., 1995). In archaebacterial 20S proteasome, the outer two rings contain a single type of α subunit and the inner two rings a single β subunit, whereas in eukaryotes the seven α and seven β subunits are distinct gene products (Rechsteiner et al., 1993; Goldberg 1995; Zwickl et al., 1992). It has been suggested that the α subunits play a role in assembling 26S proteolytic complex, binding regulatory proteins, or preventing nonspecific proteolysis, and that the β subunits carry out proteolytic function at their N-termini (Goldberg 1995; Brown et al., 1995; Tamura et al., 1992). Recently, Löwe and co-workers (1995) demonstrated that archaebacterial proteasome contains 14 proteolytic active sites in the inner

cavity, one on each β subunit. Classical families of proteases have an active-site nucleophile such as a hydroxyl or a thiol group in the case of serine or cysteine proteases, respectively, which attacks the peptide bond. In the 20S proteasome, the hydroxyl group on the threonine at the N-terminus of β subunit serves as the active-site nucleophile (Löwe et al., 1995; Seemüller et al., 1995). The existence of 14 distinct subunits of 21 to 32 kDa each that compose the eukaryotic 20S proteasome, in contrast to the bacterial 20S proteasome, confers specialized multicatalytic functions (Rechsteiner et al., 1993; Goldberg, 1995). The mammalian proteasome has at least five distinct proteolytic components referred to as trypsin-like, chymotrypsin-like, peptidyl-glutamyl peptide hydrolyzing, small neutral amino acid-preferring, and branched-chain amino acid preferring (Orlowski et al., 1993). Each of these activities is catalyzed by a distinct subunit or a set of subunits, not by a single site (Orlowski et al., 1993; Orlowski, 1990; Sepp-Lorenzino et al., 1995).

Omura and co-workers (1991) originally isolated lactacystin (Lacta), a *Streptomyces* metabolite, on the basis of its ability to induce neurite outgrowth in the mouse neuroblastoma cell line Neuro 2A (Diagram 6). Lacta was also shown to inhibit proliferation of MG-63 cells (Fenteany et al., 1994). The study in which a series of Lacta analogs were tested in Neuro 2A cells and MG-63 cells suggested that an electrophilic carbonyl at C4 was critical for the cellular

activity of Lacta and that its target might be an enzyme containing a catalytic nucleophile such as a protease (Fenteany et al., 1994). In 1995, Fenteany and co-workers found that [^{3}H]Lacta or [^{3}H]β-lactone covalently bound one type of 20S proteasome subunit, called subunit X/MB1, in extracts of cultured neuroblastoma Neuro 2A cells or bovine brain tissue. They concluded that Lacta and related β-lactone compounds that contained a reactive electrophile specifically inhibited three distinct catalytic activities of 20S proteasome (trypsin-like, chymotrypsin-like, peptidyl-glutamyl peptide hydrolyzing activity) by covalently binding to the N-terminal threonine of the β subunit. Peptidyl aldehydes, which were designed on the basis of the substrate specificity of the branched amino acid preferring component, now known as 20S proteasome substrates, block protein degradation catalyzed by 20S proteasome (Vinitsky et al., 1994). These inhibitors contain the C-terminal aldehyde, which reacts with active-site nucleophile and forms a hemiacetal or thiohemiacetal (Sepp-Lorenzino et al., 1995; Vinitsky et al., 1994). Although certain peptidyl aldehydes selectively inhibit the proteasome, others potently inhibit the cysteine proteases such as calpain and cathepsin B. On the other hand, Lacta has no effect on these or any other protease, including the serine proteases chymotrypsin and trypsin, and the cysteine protease papain (Fenteany et al., 1995).

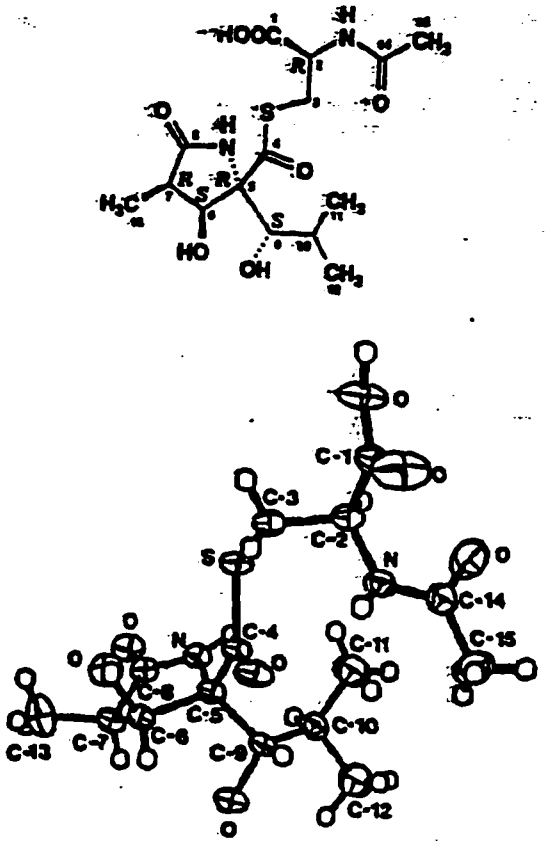

Diagram 6. Structure and absolute configuration of lactacystin (Omura et al. J. Antibiotics 44, 117, 1991).

The purpose of this study was to elucidate a mechanism by which Bryo or PMA causes PKC degradation/downregulation and a mechanism by which Bryo antagonizes the effect of PMA on PKC. The present findings indicate that treatment of LLC-MK_2 renal epithelial cells or human fibroblasts with Bryo or PMA induces autophosphorylation of 80 kDa PKC-α, which is accompanied by production of dephosphorylated, incompetent 76 kDa form, and proteolysis by the ubiquitin-proteosome mediated pathway. We suggest that dephosphorylation predisposes PKC to ubiquitination and subsequent proteosome-mediated proteolysis. In LLC-MK_2 renal epithelial cells, Bryo antagonizes PKC activation by inducing a more efficient dephosphorylation and degradation of PKC than PMA. This idea is supported by the data that proteasome inhibitors convert Bryo from a PKC antagonist to an agonist (PMA-like), with respect to a change in cell morphology.

METHODS AND MATERIALS

Cell Culture.

The LLC-MK_2 monkey line (ATCC CCL 7.2) of renal epithelial cells was grown in Dulbecco's modified Eagle's medium (DMEM) containing 5% (v/v) fetal bovine serum (FBS) (Lyu et al., 1987). Primary cultures of human dermal fibroblasts were initiated from forearm biopsies and grown in DMEM containing 10% (v/v) FBS, as described (Smith et al., 1989).

NCX mRNA, Protein and Activity.

RNA was extracted, fractionated with oligo(dT) cellulose, and electrophoresed for northern analysis, as described (Smith et al., 1995). After hybridization with NCX cDNA probe and autoradiography, the membrane was stripped and hybridized with a rat β-actin (735 bp) cDNA probe obtained from a PC12 cDNA library. Autoradiograms were scanned and analyzed with a model GS-670 Imaging Densitometer using Molecular Analyst 2.0 software (Bio-Rad Laboratories, Hercules, CA). NCX protein was quantified with a tritium labeled MAb R3F1 to canine NCX, as previously described (Smith et al., 1995). The binding assay contained 0.25 ml cell sonicate, 0.75 ml physiological salt solution (PSS) containing 1 mg/ml saponin and 1 mg/ml bovine serum albumin

(BSA), and 0.35 μg/ml [^{3}H]MAb (570 cpm/ng). PSS contained (mM) 120 NaCl, 5 KCl, 1 $CaCl_2$, 1 $MgCl_2$, and 20 HEPES-Tris, pH 7.4. Total protein was measured by the Bicinchoninic acid (BCA) method (Pierce Chemical Co., Rockford, IL). After 1 h at 37°C, bound [^{3}H]MAb was collected by filtration with glass fiber filters (Whatman GF/F, Maidstone, UK) presoaked with 1% (w/v) polyethylenimine. Filters were rinsed three times with saline containing 10 mM HEPES-Tris, pH 7.5, dried, and counted with 10 ml Budget-Solve (Research Products International Corp., Mount Prospect, IL).

NCX activity was assayed as $^{45}Ca^{2+}$ influx that required both increasing cell Na^+ and decreasing external Na^+, which competitively inhibits NCX (Lyu et al., 1987). Cells were treated with 0.1 mM ouabain to raise cell Na^+, and $^{45}Ca^{2+}$ uptake on triplicate cultures was determined in solutions containing 140 mM NaCl or KCl. The initial rate of $^{45}Ca^{2+}$ uptake in the presence of NaCl was subtracted from uptake in 140 mM KCl to obtain NCX activity (Smith et al., 1995; Lyu et al., 1987). Total protein was measured on duplicate cultures at the time of each experiment.

PKC-α Translocation.

Cultures (100 mm diameter of LLC-MK$_2$ cells) were incubated with PMA and/or Bryo for the indicated interval. The cells were rinsed with ice-cold phosphate buffered saline (PBS) and collected by scraping with ice-cold homogenization buffer (1 ml/dish). PBS contained (per liter) 8 g NaCl, 0.2 g

KCl, 0.61 g Na_2HPO_4, and 0.2 g KH_2PO_4 and was adjusted to pH 7.2 with HCl. Cells were sonicated (Sonifier cell disrupter 350, Branson Ultrasonic Corp., Danbury, CT) for 15 s with a 1/8 inch microtip at 60% maximum output (setting 3, continuous) in a thick-walled polystyrene centrifuge tube for an 80 Ti rotor (Beckman Instruments, Inc., Palo Alto, CA). Homogenization buffer contained (mM) 20 Tris-HCl, pH 7.4, 0.5 EGTA, 1 dithiothreitol, 1 benzamidine, 0.1 Na_2VO_3, 10 µg/ml leupeptin, and 10 µg/ml aprotinin. Cytosol was obtained by centrifugation at 100,000 x g for 30 min. The pellet, which contains particulate PKC, was suspended with homogenization buffer containing 1% (w/v) Triton X-100 and extracted for 1 h on ice to solubilize PKC. The supernatant obtained after centrifugation at 100,000 x g for 30 min contains solubilized PKC from the particulate fraction. Protein was measured by the BCA method, and 30 µg cytosol and 40 µg particulate fraction were fractionated by SDS-PAGE for 1.5 h at 150 V in a 10% acrylamide gel (1:38 ratio of N,N'-methylene-bis-acrylamide to acrylamide) (Laemmli, 1970), and PKC-α was detected by western analysis, as described below. Western Analysis of PKC-α.

Protein (cytosol, particulate fraction, SDS cell extract, DEAE fraction, or immunoprecipitated PKC-α) was size fractionated by SDS-PAGE and electrophoretically transferred to an Immobilon PVDF membrane. To improve the resolution of the PKC-α bands, the ratio of N,N'-methylene-bis-acrylamide to acrylamide was decreased from 1:38 to 1:25 and the duration

of electrophoresis was increased from 1.5 to 7 h. Membranes were incubated for 1 h at 37°C with blocking solution and then for 30 min in fresh blocking solution containing 0.2 µg/ml affinity purified polyclonal antibodies to PKC-α. Blocking solution contained 2% (w/v) BSA, 0.1% (w/v) Tween 20, 0.1 M NaCl, and 10 mM Tris-HCl, pH 7.5. Membranes were rinsed with solution C for 30 min, replacing solution C at 5 min intervals for 30 min. Solution C contained 0.1% Tween 20, 50 mM NaCl, and 10 mM Tris-HCl, pH 7.5. Membranes were incubated for 30 min at 37°C with blocking solution containing donkey anti-rabbit IgG conjugated to horseradish peroxidase at 1:25,000 dilution (Amersham Life Science, Buckinghamshire, UK). After rinsing with solution C as described above, PKC-α was visualized by chemiluminescence using ECL reagent (Amersham Life Science) or LumiGLO (Kirkegaard & Perry Laboratories, Gaithersburg, MD) and Konica PPB film. Incubation of PKC-α antibody with the peptide immunogen (10 µg) abolished PKC-α staining. PKC-α autoradiograms were quantified by volume densitometry with a GS-670 Imaging Densitometer (Bio-Rad Laboratories, Hercules, CA).

Extraction of Total Cellular PKC-α by SDS.

Confluent LLC-MK$_2$ line of renal epithelial cell cultures (35 mm diameter) was incubated with PMA and/or Bryo, as indicated. Cells were rinsed with ice-cold PBS and lysed with 100 µl of twice concentrated SDS sample solution without bromophenol blue. Total protein was measured by the BCA

method and fractionated by SDS-PAGE. Western analysis of PKC-α was done as described above.

PKC-α Immunoprecipitation.

Confluent cultures (60 mm diameter) were incubated with indicated additions. Cultures were rinsed with ice-cold PBS and extracted with 0.5 ml ice-cold lysis buffer which contained 1% (w/v) Triton X-100 and (mM) 10 Tris-HCl, pH 7.4, 5 EDTA, 1 phenylmethylsulfonyl fluoride, 0.1 Na_2VO_3, 30 sodium pyrophosphate, 50 NaF, 10 µg/ml leupeptin, and 10 µg/ml aprotinin. Lysates were passed through a 26 gauge needle three times and centrifuged for 20 min at 4°C at 16,000 x g. Protein was measured by the BCA method, and a 0.03 to 2 mg sample was precleared by incubation with 20 µl protein A/G agarose at 4°C for 1 h. Precleared lysates were incubated with 2.5 to 10 µg mouse monoclonal anti PKC-α antibody and 30 µl protein A/G agarose at 4°C for 3 h. Immunocomplexes were washed 6 times with ice-cold lysis buffer and extracted with 30 µl twice concentrated SDS sample solution. Protein was fractionated by SDS-PAGE, and PKC-α was detected by western analysis.

Western Analysis of Ubiquitinated PKC-α.

Proteins were immunoprecipitated with the monoclonal PKC-α antibody, separated by SDS-PAGE, and transferred to a nitrocellulose membrane. Membranes were autoclaved for 20 min, incubated for 10 min with TBS and then for 1 h with blocking solution, rinsed twice (5 min each) with TTBS (TBS containing 0.5% (v/v) Tween 20), and incubated for 1 h in

TTBS containing 0.1% dry milk and a 1000-fold dilution of a monoclonal ubiquitin antibody (4F3 ascites fluid) (Guarino et al., 1995). TBS contained (per liter) 8 g NaCl, 0.2 g KCl, and 3 g Tris base and was adjusted to pH 7.4 with HCl. Membranes were rinsed with TTBS for 15 min, replacing the solution at 5 min intervals and incubated for 1 h with TTBS containing 0.1% dry milk and a 1:20,000 dilution of goat anti-mouse IgG conjugated to horseradish peroxidase (Transduction Laboratories, Lexington, KY). After rinsing with TTBS for 15 min (replacing the TTBS at 5 min intervals), ubiquitin-containing bands were visualized by chemiluminescence with LumiGLO (Kirkegaard & Perry Laboratories, Gaithersburg, MD) and Konica PPB film. After immunostaining for ubiquitin, membranes were rinsed for 24 h with TBS and immunostained for PKC-α as described above.

^{32}P-PKC-α Labeling.

Confluent cultures (60 mm diameter) were rinsed twice with phosphate-free DMEM and incubated with 2 ml phosphate-free DMEM containing 1 mCi [^{32}P]orthophosphate for 3 h. Indicated additions were added for the indicated interval, and cultures were rinsed 8 times with ice-cold PBS and extracted with 0.5 ml ice-cold lysis buffer. Immunoprecipitation and western analysis of PKC-α were done as described above. After western analysis of PKC-α, membranes were rinsed extensively with solution C and autoradiographed at -70°C for detection of 32P-labeled PKC-α.

Pulse-Chase PKC-α Labeling.

Cultures (60 mm diameter) were rinsed with Met/Cys-free DMEM and incubated with 2 ml Met/Cys-free DMEM containing 5% dialyzed FBS for 1 h to deplete endogenous Met and Cys. Cells were incubated with 0.2 mCi EXPRE35S35S protein labeling reagent in 1.8 ml Met/Cys-free DMEM plus 0.2 ml DMEM containing 5% dialyzed FBS for 16 h. Cells were rinsed with DMEM and 35S was chased for the indicated interval with 2 ml DMEM containing 5% FBS, 5 mM unlabeled Met and Cys, and the indicated additions. Cultures were rinsed 8 times with ice-cold PBS and extracted with 0.5 ml ice-cold lysis buffer. Immunoprecipitation of PKC-α was done as described above. Protein was fractionated by SDS-PAGE, and the gel was soaked in dimethyl sulfoxide containing 10% (w/v) 2,5-diphenyloxazole (Research Products International Corp., Mount Prospect, IL), followed by soaking in water, vacuum drying, and fluorography at -70°C.

Dephosphorylation of PKC-α by Alkaline Phosphatase.

Cultures were incubated with Bryo as indicated, and PKC-αwas immunoprecipitated as described above. Immune complexes were rinsed 6 times with dephosphorylation buffer, which contained 50 mM Tris-HCl, pH 9.0, 1 mM $MgCl_2$, 20 μg/ml leupeptin, and 2 μg/ml aprotinin. Thirty units of affinity purified alkaline phosphatase purified from bovine intestinal mucosa was added to immune complex in 50 μl dephosphorylation buffer with or without 10 mM sodium pyrophosphate (pH 9.0), which inhibits phosphatase activity. After 2 h at 37°C, the

reaction was terminated by rinsing twice with 20 mM Tris-HCl, pH 7.5, and adding 30 µl twice concentrated SDS sample solution. PKC-α bands were fractionated by SDS-PAGE and detected by western analysis as described above.

PKC Activity.

Confluent cultures (100 mm diameter) were incubated with indicated additions for the indicated interval. Cultures were rinsed 3 times with PBS and lysed with 0.5 ml extraction buffer, which contained (mM) 20 Tris-HCl, pH 7.5, 0.5 EDTA, 0.5 EGTA, 10 β-mercaptoethanol, and 0.5% (w/v) Triton X-100. Extracts were homogenized on ice with 15 strokes of a Dounce homogenizer and centrifuged at 100,000 x g for 30 min. PKC was partially purified by DEAE cellulose chromatography (DE 52, Whatmann, Maidstone, UK). A 1 ml column of DE 52 was prepared with column buffer, which contained (in mM) 20 Tris-HCl, pH 7.5, 0.5 EDTA, 0.5 EGTA, 10 β-mercaptoethanol. Extracts were applied to the column, the column was washed with 5 ml column buffer, and PKC was eluted with 10 ml column buffer containing 0.2 M NaCl. Fractions (2 ml each) were assayed for protein by the BCA method and PKC activity by the mixed micelle method (Bell et al., 1986). The reaction mixture (0.2 ml) contained 20 mM Tris-HCl, pH 7.5, 50 µg histone III-SS, 10 mM $MgCl_2$, 20 µM ATP, 0.5 µCi [γ-^{32}P]ATP, 0.3% (w/v) Triton X-100 with or without 8 mol% PS plus 2 mol% DAG, and either 0.2 mM $CaCl_2$ or 1 mM EGTA. The reaction was started by adding 50 µl of a column fraction and stopped after 10 min at 27°C with 1 ml ice-cold 0.5 mg/ml BSA and 1

ml ice-cold 25% (w/v) trichloroacetic acid. Protein was collected by vacuum filtration with GF/C filters (Whatmann, Maidstone, UK). Filters were washed with 10 ml ice-cold 10% (w/v) trichloroacetic acid and counted. Ca^{2+}- and phospholipid-dependent PKC activity was calculated by subtracting ^{32}P incorporation obtained in the absence of Ca^{2+}, phosphatidyl serine, and diacylglycerol.

Cell Morphology.

Confluent LLC-MK_2 line of renal epithelial cell cultures (35 mm diameter) was incubated for 1 h with 10 μM Lacta, 50 μM Benzyloxycarbonyl-Gly-Leu-Ala-leucinal (BzGLAL-al) or Benzyloxycarbonyl-Gly-Leu-Ala-leucinol (BzGLAL-ol). Bryo, PMA, or both were added to 0.1 μM and incubation continued. After 23 h, cells were photographed by phase-contrast microscopy.

Materials.

Ascites fluid (4F3) containing the ubiquitin antibody was generously provided by Dr. Linda A. Guarino (Texas A & M University, College Station, TX). Lacta was obtained from Dr. E. J. Corey (Harvard University). BzGLAL-al and BzGLAL-ol were synthesized as described (Vinitsky et al., 1994; Sepp-Lorenzino et al., 1995). A mouse monoclonal (IgG_{2b}) to an immunogen corresponding to positions 270-427 of rat brain PKC-α was from Transduction Laboratories (Lexington, KY). Protein A/G agarose and a rabbit polyclonal IgG to an epitope corresponding to amino acids 651-672 of the C-terminus of

rabbit PKC-α was obtained from Santa Cruz Biotechnology, Inc. (Santa Cruz, CA). Bryo was isolated from *Bugula neritina* as described (Pettit et al., 1982). The purity of Bryo was >95% as routinely determined by thin layer chromatography, mass spectrometry, ultraviolet spectrophotometry, infrared spectrometry, and nuclear magnetic resonance (Pettit et al., 1982). [^{32}P] Orthophosphoric acid (9,000 Ci/mmol), EXPRE^{35}S^{35}S Protein Labeling Mix (1,175 Ci/mmol), and [γ-^{32}P]ATP (3,000 Ci/mmol) were from DuPont, NEN Research Products (Boston, MA). FBS was obtained from Atlanta Biologicals, Inc. (Norcross, GA). Acrylamide was from Bio-Rad Laboratories (Hercules, CA). Affinity purified bovine intestinal alkaline phosphatase, calf thymus histone III-SS, and fatty acid free BSA were from Sigma Chemical Co. (St. Louis, MO). 1,2-Dioleoyl-sn-glycerol-3-[phospho-L-serine] (in chloroform) and 1,2-dioleoyl glycerol (in chloroform) were from Avanti Polar Lipids (Alabaster, AL), and PMA was from LC Laboratories (Woburn, MA).

Data are expressed as mean ± SE (n = number of experiments). Analysis of variance (single factor factorial) with Scheffe F test was done with Statview II to determine whether means differed significantly at 95% confidence (Abacus Concepts, Inc., Berkeley, CA).

RESULTS

Bryo Antagonizes Phorbol Ester-Evoked Responses Of LLC-MK$_2$ Renal Epithelial Cells

Bryo prevents PMA from decreasing NCX expression. A 24 h incubation of LLC-MK$_2$ cells with 0.1 μM PMA markedly decreased NCX mRNA, protein, and activity (Fig. 1), as reported previously (Smith et al., 1995). PMA decreased the ratio of NCX to β-actin mRNA to 10% of control and NCX activity to 30% of control (Fig. 1). NCX protein, which was quantified by [^{3}H]MAb binding, decreased to 58 ± 4% of control following the incubation with PMA (Fig. 1). The presence of inactive NCX protein that binds [^{3}H]MAb in the PMA-treated cells may account for the larger decrease in NCX activity compared to NCX protein.

Bryostatins acutely activate PKC (Smith et al., 1985; Tallant et al., 1987; Kraft et al., 1986) and block the responses to PMA that they do not produce (Isakov et al., 1993; Huwiler et, al., 1994; Hennings et al., 1987). A 24 h incubation with 1 μM Bryo had no effect on NCX mRNA, [^{3}H]MAb binding, or activity (Fig. 1). Interestingly, 1 μM Bryo prevented PMA from decreasing NCX mRNA, [^{3}H]MAb binding, and

activity (Fig. 1). The remaining experiments address the mechanism by which Bryo antagonizes PMA.

Dephosphorylation of Activated PKC-α Contributes to Downregulation by Bryo or PMA in LLC-MK$_2$ Renal Epithelial Cells

PKC-α translocation by Bryo or PMA. Figure 2 shows the distribution of PKC-α in cytosol and particulate fractions from LLC-MK$_2$ cells that had been incubated with 1 μM Bryo, 0.1 μM PMA, or both for various intervals from 10 min to 24 h. Bryo, like PMA, stabilized the association of PKC-α with the particulate fraction. The cytosolic fraction from cells treated with PMA contained substantially more PKC-α than those treated with Bryo at 1 h and all subsequent intervals (Fig. 2). The effect of Bryo on depletion of cytosolic PKC was dominant to that of PMA. The combination of Bryo plus PMA depleted cytosolic PKC similarly to Bryo alone at 1 h and all subsequent intervals. Interestingly, Bryo appeared to produce a faster mobility PKC-α species (76 kDa) at 4 h and subsequent intervals (Fig. 2). The 76 kDa PKC-α species appeared to be the predominant form in the particulate fraction of cells treated with Bryo or Bryo plus PMA at 8 and 24 h. Experiments described below confirmed the production of 76 kDa PKC-α by Bryo (Figs. 3-7). PKC-α of LLC-MK$_2$ cells has an apparent molecular weight of 80 kDa, as determined by SDS-PAGE using molecular weight standards (Fig. 3). At 4, 8, and 24 h there was markedly more particulate 80 kDa PKC-α in PMA-treated cells compared to those treated with Bryo or Bryo

plus PMA. The rapid depletion of 80 kDa PKC-α by Bryo may largely explain Bryo's antagonism of PMA with respect to NCX expression and cell morphology because PKC-α appears to be the predominant PMA-sensitive isoform of PKC expressed by LLC-MK$_2$ cells. PKC-β, -γ, -δ, or -ε were not detected by western analysis in LLC-MK$_2$ cells (H.-W. Lee and J. B. Smith, unpublished data).

Production of 76 kDa PKC-α by Bryo or PMA. Figure 3 shows a PKC-α western blot of total cell protein, which was extracted with SDS and fractionated by SDS-PAGE under conditions that improved the resolution of the PKC-α bands. The cells were incubated for 2, 4, and 8 h with 0.1 or 1 μM Bryo or PMA. Bryo (0.1 μM and 1 μM) produced substantial 76 kDa PKC-α at each time interval. The amount of the 76 kDa species was much greater with Bryo than PMA (Fig. 3). The 76 kDa band was produced by 1 μM PMA (Figs. 3-6) but was not readily detectable at the lower PMA concentration (Fig. 3). The production of the 76 kDa band by 1 μM PMA was more readily demonstrated in PKC-α immunoprecipitates (Figs. 4-6) than in detergent extracts of the cells (Figs. 2 and 3). There was no detectable 76 kDa PKC-α in cells that were incubated in the absence of Bryo or PMA (Figs. 3-7).

Disappearance of 80 kDa PKC-α by Bryo or PMA. Concomitant with the production of the 76 kDa PKC-α, the 80 kDa form disappeared. The disappearance of the 80 kDa PKC-α was somewhat faster at the higher Bryo concentration (Fig. 3

and Table 1). The effect of Bryo or PMA on the half life of the 80 kDa band was determined by western analysis (Fig. 3 and Table 1). The 80 kDa band was quantified by volume densitometry relative to that of cells that were not treated with PMA or Bryo. The amount of the 80 kDa PKC-α was constant from 0, 2, 4, 8, and 24 h in the absence of Bryo or PMA. The half-life of the 80 kDa band was 4.6 ± 0.9 and 2.9 ± 0.9 h (n = 3) at 0.1 and 1 μM Bryo, respectively (Table 1). The half-life of 80 kDa PKC-α was 8.6 ± 1.4 and 4.5 ± 1.0 h (n = 3) in the presence of 0.1 and 1 μM PMA, respectively (Table 1).

Table 1. Half-life of 80 kDa PKC-α in renal epithelial cells treated with 0.1 or 1 μM Bryo or PMA

control	>24 h
0.1 μM Bryo	4.9 ± 0.9 h
1 μM Bryo	2.9 ± 0.9 h
0.1 μM PMA	8.6 ± 1.4 h
1 μM PMA	4.5 ± 1.0 h

Values represent mean ± S.E. of three independent experiments.

Decrease in PKC activity produced by Bryo or PMA. LLC- MK_2 cells were incubated with 0.1 or 1 μM Bryo or PMA for 4 h (n = 3 experiments) and 8 h (n = 3 experiments). PKC was extracted with Triton X-100, partially purified by DEAE cellulose chromatography, and assayed for Ca^{2+}- and phospholipid-dependent PKC activity with histone as substrate

(See "Methods and Materials"). Treatment of the cells with Bryo or PMA had no effect on the amount of protein extracted by Triton X-100 or eluted from the DEAE colum (Table 2). At 4 and 8 h, 0.1 μM Bryo decreased total PKC activity to 40% and 28% of control, respectively (Table 3). One μM Bryo decreased PKC activity to 17 and 6% control in 4 and 8 h, respectively (Table 3). PMA (0.1 μM) decreased PKC activity to 62% and 56% of control in 4 and 8 h, respectively (Table 3). One μM PMA decreased activity to 31% and 15% of control at 4 and 8 h, respectively (Table 3). These data indicate that 1 μM Bryo produced greater decreases in PKC activity than 1 μM PMA. One μM PMA produced decreases in PKC activity similar to those produced with 0.1 μM Bryo.

Pulse-chase ^{35}S-labeling of 76 kDa PKC-α by Bryo or PMA. Bryo produced a substantial amount of 76 kDa PKC-α in 2 h (Fig. 3) or 1 h (Fig. 19); therefore, ^{35}S pulse-chase experiments were done to determine whether the 80 kDa PKC-α was the precursor of the 76 kDa form. LLC-MK$_2$ cells were incubated with ^{35}S-Met/Cys for 16 h to label PKC-α. Then the labeling solution was removed, excess unlabeled Cys and Met were added, and the cells were incubated with or without 1 μM Bryo or PMA for 2, 4, and 8 h. PKC-α was extracted and immunoprecipitated, and the 76 and 80 kDa forms were resolved by SDS-PAGE (Fig. 4). In the absence of PMA or Bryo, the ^{35}S-labeled 80 kDa PKC-α had a >24 h half-life (Lee et al., unpublished data), which is similar to that reported in human

Table 2. Amount of protein (mg) extracted by TX-100 and eluted by NaCl from DEAE column

total	4 h	8 h
control	5.3 ± 0.6	4.9 ± 0.2
0.1 μM Bryo	5.2 ± 0.5	4.8 ± 0.3
1 μM Bryo	4.8 ± 0.3	5.1 ± 0.6
0.1 μM PMA	4.8 ± 0.4	4.9 ± 0.5
1 μM PMA	4.7 ± 0.2	5.4 ± 0.7

DEAE	4 h	8 h
control	2.3 ± 0.1	2.6 ± 0.1
0.1 μM Bryo	2.6 ± 0.2	2.5 ± 0.1
1 μM Bryo	2.4 ± 0.0	2.8 ± 0.6
0.1 μM PMA	2.6 ± 0.1	2.6 ± 0.3
1 μM PMA	2.4 ± 0.2	2.8 ± 0.1

Amount of protein (mg) in total cell lysate and DEAE purified fractions. Values represent mean ± S.E. of same three independent experiments.

Table 3. Ca^{2+} and lipid-dependent PKC activity of renal epithelial cells treated with Bryo or PMA for 4 or 8 h

	4 h	8 h
0.1 μM Bryo	40 ± 3	28 ± 3
1 μM Bryo	17 ± 2	6 ± 1
0.1 μM PMA	62 ± 6	56 ± 4
1 μM PMA	31 ± 2	15 ± 1

Values represent % control ± S.E. of three independent experiments. PKC activity of controls was 3.8 ± 0.2 nmol phosphate incorporated (μg protein x 10 min)$^{-1}$. All values are significantly different from control at 95% confidence, as determined by ANOVA.

breast cancer cell lines (Borner et al., 1989). Addition of Bryo or PMA markedly decreased the half-life of the ^{35}S-labeled 80 kDa band (Fig. 4). Moreover, Bryo or PMA chased ^{35}S into the 76 kDa band, which was readily apparent in 2 h (Fig. 4). The amount of ^{35}S-labeled 76 kDa band did not appear to change between 2 and 8 h of treatment with Bryo or PMA (Fig. 4). Between 2 and 8 h, Bryo or PMA increased the relative amount of ^{35}S in the 76 versus the 80 kDa band, largely because the 80 kDa band gradually disappeared. Bryo decreased the amount of the ^{35}S-labeled 80 kDa protein more rapidly than PMA (Fig. 4). The half-lives of the ^{35}S-labeled 80 kDa band in cells treated with 0.1 or 1 μM Bryo were 3.7 ($n = 2$) and 2.8 h ($n = 5$), respectively. These half-lives are similar to those obtained by western analysis (Figs. 3 and 4).

The pulse-chase data suggest that 76 kDa PKC-α is produced from the 80 kDa protein. These data, however, are not sufficient to prove a precursor-product relationship between the 80 and 76 kDa proteins, and the immunoprecipitates contained ^{35}S-labeled proteins other than PKC-α. However, the relative amounts of ^{35}S-labeled 76 and 80 kDa bands at 2, 4, and 8 h of treatment with Bryo or PMA (Fig. 4) are similar to those observed by immunostaining (Fig. 5), which suggests that the ^{35}S-labeled 76 kDa band is predominantly PKC-α. Furthermore, the pulse-chase data are

corroborated by western blot experiments showing that the production of 76 kDa PKC-α by Bryo is independent of protein synthesis (see Fig. 6). Bryo or PMA also chased ^{35}S into a 90 kDa band (Fig. 5). We have found that the ~90 kDa band immunostains with antibodies to PKC-α and ubiquitin (Figs. 16 and 25). Next we investigated PKC-α phosphorylation, which is known to influence its mobility by SDS-PAGE.

Bryo or PMA evokes ^{32}P labeling of PKC-α. Incubation of [^{32}P]orthophosphate labeled cells for 2, 4, or 8 h in the absence of Bryo or PMA gradually increased ^{32}P incorporation by nonactivated, competent PKC-α (Fig. 5). A 1 h incubation with 1 μM Bryo or PMA maximally increased ^{32}P-labeling of the 80 kDa PKC-α (Lee et al., unpublished data). Activation of PKC by PMA is known to evoke autophosphorylation (Borner et al., 1989; Cazaubon and Parker, 1993; Pears et al., 1992), which probably accounts for PMA- and Bryo-evoked ^{32}P-labeling of PKC-α. From 1 to 2 h, ^{32}P-labeling of PKC-α remained at the maximal level in the presence of PMA but decreased in the Bryo-treated cells (Fig. 5). From 2 to 8 h, Bryo or PMA concomitantly decreased 80 kDa protein and its ^{32}P content (Fig. 5 and unpublished data). At 2, 4, and 8 h, Bryo produced greater increases in 76 kDa PKC-α and decreases in the 80 kDa form than PMA (Fig. 5). The combination of Bryo plus PMA (1 μM each) produced similar changes in 76 and 80

kDa proteins as Bryo alone, indicating that the effect of Bryo was dominant over that of PMA.

Lack of detectable ^{32}P in 76 kDa PKC-α. There was no detectable ^{32}P in 76 kDa PKC-α (Figs. 5 and 6). For example, a 2 or 4 h incubation with 1 μM Bryo or PMA produced a substantial amount of the 76 kDa PKC-α and ^{32}P labeling of the 80 kDa form, as indicated above, but no detectable ^{32}P-labeling of the 76 kDa form (Figs. 5 and 6). These data suggest that the 76 kDa form is dephosphorylated.

We used a mouse monoclonal (IgG_{2b}) to an immunogen corresponding to positions 270-427 of rat brain PKC-α and a rabbit polyclonal IgG to an epitope corresponding to amino acids 651-672 of the C-terminus of rabbit PKC-α for immunoprecipitation and western analysis of PKC-α, respectively. Smilar proportions of 80 kDa and 76 kDa PKC-α were detected by western analysis of total SDS-extractable cell proteins, western analysis of immunoprecipitated PKC-α, or fluorography of ^{35}S labeled immunoprecipitated PKC-α. In addition, the immunogenic polypeptide (rat brain PKC-α residues 270-427) that was used to produce the mouse monoclonal PKC-α antibody contains no known trans- or auto-phosphorylation sites. These data suggest that the mouse monoclonal PKC-α antibody immunoprecipitates 80 kDa and 76 kDa forms with similar efficiency.

Production of 76 kDa PKC-α is independent of protein synthesis in LLC-MK_2 renal epithelial cells. Because PMA

has been shown to produce non-phosphorylated PKC by de novo synthesis (Borner et al., 1989), the effect of cycloheximide on the production of the 76 kDa form was tested. A 4 h incubation of renal epithelial cells with 1 μM Bryo or PMA produced similar amounts of 76 kDa band in the presence and absence of 30 μg/ml cycloheximide (Fig. 6). Under these conditions, cycloheximide inhibited ^{35}S-Met/Cys incorporation into trichloroacetic acid precipitable protein by 97% (Lee et al., unpublished data). The cycloheximide data exclude de novo synthesis as the source of 76 kDa PKC-α in cells treated with Bryo or PMA.

Dephosphorylation of immunoprecipitated PKC-α by alkaline phosphatase in LLC-MK$_2$ renal epithelial cells. PKC-α was extracted and immunoprecipitated from renal epithelial cells that had been incubated for 4 h in the presence or absence of 1 μM Bryo. In order to demonstrate directly the effect of dephosphorylation on the electrophoretic mobility of PKC-α, the immunoprecipitates were incubated with alkaline phosphatase in the presence or absence of 10 mM pyrophosphate, which inhibits its activity. Treatment with alkaline phosphatase increased the mobility of 80 kDa PKC-α from control cells (Fig. 7). After the alkaline phosphatase treatment, PKC-α from control cells had the same electrophoretic mobility as the 76 kDa species from Bryo-treated cells (Fig. 7). This result indicates that in vitro

dephosphorylation of PKC-α from control cells is sufficient to increase its electrophoretic mobility from 80 to 76 kDa.

Treatment with alkaline phosphatase increased the electrophoretic mobility of PKC-α from cells incubated with Bryo from 80 to 76 kDa. Treatment with alkaline phosphatase had no effect on the mobility of the 76 kDa band, which suggests that 76 kDa form is not phosphorylated, in agreement with the ^{32}P labeling experiments (Figs. 5 and 6). The combination of 1 μM Bryo and 0.1 μM PMA produced similar amounts of 76 and 80 kDa forms as Bryo alone, which indicates that the effect of Bryo is dominant to that of PMA as shown previously (Figs. 3 and 5).

Bryo- or PMA-Induced PKC-α Downregulation by the Production of Incompetent, Nonphosphorylated Enzyme from Activated, Autophosphorylated Form and Degradation by the Ubiquitin-Proteasome Pathway in Human Fibroblasts

Phosphatase inhibitors block formation of 76 kDa PKC-α and concomitantly accumulate 80 kDa form. To test whether dephosphorylation of activated PKC-α occurs generally in mammalian cells, we used non-immortalized early passage of human dermal fibroblasts. In addition, phosphatase inhibitors were used in human fibroblasts to test the hypothesis that dephosphorylation predisposes to degradation of PKC-α. A 6 h incubation of human fibroblasts with 1 μM Bryo markedly decreased 80 kDa PKC-α and concomitantly produced 76 kDa form (Fig. 8), as in LLC-MK$_2$ cells (Figs. 4 and 5). PMA was much less effective than Bryo with respect to downregulation of 80 kDa PKC-α and production of 76 kDa form (Fig. 8), as

in LLC-MK$_2$ cells (Figs. 4 and 5). Figure 8 shows that 5 mM orthovanadate, a non-specific phosphatase inhibitor, prevented production of 76 kDa PKC-α by Bryo and accumulated 80 kDa form. Incubation with 1 or 0.3 μM okadeic acid, a type 2B phosphatase inhibitor, also accumulated 80 kDa form (Fig. 10). The phosphatase inhibitor data support the idea that dephosphorylation of 80 kDa PKC-α produces the 76 kDa form. Because okadeic acid prevented 80 kDa PKC-α from degradation, the production of the 76 kDa species may be a prerequisite for degradation.

Proteasome inhibitors protect PKC-α from downregulation. Incubation of human fibroblasts with 1 μM Bryo for 8 h markedly decreased 80 kDa PKC-α (Figs. 11-13 and 18). Lacta, which selectively inhibits proteolysis by the proteasome (Fenteany et al., 1995), strongly protected PKC-α from downregulation by Bryo whereas E64d, a calpain inhibitor, had no effect on the prevention of PKC-α from downregulation by Bryo (Figs. 11-13 and 18). Peptidyl aldehydes such as BzGLAL-al selectively inhibit the proteolytic activities of the 20S proteasome in vitro and 26S proteasome-mediated intracellular degradation of ubiquitinated proteins (Sepp-Lorenzino et al., 1995; Vinitsky et al., 1994). The corresponding peptidyl alcohols from which the aldehydes were prepared are inactive, showing that the C-terminal aldehyde group is essential for activity towards the proteasome (Sepp-Lorenzino et al., 1995; Vinitsky et al., 1994). BzGLAL-al prevented 80 kDa PKC-α from degradation,

whereas BzGLAL-ol had no effect on the degradation (Figs. 11 and 14). Protection of PKC-α from downregulation by Bryo was significant at 1 μM Lacta and maximal at 20 μM (Fig. 13). The concentration dependence for the preservation of PKC-α by Lacta is similar to that of proteasome inhibition (Fenteany et al., 1995). Lacta or BzGLAL-al by itself had no effect on preservation of PKC-α protein from Bryo- or PMA-evoked degradation (Figs. 12-15). Besides decreasing 80 kDa PKC-α, Bryo produced a 76 kDa form of the kinase (Figs. 11-14), as previously shown. Lacta protected 80 kDa PKC-α from degradation by 40 h treatment of 50 nM Bryo or PMA (Fig. 15). Lacta modestly increased the accumulation of the 76 kDa form produced by 50 nM Byro or PMA (Fig. 15).

In vivo ubiquitination of PKC-α. Proteasome inhibitors strongly increased accumulation of a ladder of >80 kDa PKC-α bands (Figs. 11-14,18,19). Total lysate of human fibroblasts (2 mg) incubated with Bryo plus Lacta for 12 h was used to immunoprecipiate PKC-α with 10 μg of mouse PKC-α monoclonal antibody to increase the yield of PKC-α. Western analysis of immunoprecipitated PKC-α with the mouse 4F3 monoclonal antibodies to ubiquitin indicated that the ladder of PKC-α bands contained ubiquitin (Fig. 16). There was no detectable ubiquitin in PKC-α immunoprecipitated from cells that were incubated in the absence of Lacta plus Bryo (Fig. 16). The 80 and 76 kDa bands from the Lacta plus Bryo treated cells also lacked detectable ubiquitin (Fig. 16). Note that the most prominent band of the ladder with respect to PKC-α

immunostaining, the one just above the 80 kDa band, was the weakest with respect to ubiquitin staining (Fig. 16). The first band of the ladder presumably is mono-ubiquitinated, whereas the others contain more than one ubiquitin per PKC, which would account for the differences in the relative intensities of the bands on the ubiquitin and PKC-α westerns. To maximize the amount of PKC-α immunoprecipitated for ubiquitin immunostaining, an excess of cell extract was used relative to the amount of PKC-α antibody, which accounts for the apparent lack of disappearance of the 80 kDa band in the Bryo plus Lacta treated cells (Fig. 16). Figure 17 shows that 76 kDa and 90 kDa PKC-α proteins produced by Bryo or PMA are located in the particulate fraction. This finding suggests that the 76 and 90 kDa forms are derived from membrane-bound activated PKC-α rather than inactive cytosolic enzyme.

Lacta preserves active PKC-α in vivo. To determine whether Lacta preserved activated, autophosphorylated PKC-α, human fibroblasts were labeled with [^{32}P]orthophosphate and treated with Bryo and/or Lacta in the labeling medium for 8 h (Fig. 18) or 1 h (Fig. 19). A 1 h incubation with Bryo maximally increased ^{32}P-labeled PKC-α (Fig. 19), which subsequently decreased as PKC-α protein was degraded. Lacta preserved a substantial amount of Bryo-induced ^{32}P-labeled PKC-α after the 8 h incubation which was immunoprecipitated from the cells (Fig. 18). Lacta alone had no effect on ^{32}P-labeled PKC-α (Fig. 18). Lacta had no effect on the amount of

^{32}P-labeled PKC-α in the cells following a 1 h incubation with Bryo (Fig. 19). Therefore, Lacta has no effect on production of autophosphorylated 80 kDa PKC-α. Note that an excess of cell lysate relative to the antibody was used in order to maximize the detection of ^{32}P labeled bands. Therefore, a moderate decrease in 80 kDa PKC-α would not be detected because the antibody was not in excess relative to PKC-α.

Ubiquitinated PKC-α lacks detectable ^{32}P. ^{32}P was not detected in the most abundant, presumably mono-ubiquitinated, 90 kDa PKC-α band, which is just above the 80 kDa band in the western blots (Figs. 18 and 19). Note also that treatment of the cells with Bryo alone produced the apparently mono-ubiquitinated PKC-α band in 1 h (Fig. 19), as did PMA (Figs. 17 and 20). Interestingly, the 76 kDa PKC-α band produced by Bryo or PMA lacked detectable ^{32}P (Figs. 18-20), like the apparently mono-ubiquitinated band (Fig. 19). Bisindolylmaleimide, which selectively inhibits PKC (Toullec et al., 1991), inhibited Bryo-induced ^{32}P-labeling of PKC-α, as would be expected for ^{32}P-labeling by autophosphorylation (Fig. 20). Bisindolylmaleimide also inhibited the downregulation of 80 kDa PKC-α and production of 76 kDa form by Bryo or PMA. Interestingly, 90 kDa PKC-α accumulated in the cells treated with bisindolylmaleimide plus Bryo (Fig. 20), suggesting that activation and autophosphorylation of PKC-α is necessary for dephosphorylation and degradation. A

plausible explanation for 90 kDa PKC-α accumulation by bisindolylmaleimide, which is a competitive inhibitor with respect to ATP, is that it would also inhibit the activity of 26S proteasome. PA700 has been shown to have unique ATPases which apparently inject ubiquitinated substrates into the inner cavity of the proteasome (Goldberg, 1995; Hochstrasser, 1995). There was approximately half as much ^{32}P in the 80 kDa PKC-α band immunoprecipitated from the cells treated with Bryo plus bisindolylmaleimide as from cells treated with Bryo alone, as determined by volume densitometry (Fig. 20). ^{32}P should have been readily detectable in the 76 kDa band because densitometric analysis indicates that there was about half as much 76 kDa as 80 kDa PKC-α protein in the Bryo plus cycloheximide immunoprecipitate (Fig. 20). In this experiment, PKC-α protein in the control samples was underestimated because the antibody was saturated with PKC-α in order to maximize immunoprecipitation of the 76 kDa band and detection of ^{32}P.

Production of 76 kDa PKC-α by Bryo is independent of protein synthesis in human fibroblasts. Experiments with cycloheximide excluded the possibility that the 76 kDa form was produced by de novo synthesis in human fibroblasts. Production of 76 kDa PKC-α by Bryo or PMA was unaffected by 30 μg/ml cycloheximide, indicating that it was not produced by de novo synthesis (Fig. 20). Cycloheximide at this level essentially abolished protein synthesis, as determined by

[^{3}H]leucine incorporation into trichloroacetic acid precipitable protein (Lee et al., unpublished data).

Dephosphorylation of PKC-α immunoprecipitated from human fibroblasts by alkaline phosphatase. If Bryo produces 76 kDa PKC-α by dephosphorylation of 80 kDa kinase, then treatment with alkaline phosphatase in vitro would be expected to convert the 80 kDa form to 76 kDa. PKC-α immunoprecipitated from Bryo-treated or control cells was incubated with alkaline phosphatase in the presence or absence of pyrophosphate, which inhibits alkaline phosphatases. Alkaline phosphatase converted the 80 kDa form to 76 kDa in the absence but not in the presence of pyrophosphate, as expected (Fig. 21). Furthermore, if Bryo produced the 76 kDa band by a mechanism other than dephosphorylation, then dephosphorylation by alkaline phosphatase would be expected to increase further the electrophoretic mobility of the 76 kDa band, which was not observed (Fig. 21).

Inhibitors of proteolysis by the proteasome protect Ca^{2+} and lipid-dependent kinase activity from downregulation by PMA or Bryo. Incubation of human fibroblasts with 50 nM Bryo or 0.1 μM PMA for 20 h strongly downregulated PKC-α protein and Ca^{2+} and lipid-dependent kinase activity (Fig. 22). Lacta protected PKC-α protein and Ca^{2+} and lipid-dependent kinase activity from downregulation by Bryo or PMA (Fig. 22). Cells treated with Bryo or PMA in the presence of

Lacta retained 7- and 14-fold higher specific activity in the same amount of protein than those incubated with Bryo or PMA alone (Fig. 22). PKC activity was calculated as the difference between kinase activity in the absence or presence of Ca^{2+}, diacylglycerol, and phosphatidyl serine. None of the treatments had any effect on kinase activity determined in the absence of Ca^{2+} and lipids, which was 3 to 7% of that determined in their presence (data not shown).

Figure 23 shows that BzGLAL-al protected PKC-α protein from Bryo-induced downregulation, whereas the BzGLAL-ol had no effect on downregulation. The peptidyl aldehyde but not the alcohol protected Ca^{2+} and lipid-dependent PKC activity from downregulation by Bryo (Fig. 23). There was approximately 2.5 times more PKC activity in the cells treated with the peptidyl aldehyde plus Bryo compared to Bryo alone (Fig. 23). The peptidyl aldehyde but not the alcohol similarly protected PKC activity from downregulation by a 20 h incubation of the cells with 0.1 μM PMA. Neither BzGLAL-al nor BzGLAL-ol by itself affected PKC-α protein or Ca^{2+} and lipid-dependent PKC activity (Fig. 23).

Lactacystin Preserves Activated PKC-α and Proteasome Inhibitors Convert Bryo from a PKC Antagonist to an Agonist by Preventing Downregulation by Ubiquitin-Proteasome Pathway in LLC-MK$_2$ Renal Epithelial Cells

Lacta preserves ^{32}P-labeled PKC-α produced by Bryo. Determinations of Bryo-induced ^{32}P-labeling of PKC in vivo are important because autophosphorylated PKC is the most direct

method for estimating the amount of PKC that is active in vivo. When [^{32}P]orthophosphate-labeled cells were incubated for 8 h with Lacta and Bryo, the amount of ^{32}P-labeled PKC-α increased markedly compared to treatment with Bryo alone (Fig. 24, middle panel). This finding indicates that Lacta preserved activated PKC-α in vivo. The inhibition of Bryo-evoked PKC-α degradation by Lacta accounts, at least in part, for the increase in ^{32}P-labeled enzyme (Fig. 24). PKC-α was immunoprecipitated from 0.03 (Fig. 24, left panel) or 0.5 mg (Fig. 24, middle and right panels) of cell lysate. The lower amount of lysate was better for quantifying the 76 and 80 kDa forms of PKC-α by western analysis, and the latter increased immunoprecipitation of all PKC-α bands, which improved the detectability of ^{32}P-labeled bands. The 76 kDa form of the enzyme, which was produced by Bryo in the presence or absence of Lacta, lacked detectable ^{32}P (Figs. 18-20,24, and 26). In contrast to the marked increase in Bryo-induced ^{32}P-labeled PKC-α produced by Lacta in 8 h, Lacta had no effect on the amount of ^{32}P-labeled PKC-α produced by a 1 h incubation with Bryo (Fig. 26). These data show that Lacta principally affected the disappearance of ^{32}P-labeled PKC-α rather than its formation.

Ubiquitination of PKC-α. PKC-α from total lysate of renal epithelial cells (2 mg) incubated with Bryo plus Lacta for 12 h was immunoprecipitated with 10 μg of mouse

monoclonal PKC-α antibody to increase the yield of PKC-α. Figure 25 shows ubiquitin immunostaining of immunoprecipitated PKC-α, separated by SDS-PAGE, transferred to a nitrocellulose membrane, and detected by western analysis with mouse 4F3 monoclonal ubiquitin antibody. Incubation with Bryo plus Lacta for 12 h produced a ladder of >80 kDa PKC-α bands (Fig. 25) which was similar to that produced by a 1 or 8 h incubation with Bryo and Lacta (Figs. 26 and 24, right panels). Immunostaining with 4F3 monoclonal antibody indicated that the >80 kDa PKC-α bands were ubiquitinated (Fig. 25). Neither the 76 nor the 80 kDa PKC-α bands immunostained for ubiquitin (Fig. 25). The band with a similar mobility as the 116 kDa molecular weight marker was the most prominent ubiquitinated PKC-α band (Fig. 25). In addition, there was a broad band in the 200 kDa region, as would be expected for polyubiquitinated PKC-α in renal epithelial cells treated with Bryo plus Lacta (Fig. 25). There was no detectable ubiquitin in PKC-α immunoprecipitated from cells that were incubated in the absence of Bryo and Lacta (Fig. 25).

Importantly, Bryo alone produced the ladder of >80 kDa PKC-α bands (Fig. 24). The ladder was readily detected when an excess of lysate relative to antibody was used for the immunoprecipitation (Fig. 24, right panel). Lacta preserved the ladder of PKC-α bands during the 8 h incubation with Bryo (Fig. 24, right panel). The only known post-translational

mechanism that produces a ladder of bands larger than the native protein is ubiquitination. Interestingly, ^{32}P was not detected in the >80 kDa PKC-α bands after either a 1 or an 8 h incubation with Bryo plus Lacta (Figs. 26 and 24). The lack of detectable ^{32}P in the >80 kDa PKC-α bands supports the idea that dephosphorylation precedes ubiquitination.

BzGLAL-al preserves PKC-α protein from downregulation by Bryo. Figure 27 shows that BzGLAL-al preserved 80 kDa PKC-α protein similarly to Lacta in Bryo-treated cells. The corresponding alcohol, BzGLAL-ol, had no effect on the disappearance of PKC-α evoked by Bryo (Fig. 27), indicating C-terminal aldehyde of BzGLAL-al is critical for its activity towards the 20S proteasome.

Lacta preserves Ca^{2+} and lipid-dependent kinase activity in Bryo- or PMA-treated cells. LLC-MK$_2$ cells were incubated with 1 μM Bryo for 4 h (Fig. 28A) or with 0.1 μM Bryo or 0.2 μM PMA for 20 h (Fig. 28B). Following the incubation, PKC was extracted with Triton X-100, partially purified by DEAE cellulose chromatography, and assayed with histone as substrate using the mixed micelle system. PKC-α protein was determined by western analysis of first fraction from the DEAE cellulose column, which contained most PKC activity. Bryo decreased 80 kDa PKC-α protein by ~70% and produced the 76 kDa inactive form of the kinase (Fig. 28A, inset), as shown previously. The 76 kDa band was excluded from the analysis of PKC-α protein because dephosphorylated,

76 kDa PKC-α is inactive, probably due to the lack of phosphate at a trans site, Thr^{497} and possibly Thr^{495} (Cazaubon and Parker, 1993; Cazaubon et al., 1994). Bryo (1 μM) decreased Ca^{2+} and lipid-dependent PKC activity by ~90% in 4 h (Fig. 28A). Lacta (20 μM) preserved PKC activity and protein from downregulation by Bryo (Fig. 28A). There was approximately 3.3-fold more PKC activity and approximately twice as much 80 kDa PKC-α protein in Bryo plus Lacta treated cells compared to those treated with Bryo alone. The similar decreases in 80 kDa protein and Ca^{2+} and lipid-dependent PKC activity produced by Bryo are consistent with the finding that PKC-α is the predominant diacylglycerol-dependent PKC expressed by LLC-MK_2 cells. Decreases in the activity of other relatively minor PKC isoforms, however, may account for the somewhat larger decrease in PKC activity compared to PKC-α protein. Figure 28B shows that a 20 h incubation of the cells with 0.2 μM PMA or 0.1 μM Bryo strongly decreased Ca^{2+} and lipid-dependent PKC activity, which was assayed in vitro. Lacta similarly preserved PKC activity and PKC-α protein from downregulation by PMA or Bryo (Fig. 28B). Lacta preserved 2.7 and 2.2 times more PKC activity in PMA- or Bryo-treated cells, respectively (Fig. 28B).

Bryo prevents PMA-evoked change in cell morphology. A 23 h incubation with 0.1 μM PMA altered the morphology of LLC-MK_2 cells (Fig. 29). Prior to the PMA treatment, the cells had a cobblestone appearance with bright cell-cell borders, as

observed by phase-contrast microscopy. PMA rounded the cells, which disrupted cell-cell interactions (Fig. 29). In contrast to PMA, Bryo had no effect on cell shape at 0.1 μM (Fig. 29) or other concentrations (1-10^3 nM) (data not shown). Moreover, 0.1 μM Bryo prevented 0.1 μM PMA from rounding the cells (Fig. 29). Therefore, with respect to the morphology change, Bryo is a PMA antagonist.

Proteasome inhibitors convert Bryo from a PMA-antagonist to a long-term PKC agonist. Proteasome inhibitors potentiated the effect of PMA on cell morphology (Fig. 29). Interestingly, in the presence of 10 μM Lacta, Bryo changed cell morphology similarly to PMA (Fig. 29). BzGLAL-al, a peptidyl aldehyde that blocks proteolysis by the proteasome, also converted Bryo from a PMA antagonist to an agonist (Fig. 29). Lacta or BzGLAL-al alone slightly affected cell shape, although neither compound rounded the cells like PMA (Fig. 29). The corresponding peptidyl alcohol (BzGLAL-ol), which is inactive as a proteasome inhibitor, was inactive with respect to the conversion of Bryo to a long-term PKC agonist (Fig. 29). These findings indicate that the proteasome inhibitors converted Bryo from a PKC antagonist to an agonist with respect to the morphology change.

DISCUSSION

Proteolytic degradation of PKC is generally responsible for the downregulation produced by phorbol esters without change in its rate of synthesis (Mahoney and Huang, 1994; Young et al., 1987). Although much is known about acute activation of PKC by DAG and PS (Quest and Bell, 1994; Goode et al., 1995), there is little understanding of PKC downregulation. A recent study suggests that downregulation by PMA depends on the kinase function of PKC (Ohno et al., 1990; Goode et al., 1995). A role of Ca^{2+}-activated neutral proteases (calpain) in PKC downregulation was suggested by the relative sensitivity of PKC to various proteases in vitro (Kishimoto et al., 1989). However, recent studies of PKC mutants expressed in COS and yeast cells implicate membrane trafficking and multiple proteases in downregulation (Junco et al., 1994). Our Bryo data indicate that dephosphorylation, which is known to inactivate PKC (Cazaubon and Parker, 1993; Dutil et al., 1994; Pears et al., 1992), contributes to downregulation and may be a prerequisite for ubiquitin-proteasome-mediated degradation. Bryo activated PKC-α similarly to PMA, as indicated by autophosphorylation (Figs. 5,6, and 20) and translocation from the cytosol to the

particulate fraction (Figs. 2 and 17). Bryo, however, was a more potent inducer of PKC downregulation than PMA. Bryo produced a more rapid loss of 80 kDa PKC-α protein and Ca^{2+}- and lipid-dependent PKC activity than PMA (Figs. 2-5,15,20,22,23, and 28 and Tables 1 and 3), in agreement with recent findings in other cell types (Huwiler et al., 1994; Isakov et al., 1993; Jalava et al., 1993). The 76 kDa form of PKC-α was inactive in vivo because it lacked ^{32}P, in contrast to the highly labeled 80 kDa form produced by autophosphorylation in response to Bryo or PMA (Figs. 5,6,18-20,24, and 26). The 76 kDa form of PKC-α was in the particulate rather than the cytosolic fraction (Figs. 2 and 17), indicating it was probably derived from activated kinase. One of the most novel and unexpected findings of the present study is the rapid (≤ 2 h) production of inactive 76 kDa PKC-α following PKC activation by Bryo or PMA. Previously, it was shown that PMA caused the accumulation of nonphosphorylated PKC in breast cancer cell lines (Borner et al., 1989); however, nonphosphorylated PKC was produced by de novo synthesis rather than by dephosphorylation of existing PKC, as shown here. The possibility that Bryo or PMA produced 76 kDa PKC-α by de novo synthesis was excluded because blocking protein synthesis had no effect on its generation (Figs. 6 and 20). Furthermore, pulse-chase experiments suggest that ^{35}S-labeled 80 kDa PKC-α is the precursor of the 76 kDa species (Fig. 4).

Both termini of the 76 kDa form of PKC-α appear to be intact. There are trans- (Thr^{495}, Thr^{497}) and auto- (Thr^{631}, Thr^{638}) phosphorylation sites in the C-terminal portion of PKC-α (Cazaubon and Parker, 1993; Dutil et al., 1994; Orr and Newton, 1994; Pears et al., 1992; Zhang et al., 1993, 1994). Accordingly, removal of an N-terminal segment would not dephosphorylate PKC-α; however, the 76 kDa form was derived from highly ^{32}P-labeled PKC-α and lacked detectable radioactivity (Figs. 18-20,24, and 26). Furthermore, if Bryo produced the 76 kDa band by removal of an N-terminal segment, then dephosphorylation by alkaline phosphatase would be expected to increase further its electrophoretic mobility, which was not observed (Figs. 7 and 21). The antibody used for western analysis reacts with the C-terminus (residues 651-672), so 76 kDa PKC-α has an intact C-terminus and probably an intact N-terminus.

Diagram 7 shows a hypothetical pathway of PKC synthesis and downregulation. Transphosphorylation of the nascent protein by an unidentified kinase ("PKC kinase") converts PKC to a competent, cytosolic form, which translocates to the plasma membrane and phosphorylates itself upon activation by DAG (or Bryo) and PS (Borner et al., 1989; Cazaubon and Parker, 1993; Dutil et al., 1994; Orr and Newton, 1994; Pears et al., 1992). Our findings indicate that, following PKC-α activation by Bryo, removal of phosphate from both trans and auto sites, which is known to inactivate the kinase,

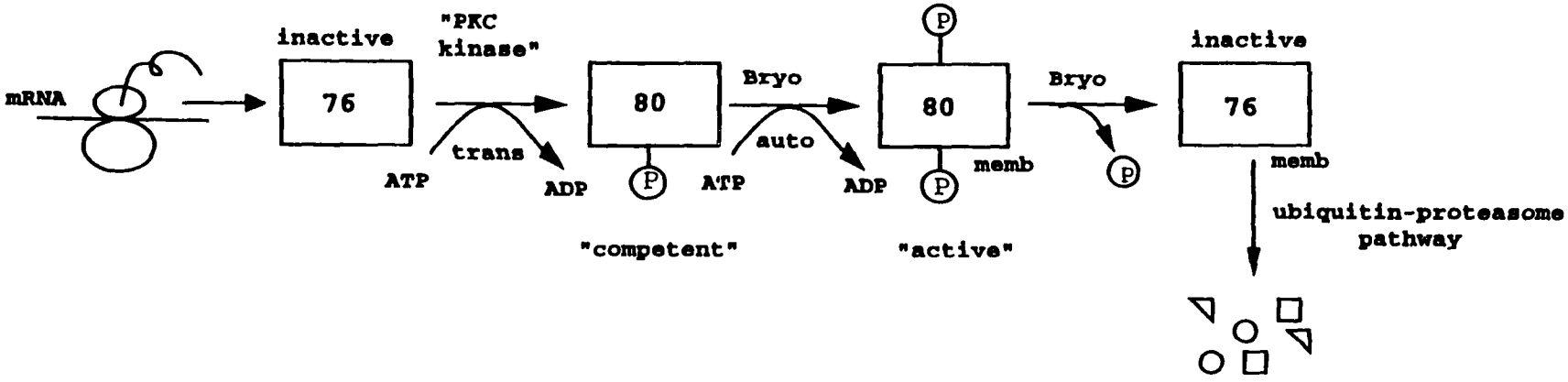

Diagram 7. Hypothetical pathway of PKC synthesis, activation, dephosphorylation, and degradation by Bryo. Transphosphorylation of the 76 kDa nascent protein by an unidentified "PKC kinase" converts it to a competent form, which migrates as an 80 kDa protein by SDS-PAGE. Concomitant with activation and intramolecular autophosphorylation, PKC translocates from the cytosol to the plasma membrane. Autophosphorylation is known to slightly decrease the electrophoretic mobility of PKC-α, as suggested in Fig. 7; however, the resolution of the autophosphorylated PKC-α was not sufficiently resolved from the 80 kDa form under the electrophoretic condition used here. In the presence of Bryo, catalytically active 80 kDa PKC is bound to the plasma membrane where it becomes dephosphorylated and degraded. The incompetent 76 kDa forms are not equivalent because the one produced de novo is cytosolic, whereas the one produced by dephosphorylation is membrane bound.

contributes to downregulation. Dephosphorylated, 76 kDa PKC-α was produced by PMA, as well as Bryo (Figs. 4,5, and 20). The following correlative evidence suggests that dephosphorylation is a prerequisite for rapid degradation of PKC-α. First, production of 76 kDa PKC-α and disappearance of 80 kDa form occurred concomitantly and were similarly affected by the concentration of Bryo (Figs. 3-5). Second, PMA was less potent than Bryo with respect to the production of dephosphorylated, 76 kDa PKC-α and the disappearance of the 80 kDa form (Figs. 3,5,8,15,17,20, and 22). Although the 76 kDa form was not detected after a 4 h incubation with 0.1 μM PMA (Fig. 3), higher PMA (1 μM) produced the 76 kDa form (Figs. 3-6,8,17, and 20). Because the disappearance of the 80 kDa PKC-α protein was much slower at the lower PMA concentration ($t_{1/2}$ of 8.6 versus 4.5 h), it seems likely that the 76 kDa form was produced by 0.1 μM PMA, but its level was too low to detect. A 20 h incubation of LLC-MK_2 cells with 0.2 μM PMA produced 76 kDa PKC-α (Fig. 28). Third, Bryo or PMA produced 76 kDa PKC-α from the 80 kDa form in early passage cultures of human dermal fibroblasts, as well as LLC-MK_2 cells, suggesting that dephosphorylation of activated PKC-α occurs generally in mammalian cells. Fourth, phosphatase inhibitors, orthovanadate and okadeic acid, retarded the production of 76 kDa PKC-α and the degradation of the 80 kDa form in Bryo-treated fibroblasts (Figs. 9 and 10). Production of nonphosphorylated PKC from active kinase requires

dephosphorylation at the trans and auto sites, which may occur in a random or an ordered fashion. Initial dephosphorylation at a trans site is attractive because this would inactivate the kinase and curtail the futile cycle of dephosphorylation followed by intramolecular autophosphorylation.

The most important finding of this study is that the ubiquitin-proteasome system is responsible for the rapid degradation of PKC that follows acute activation by Bryo or phorbol ester. The following evidence implicates the ubiquitin-proteasome system in PKC-α degradation. First, western analysis indicated that Bryo produced a ladder of ubiquitinated PKC-α bands that were larger than the native enzyme in human fibroblasts (Figs. 11-14 and 16-19) and renal epithelial LLC-MK_2 cells (Figs. 24-27). Second, two structurally dissimilar proteasome inhibitors, Lacta and BzGLAL-al, antagonized Bryo-induced PKC-α degradation in both cell types (Figs. 11-19 and 22-28). Lacta also antagonized PMA-induced PKC-α degradation (Figs. 14,21, and 27). Because Bryo was more efficacious than PMA with respect to PKC-α downregulation, Lacta preserved more PKC-α protein and Ca^{2+} and lipid-dependent PKC activity in PMA- compared to Bryo-treated cells (Figs. 15, 22, and 28). Proteasome inhibitors preserved PKC activity and PKC-α protein in LLC-MK_2 cells similarly to human fibroblasts. Third, ^{35}Smet/Cys pulse-chase labeling experiments in LLC-MK_2 cells suggest that there

is a precursor-product relationship between 80 kDa PKC-α and the ladder of >80 kDa PKC-α bands (Fig. 4).

According to our view, dephosphorylated, incompetent kinase is a better substrate for ubiquitination than phosphorylated PKC-α. ^{32}P was not detected in the most abundant ubiquitinated PKC-α band, which is the presumably mono-ubiquitinated band that is just above the 80 kDa band in the western blots (Figs. 11-14,16,18,19, and 24-27). The lack of ^{32}P in mono-ubiquitinated PKC-α is consistent with the idea that the nonradiolabeled 76 kDa form, rather than the highly ^{32}P-labeled 80 kDa form, becomes ubiquitinated. The possibility that the autophosphorylated 80 kDa form is the exclusive substrate for ubiquitination is unattractive because rephosphorylation of the 76 kDa form would be required for its degradation. The following evidence supports the idea that the 76 kDa form is an essential intermediate in the degradation pathway. Phosphatase inhibitors, orthovanadate and okadeic acid, retarded the degradation of the 80 kDa form in Bryo-treated fibroblasts (Figs. 9 and 10).

The mechanism by which inhibition of proteolysis via the proteasome preserved active PKC-α is unknown. It is not known whether active PKC was produced from ubiquitinated enzyme by ubiquitin hydrolase enzymes and possibly "PKC kinase" or whether less PKC became ubiquitinated due to depletion of free ubiquitin. Ubiquitin is known to be

recycled as proteins are degraded by the proteasome (Rechsteiner et al., 1993). Because nonphosphorylated 76 kDa PKC-α is known to be inactive (Dutil et al., 1994; Orr and Newton, 1994; Pears et al., 1992; Zhang et al., 1993, 1994; Cazaubon et al., 1994), the unidentified "PKC kinase" responsible for phosphorylation of the trans sites would be required for restoring kinase function (Cazaubon and Parker, 1993; Cazaubon et al., 1994; Dutil et al., 1994; Pears et al., 1992; Zhang et al., 1993, 1994).

While the structure of Bryo differs substantially from that of PMA, they both have structural features in common with DAG which are probably responsible for high affinity binding to the zinc finger site of PKC (Diagram 2 and Wender et al., 1988). Bryostatins acutely activate PKC and elicit some of the same cellular responses as PMA but not others (Smith et al., 1985; Kraft et al., 1986). Moreover, Bryo antagonizes those responses to phorbol esters that it does not evoke (Hennings et al., 1987; Kraft et al., 1986; Sako et al., 1987), as exemplified by antagonism of PMA-evoked change in the cell morphology (Fig. 29) and of PMA-induced NCX expression (Fig. 1). Bryo apparently antagonizes PMA by rapidly and efficiently downregulating PKC (Huwiler et al., 1994; Isakov et al., 1993; Jalava et al., 1993). Thus, proteasome inhibitors such as Lacta or BzGLAL-al converted Bryo to a long-acting PKC agonist (Figs. 18,22-24,28, and 29). In agreement with the idea that Bryo fails to elicit cellular responses that depend on a long-term activation of

PKC, Bryo alone had no effect on the cell morphology or NCX expression. Bryo, however, evoked the shape change in the presence of Lacta or BzGLAL-al but not BzGLAL-ol, which is inactive as a proteasome inhibitor (Fig. 29). The present findings confirm previous reports that Bryo and PMA differ with respect to potency and efficacy to downregulate PKC (Huwiler et al., 1994; Isakov et al., 1993; Jalava et al., 1993). Bryostatins have a far higher PKC affinity for PKC than phorbol esters, and the release of Bryo from PKC is so slow that binding is virtually irreversible for biologically relevant periods (Kazanietz et al., 1994; Lewin et al., 1992). Dissociation of phorbol esters from PKC occurs rapidly ($t_{1/2}$ ~1.75 min at 30°C) (Dunphy et al., 1981). The extraordinary stability of the PKC-Bryo complex may dispose it to accelerated dephosphorylation and degradation by ubiquitin-proteasome pathway. By accelerating dephosphorylation that accompanies degradation, Bryo may antagonize those responses to PMA that depend on sustained kinase activation. Conceivably, differences between the structure of the PKC complex with Bryo versus PMA influences its susceptibility to "PKC phosphatase and/or PKC kinase" and ubiquitinating enzymes. In some cell types, Bryo may influence differentially the catalytic function or subcellular distribution of individual PKC isozymes (Hocevar and Fields, 1991; Szallasi et al., 1994), and thereby produce different cellular responses or antagonize PMA. Bryo has similar binding affinities (Kd 1.2 to 5.6 nM) for a variety

of recombinant PKC isozymes (α, β, γ, δ, ε, and η) (Kazanietz et al., 1994), so the isozyme specific effects of Bryo probably involve intricate interactions between a particular isoform and its lipid microenvironment. Differential regulation of PKC isozymes by Bryo versus PMA, however, would not explain Bryo's antagonism of PMA-regulated NCX expression and change in cell morphology because LLC-MK_2 cells appear to express a single PMA-sensitive isozyme, PKC-α (H.-W. Lee and J. B. Smith, unpublished data). Although PKC has been considered to be the main target for phorbol esters or Bryo, Vav, *n*-chimaerin, and Unc-13, which have a consensus DAG binding domain, may be regulated by phorbol esters (Areces et al., 1994; Ahmed et al., 1992). A DAG kinase was also shown to possess an homologous Cys-rich motif, and phorbol esters inhibited its enzymatic activity (Sakane et al., 1990). It is also possible that the differential effects of Bryo and PMA on other proteins than PKC may cause antagonism of Bryo to the cellular responses evoked by PMA. Having identified the proteolytic pathway that degrades PKC, the hypothesis that dephosphorylation strongly enhances its susceptibility to ubiquitination becomes readily testable in vitro and in vivo.

Further understanding of the mechanism of action of Bryo is urgent because it is in Phase I clinical trials as a chemotherapeutic agent for several malignancies (Philip et al., 1993; Prendiville et al., 1993) and because the dephosphorylation and degradation of activated PKC, as elicited by Bryo, constitute a powerful negative feedback

mechanism with vital consequences for the regulation of metabolism and growth. In summary, the present findings suggest that nonphosphorylated, 76 kDa PKC-α from active, autophosphorylated enzyme produced by Bryo or PMA and dephosphorylation predisposes PKC-α to degradation by ubiquitin proteasome pathway.

Figure 1. Bryo prevents PMA from decreasing NCX mRNA, [^{3}H]MAb binding, and activity. Cultures were incubated with 0.1 μM PMA, 1 μM Bryo, or both in serum-free DMEM for 24 h. For northern analysis (A), RNA was extracted, fractionated by oligo(dT) cellulose chromatography, and size fractionated. The northern blot is representative of three independent experiments. NCX protein (B) was determined by specific binding of [^{3}H]MAb. Values are mean ± SE (n = 5 experiments). [^{3}H]MAb binding to sonicate from control cells was 68 ± 4 ng/mg protein. To assay NCX activity (C), 1 mM ouabain was added directly to each dish and the incubation continued for 1 h before determining $^{45}Ca^{2+}$ uptake with Na^+ or K^+ as the principal external cation. Values are means ± SE (n = 6). NCX activity of control cultures was 14.9 ± 0.3 nmol Ca^{2+} uptake per min per mg protein. The asterisks indicate a significant difference from control at 95% confidence, as determined by ANOVA.

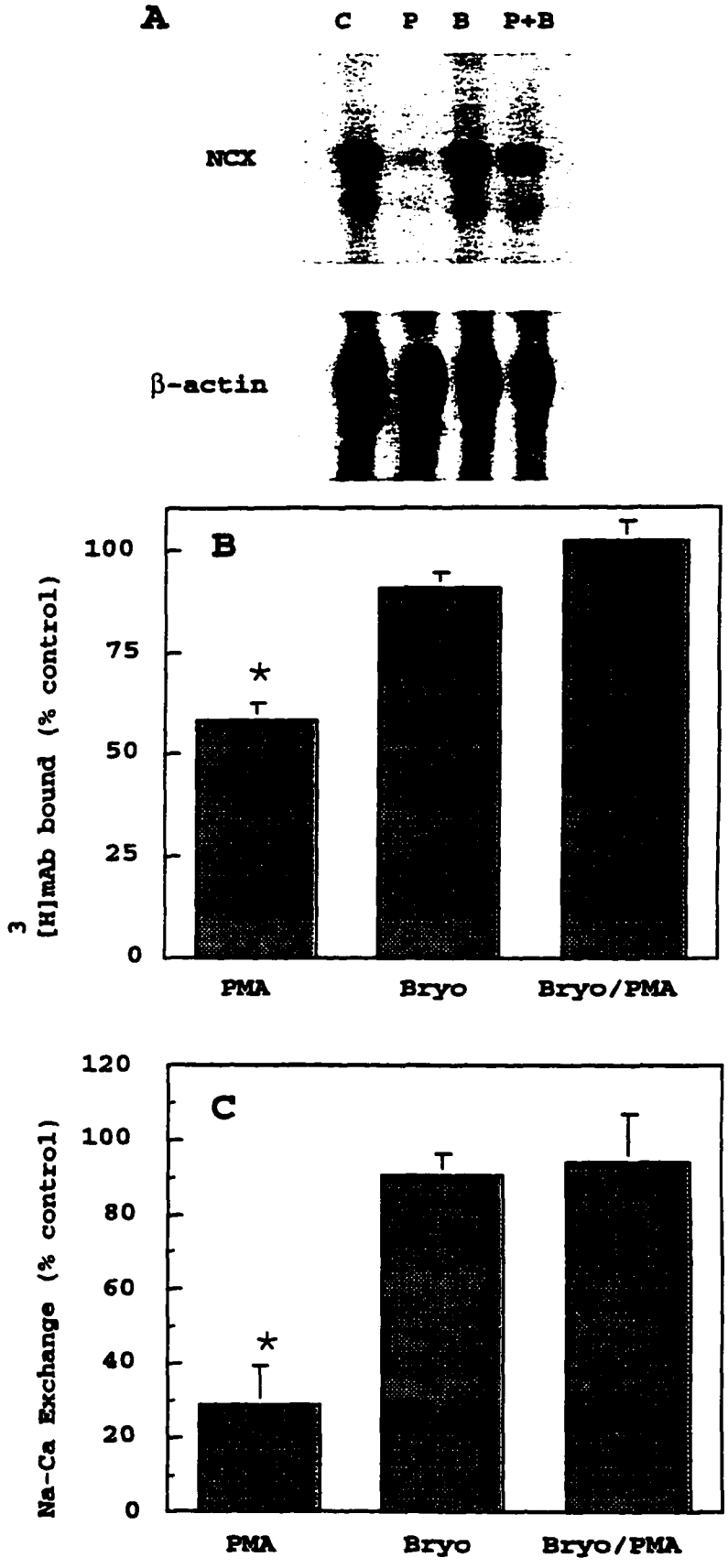

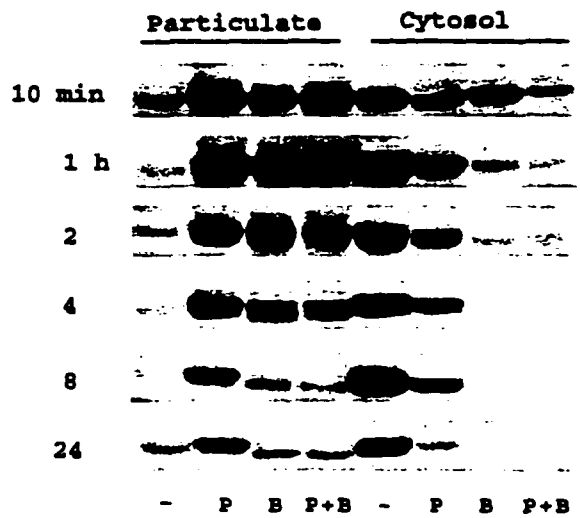

Figure 2. PKC-α translocation and downregulation by Bryo, PMA, or both in renal epithelial cells. Cultures were incubated in serum-free DMEM in the presence or absence of 0.1 μM PMA ("P"), 1 μM Bryo ("B"), or both ("P+B") for 10 min to 24 h, as indicated. Cytosol and particulate fractions were prepared and a constant amount of protein was subjected to SDS-PAGE. PKC-α was detected by western analysis. Data are representative of three independent experiments.

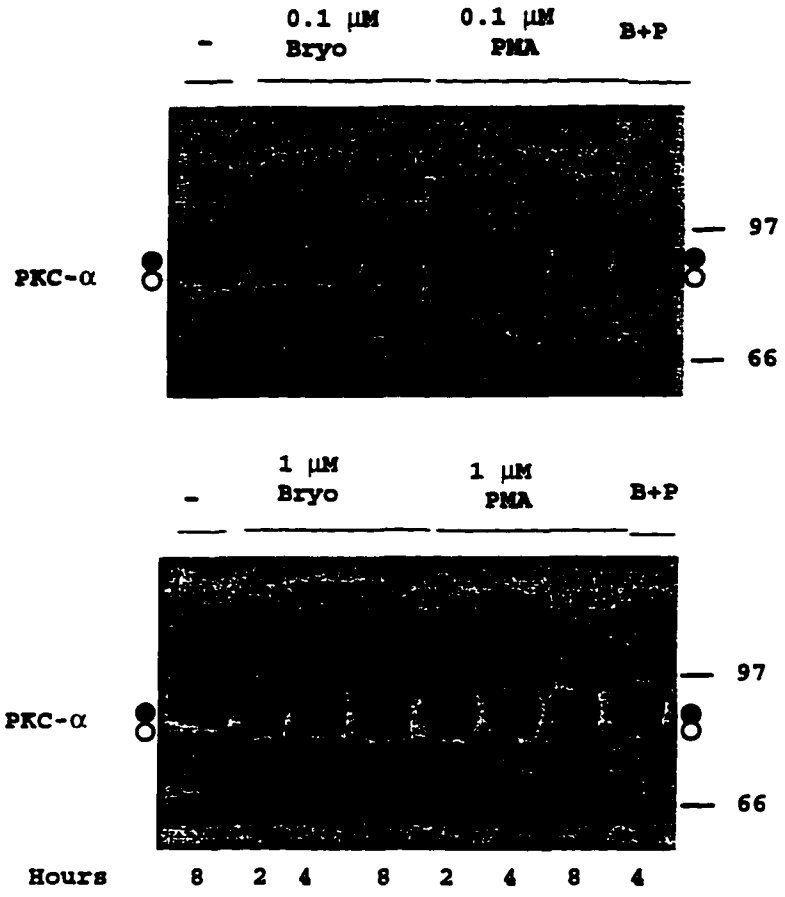

Figure 3. Effect of Bryo, PMA, or both on depletion of 80 kDa PKC-α and production of 76 kDa form in renal epithelial cells. Cultures were incubated in serum-free DMEM with or without 0.1 or 1 μM Bryo or PMA for 2, 4, and 8 h, as indicated. Total cell protein was extracted with SDS and fractionated by SDS-PAGE, and PKC-α was detected by western analysis. The positions of molecular weight standards (in kDa) are indicated. The blots are from separate experiments and representative of at least four independent experiments. Filled and unfilled circles indicate 80- and 76-kDa PKC-α bands, respectively

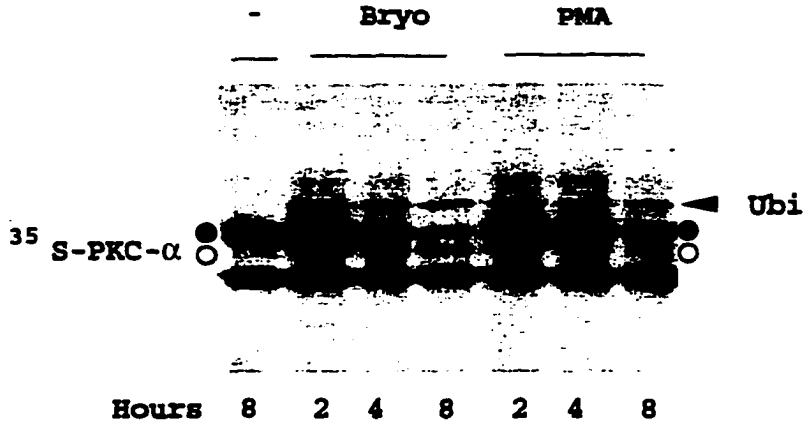

Figure 4. Pulse-chase labeling of PKC-α with ^{35}S-Met/Cys in renal epithelial cells. Cultures were incubated with 0.2 mCi ^{35}S-Met/Cys in 1.8 ml Met/Cys-free DMEM plus 0.2 ml DMEM containing 5% dialyzed FBS for 16 h. Then they were rinsed and incubated with 2 ml DMEM containing 5% FBS, 5 mM Met and Cys, and 1 μM Bryo or PMA for 0, 2, 4, or 8 h, as indicated. PKC-α was extracted, immunoprecipitated, and fractionated by SDS-PAGE. The gel was fluorographed to visualize radiolabeled bands. Data are representative of four independent experiments. Filled and unfilled circles indicate 80- and 76-kDa PKC-α bands, respectively. Arrowhead indicates the position of PKC-α band that has the same mobility as ubiquitinated PKC-α, as determined by immunostaining with ubiquitin antibody (See Fig. 25)

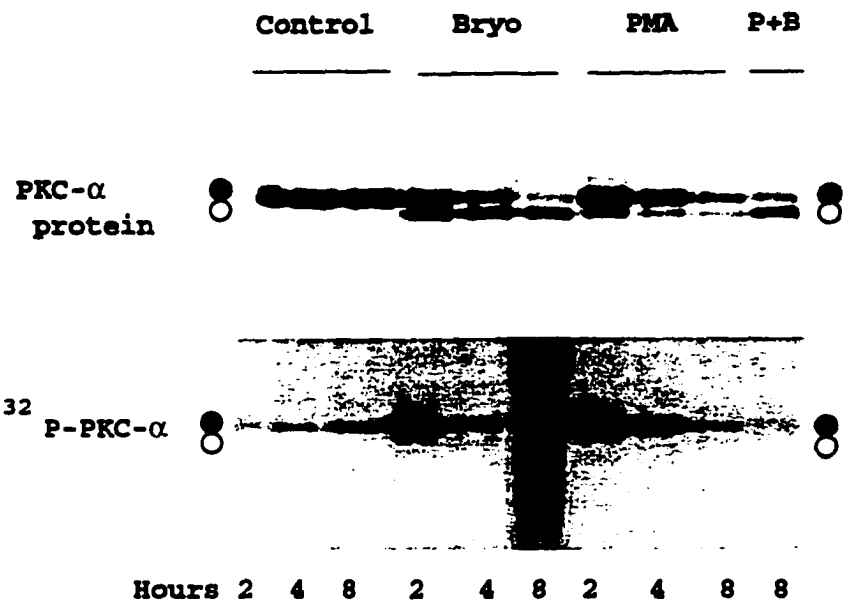

Figure 5. Autophosphorylation of PKC-α by Bryo and PMA and lack of ^{32}P in the 76 kDa form in renal epithelial cells. Cultures were incubated in serum- and phosphate-free DMEM with 1 mCi [^{32}P]orthophosphate for 3 h. One μM Bryo, 1 μM PMA, or both ("P+B") were added directly to the labeling medium and the incubation continued for 2, 4, or 8 h, as indicated. PKC-α was extracted, immunoprecipitated, fractionated by SDS-PAGE, and transferred to a membrane. After western analysis, the membrane was autoradiographed to detect ^{32}P. Filled and unfilled circles indicate 80- and 76-kDa PKC-α bands, respectively. The 8 h Bryo immunoprecipitate was contaminated with ^{32}P labeled material, which occurred occasionally, but another sample ("P+B", 8 h) had similar amounts of 80- and 76-kDa bands, as the 8 h Bryo sample and was not contaminated. Data are representative of three independent experiments.

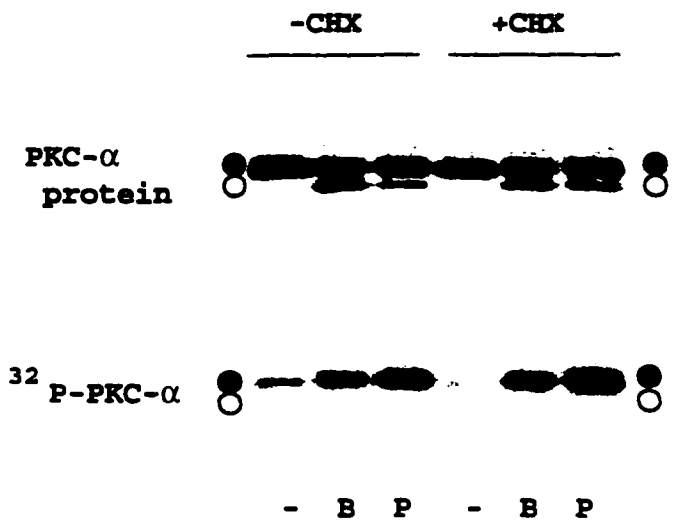

Figure 6. Production of 76 kDa PKC-α is independent of protein synthesis in renal epithelial cells. Cultures were incubated in serum- and phosphate-free DMEM with 1 mCi [^{32}P]orthophosphate for 3 h. One μM Bryo ("B"), 1 μM PMA ("P"), and 30 μg/ml cycloheximide ("CHX") were added directly to the labeling medium, as indicated, and the incubation continued for 4 h. PKC-α was extracted, immunoprecipitated, fractionated by SDS-PAGE, and transferred to a membrane. After western analysis, the membrane was autoradiographed to detect ^{32}P. Data are representative of three independent experiments. Filled and unfilled circles indicate 80- and 76-kDa PKC-α bands, respectively.

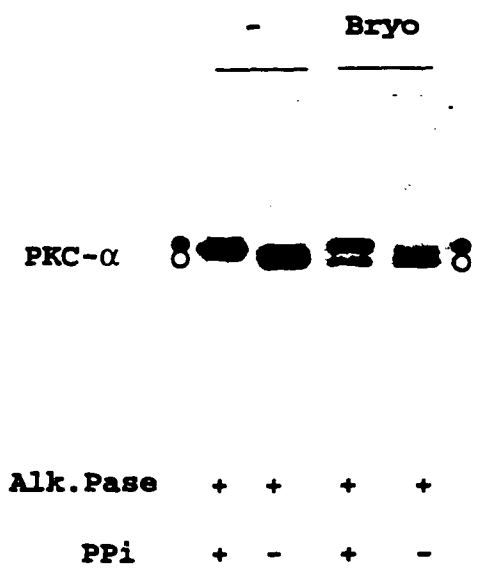

Figure 7. Effect of alkaline phosphatase on the electrophoretic mobility of PKC-α immunoprecipitated from renal epithelial cells treated with Bryo. Cultures were incubated in serum-free DMEM in the absence or presence of 1 μM Bryo for 4 h. PKC-α was extracted, immunoprecipitated, and incubated with alkaline phosphatase ("Alk.Pase") in the presence or absence of 10 mM sodium pyrophosphate ("PPi") for 2 h at 37°C, as described in "Methods and Materials." The reaction was stopped by rinsing the immunoprecipitates with 20 mM Tris-HCl, pH 7.5, and extraction with SDS. PKC-α bands were resolved by SDS-PAGE and visualized by western analysis. Three independent experiments gave similar results. Filled and unfilled circles indicate 80- and 76-kDa PKC-α bands, respectively.

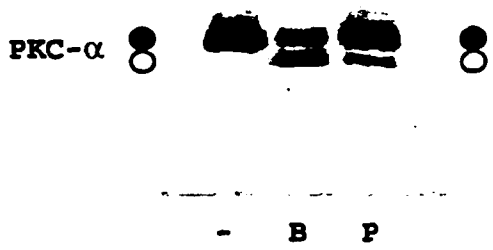

Figure 8. Production of the 76 kDa PKC-α and depletion of 80 kDa form by Bryo or PMA in human fibroblasts. Human fibroblasts were incubated with 1 μM Bryo or PMA for 6 h. PKC-α was extracted and immunoprecipitated from 0.5 mg protein. Immunoprecipitated proteins were separated by SDS-PAGE and visualized by western analysis. Filled and unfilled circles indicate 80- and 76-kDa PKC-α bands, respectively.

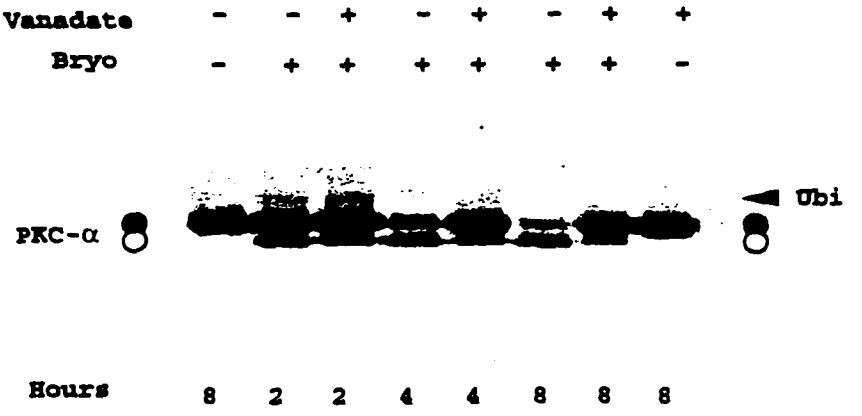

Figure 9. Effect of orthovanadate on Bryo-induced depletion of 80 kDa PKC-α and production of the 76 kDa form in human fibroblasts. Human fibroblasts were incubated with 5 mM orthovanadate for 1 h before adding 1 μM Bryo, as indicated. After the indicated interval, PKC-α was extracted and immunoprecipitated from 0.19 mg protein. Immunoprecipitated proteins were separated by SDS-PAGE and visualized by western analysis. Filled and unfilled circles indicate 80- and 76-kDa PKC-α bands, respectively. Arrowhead indicates the position of PKC-α band that has the same mobility as ubiquitinated PKC-α, as determined by immunostaining with ubiquitin antibody (See Fig. 16).

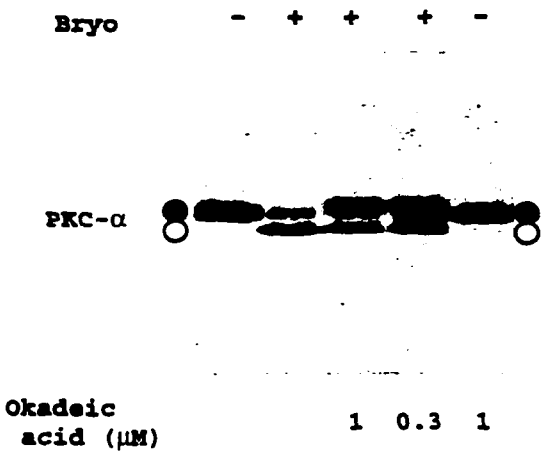

Figure 10. Effect of okadeic acid on Bryo-induced depletion of 80 kDa PKC-α and production of the 76 kDa form in human fibroblasts. Cultures were incubated with 0.3 or 1 μM okadeic acid for 1 h before adding 1 μM Bryo, as indicated. Twelve h later, PKC-α was extracted and immunoprecipitated from 0.16 mg protein. Immunoprecipitated proteins were separated by SDS-PAGE and visualized by western analysis. Filled and unfilled circles indicate 80- and 76-kDa PKC-α bands, respectively.

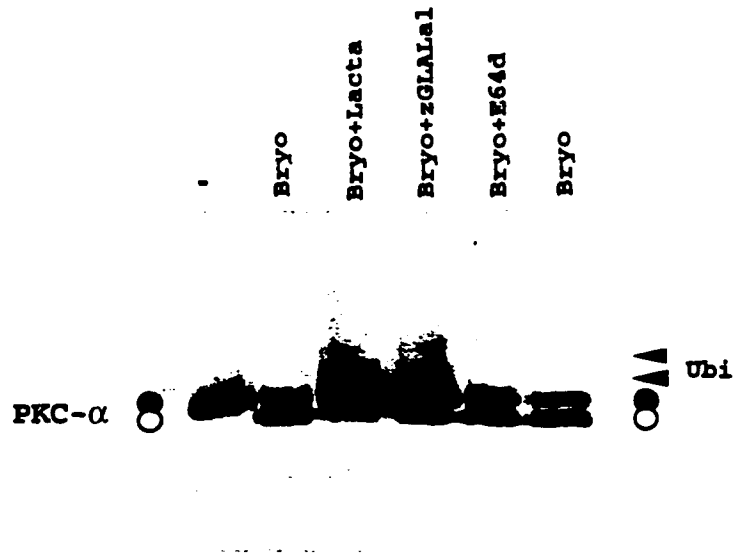

Figure 11. In vivo protection of PKC-α from degradation by proteasome inhibitors but not by a calpain inhibitor in human fibroblasts. Human fibroblasts were incubated with 50 μM Lacta, 50 μM BzGLAL-al, or 50 μM E64d for 1 h before adding 1 μM Bryo, as indicated. Eight h later, PKC-α was extracted and immunoprecipitated from 0.185 mg protein. Immunoprecipitated proteins were separated by SDS-PAGE and visualized by western analysis. Filled and unfilled circles indicate 80- and 76-kDa PKC-α bands, respectively. Arrowheads indicate the position of PKC-α bands that have the same mobility as ubiquitinated PKC-α, as determined by immunostaining with ubiquitin antibody (See Fig. 16).

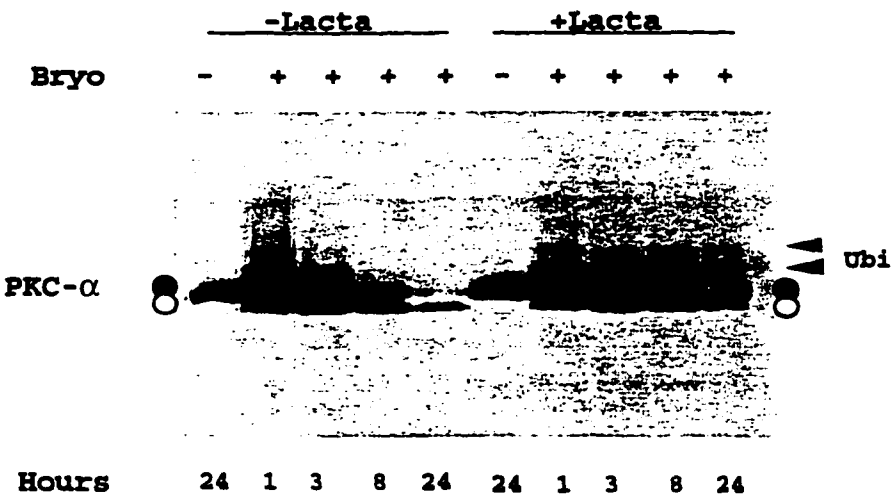

Figure 12. Effect of Lacta on Bryo-induced PKC-α degradation in human fibroblasts. Human fibroblasts were incubated with 50 μM Lacta for 1 h before adding 1 μM Bryo, as indicated. One to 20 h later, PKC-α was extracted and immunoprecipitated from 0.41 mg protein. Immunoprecipitated proteins were separated by SDS-PAGE and visualized by western analysis. Filled and unfilled circles indicate 80- and 76-kDa PKC-α bands, respectively. Arrowheads indicate the position of PKC-α bands that have the same mobility as ubiquitinated PKC-α, as determined by immunostaining with ubiquitin antibody (See Fig. 16).

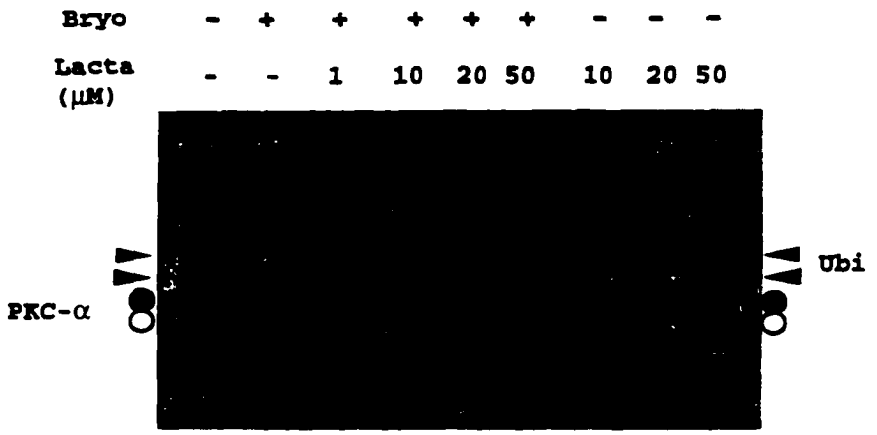

Figure 13. Concentration dependence of Lacta for the preservation of PKC-α in human fibroblasts. Human fibroblasts were incubated with the indicated concentration of Lacta for 1 h before adding 1 μM Bryo, as indicated. Eight h later, PKC-α was extracted and immunoprecipitated from 0.23 mg protein. Immunoprecipitated proteins were separated by SDS-PAGE and visualized by western analysis. Filled and unfilled circles indicate 80- and 76-kDa PKC-α bands, respectively. Arrowheads indicate the position of PKC-α bands that have the same mobility as ubiquitinated PKC-α, as determined by immunostaining with ubiquitin antibody (See Fig. 16).

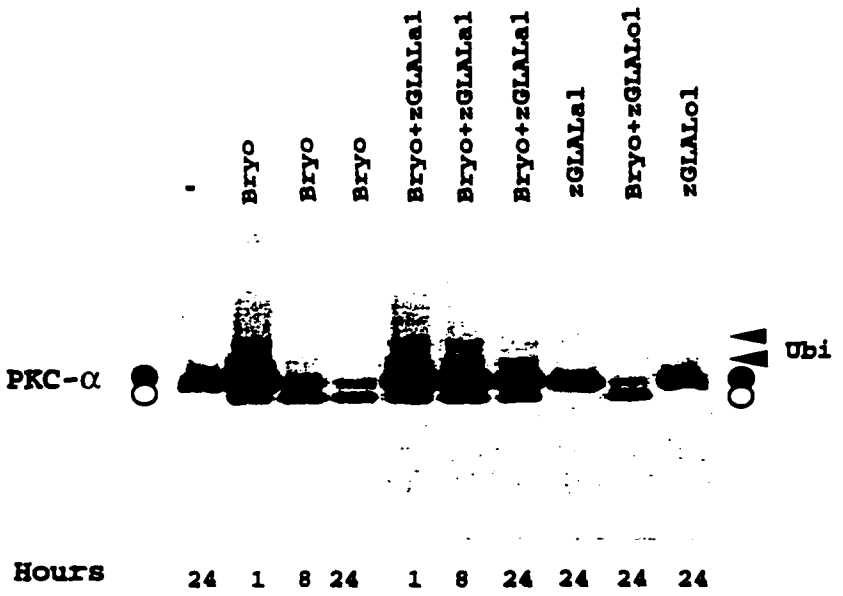

Figure 14. Effect of BzGLAL-al or BzGLAL-ol on Bryo-induced PKC-α degradation in human fibroblasts. Human fibroblasts were incubated with 50 μM BzGLAL-al or BzGLAL-ol for 1 h before adding 1 μM Bryo, as indicated. One to 20 h later, PKC-α was extracted and immunoprecipitated from 0.21 mg protein. Immunoprecipitated proteins were separated by SDS-PAGE and visualized by western analysis. Filled and unfilled circles indicate 80- and 76-kDa PKC-α bands, respectively. Arrowheads indicate the position of PKC-α bands that have the same mobility as ubiquitinated PKC-α, as determined by immunostaining with ubiquitin antibody (See Fig. 16).

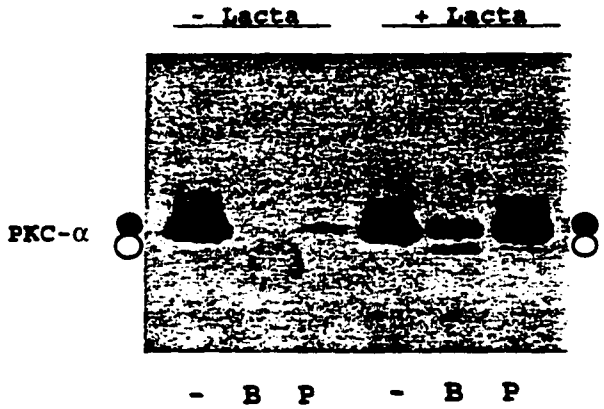

Figure 15. Inhibition of Bryo- or PMA-induced PKC-α degradation by Lacta in human fibroblasts. Human fibroblasts were incubated with 50 μM Lacta for 1 h before adding 0.05 μM Bryo or PMA, as indicated. Forty h later, PKC-α was extracted and immunoprecipitated from 0.25 mg protein. Immunoprecipitated proteins were separated by SDS-PAGE and visualized by western analysis. Filled and unfilled circles indicate 80- and 76-kDa PKC-α bands, respectively.

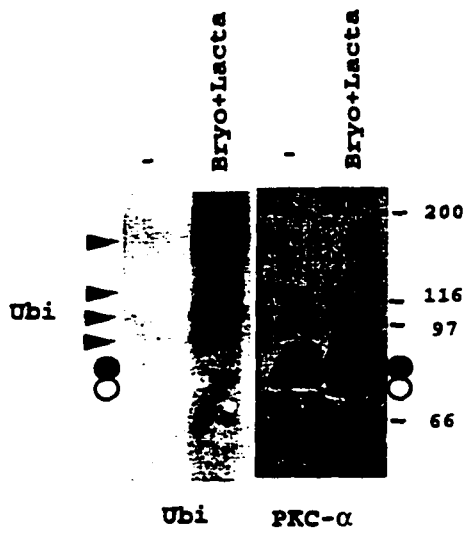

Figure 16. Ubiquitination of >80 kDa PKC-α immunoprecipitated from human fibroblasts treated with Bryo plus Lacta. Cultures were incubated in the presence or absence of 50 μM Lacta for 1 h before adding 1 μM Bryo (Lacta + Bryo). Twelve h later, the cultures were extracted with lysis buffer. PKC-α was immunoprecipitated from 2 mg lysate protein with 10 μg of antibody. Proteins were separated by SDS-PAGE and transferred to a nitrocellulose membrane, and ubiquitin ("Ubi") was detected with the 4F3 monoclonal antibody. Molecular weight markers are indicated in kDa. PKC-α bands were immunostained after detection of ubiquitinated proteins. Filled and unfilled circles indicate 80- and 76-kDa PKC-α bands, respectively. Arrowheads indicate the positions of ubiquitinated PKC-α bands.

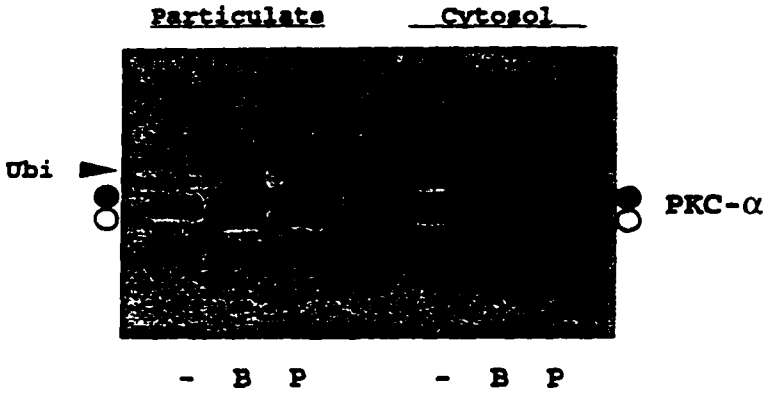

Figure 17. Localization of 76 kDa and >80 kDa PKC-α in the particulate fraction from human fibroblasts. Human fibroblasts were incubated with 1 μM Bryo or PMA for 6 h. Cytosol and particulate fractions were prepared. PKC-α was extracted and immunoprecipitated from same amount of protein (0.12 mg) in each fraction. Immunoprecipitated proteins were separated by SDS-PAGE and visualized by western analysis. Filled and unfilled circles indicate 80- and 76-kDa PKC-α bands, respectively. Arrowhead indicates the position of PKC-α band that has the same mobility as ubiquitinated PKC-α, as determined by immunostaining with ubiquitin antibody (See Fig. 16).

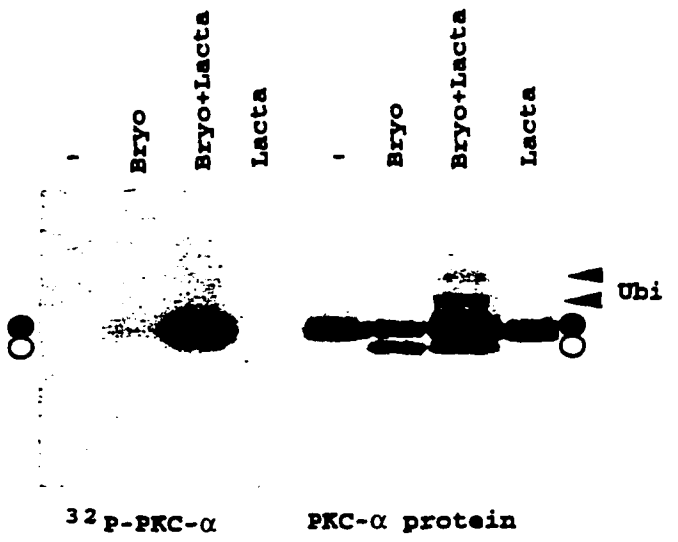

Figure 18. Preservation of Bryo-evoked ^{32}P-labeled PKC-α by Lacta in human fibroblasts. Cultures were incubated in phosphate-free DMEM with 1 mCi [^{32}P]orthophosphate for 2 h before adding 50 μM Lacta. One h later, 1 μM Bryo was added, and the incubation continued for 8 h. PKC-α was extracted and immunoprecipitated from 0.24 mg protein with 5 μg of antibody. Proteins were separated by SDS-PAGE and transferred to a membrane. After western analysis of PKC-α, the membrane was autoradiographed to detect ^{32}P. Filled and unfilled circles indicate 80- and 76-kDa PKC-α bands, respectively. Arrowheads indicate the position of PKC-α bands that have the same mobility as ubiquitinated PKC-α, as determined by immunostaining with ubiquitin antibody (See Fig. 16).

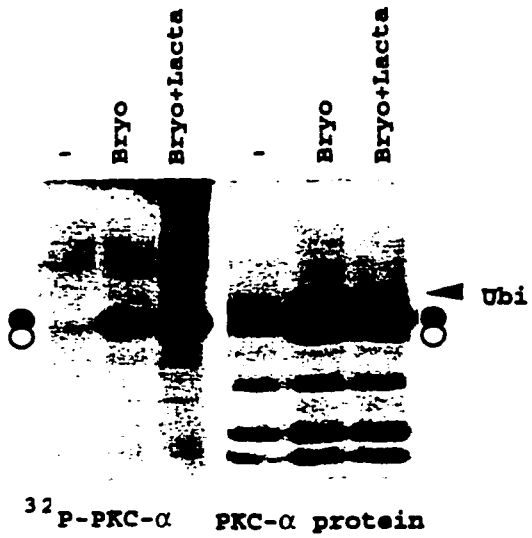

Figure 19. Lack of detectable ^{32}P in monoubiquitinated PKC-α from human fibroblasts. Cultures were incubated in phosphate-free DMEM with 1 mCi [^{32}P]orthophosphate for 2 h, and 20 μM Lacta was added, as indicated. One h later, 1 μM Bryo was added to the labeling medium, as indicated. After an additional 1 h, the cultures were extracted with Triton X-100, and PKC-α was immunoprecipitated from 1 mg protein with 10 μg of antibody. After immunoprecitation of PKC-α, immunocomplexes were washed 7 times with ice-cold lysis buffer and then once with ice-cold water. This may cause degradation of PKC-α during the washing in this particular experiment. Proteins were separated by SDS-PAGE and transferred to a membrane. After western analysis of PKC-α, the membrane was autoradiographed to detect ^{32}P. Filled and unfilled circles indicate 80- and 76-kDa PKC-α bands, respectively. Arrowhead indicates the position of PKC-α band that has the same mobility as ubiquitinated PKC-α, as determined by immunostaining with ubiquitin antibody (See Fig. 16).

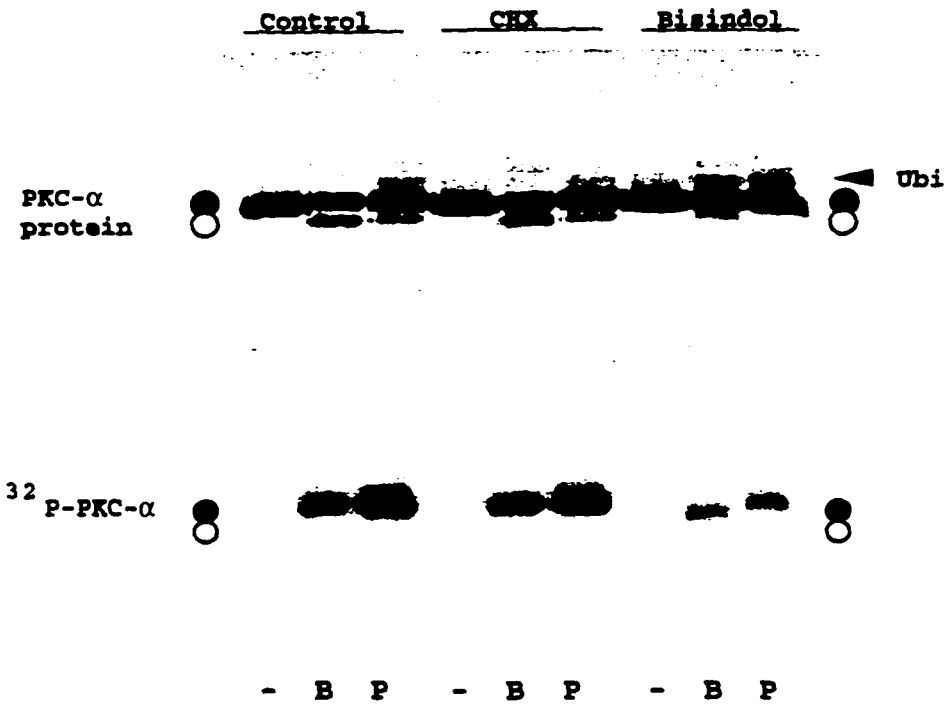

Figure 20. Lack of detectable ^{32}P in 76 kDa PKC-α produced by PMA or Bryo in the presence or absence of cycloheximide or bisindolylmaleimide in human fibroblasts. Cultures were incubated in phosphate-free DMEM with 1 mCi [^{32}P]orthophosphate for 3 h. One μM Bryo ("B"), 1 μM PMA ("P"), 2 μM bisindolylmaleimide ("Bisindol"), and 30 μg/ml cycloheximide ("CHX") were added directly to the labeling medium, as indicated, and the incubation continued for 6 h. PKC-α was extracted and immunoprecipitated from 0.5 mg protein. Proteins were separated by SDS-PAGE and transferred to a membrane. After western analysis of PKC-α, the membrane was autoradiographed to detect ^{32}P. Arrowhead indicates the position of PKC-α band that has the same mobility as ubiquitinated PKC-α, as determined by immunostaining with ubiquitin antibody (See Fig. 16).

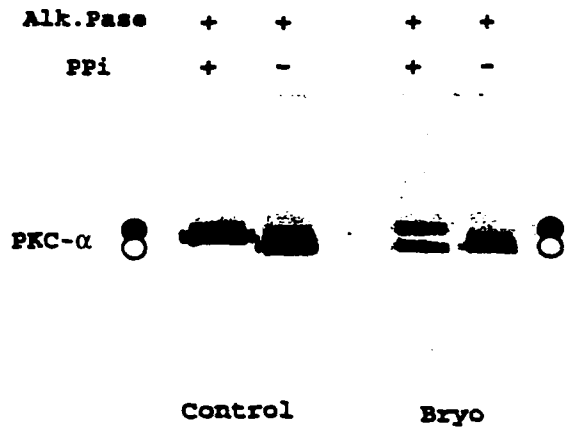

Figure 21. Effect of alkaline phosphatase on the electrophoretic mobility of PKC-α immunoprecipitated from human fibroblasts treated with Bryo. Cultures were incubated in DMEM containing 10% FBS in the absence or presence of 1 μM Bryo for 6 h. PKC-α was extracted, immunoprecipitated from 0.25 mg protein, and incubated with alkaline phosphatase ("Alk.Pase") in the presence or absence of 10 mM sodium pyrophosphate ("PP_i") for 2 h at 37°C, as described in "Methods and Materials." The reaction was stopped by rinsing the immunoprecipitates with 20 mM Tris-HCl, pH 7.5, and extraction with SDS. Proteins were resolved by SDS-PAGE and visualized by western analysis. Filled and unfilled circles indicate 80- and 76-kDa PKC-α bands, respectively.

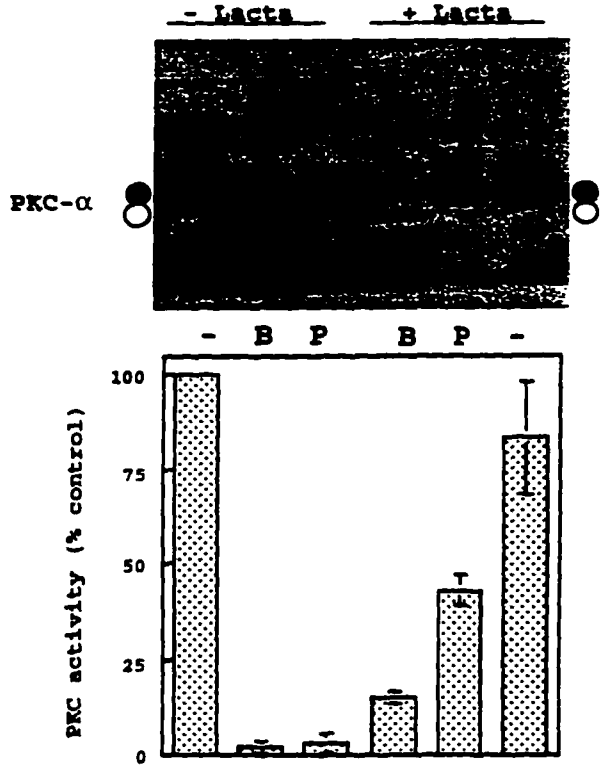

Figure 22. Lacta protects PKC-α protein and PKC activity from degradation evoked by Bryo or PMA in human fibroblasts. The indicated cultures were incubated with 20 μM Lacta for 1 h before adding 50 nM Bryo or 0.1 μM PMA. After 20 h, PKC was extracted with Triton X-100 and partially purified by DEAE-cellulose chromatography. Fractions were assayed for PKC activity. Proteins (6 μg) of the first fraction, which contained most of the activity, were separated by SDS-PAGE and subjected to western analysis of PKC-α. PKC activities are the total activity divided by total protein eluted from the DEAE cellulose column and are the mean ± S.E. (n = 3). PKC activity was 4-5 nmol phosphate incorporated (μg protein x 10 min)$^{-1}$ in the first fraction from control cells. None of the treatments significantly affected the amount of protein that was applied or eluted from the column. Filled and unfilled circles indicate 80- and 76-kDa PKC-α bands, respectively.

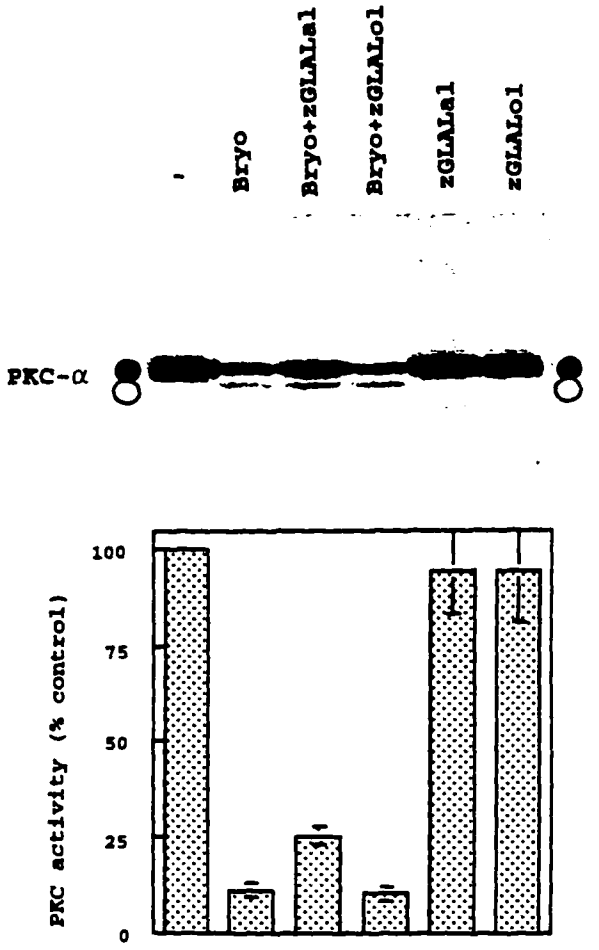

Figure 23. BzGLAL-al protects PKC-α protein and PKC activity from Bryo- or PMA-induced degradation in human fibroblasts. Cultures were incubated with 50 μM zGLAL-al or zGLAL-ol, as indicated, and, after 2 h, 1 μM Bryo was added. Three h later, PKC was extracted with Triton X-100 and partially purified by DEAE-cellulose chromatography. Fractions were assayed for PKC activity. Proteins (10 μg) of the first fraction, which contained most of the activity, were separated by SDS-PAGE and subjected to western analysis of PKC-α. PKC activities are the total activity divided by total protein eluted from the DEAE cellulose column and are the mean ± S.E. (n = 3). PKC activity was 4-5 nmol phosphate incorporated (μg protein x 10 min)$^{-1}$ in the first fraction from control cells. None of the treatments significantly affected the amount of protein that was applied or eluted from the column. Filled and unfilled circles indicate 80- and 76-kDa PKC-α bands, respectively.

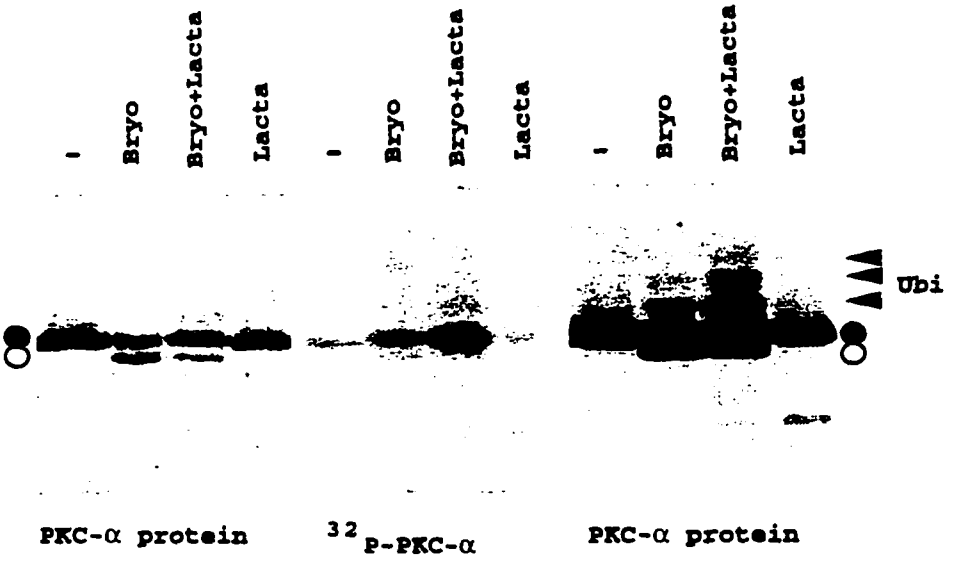

Figure 24. Preservation of Bryo-evoked ^{32}P-labeled PKC-α by Lacta in renal epithelial cells. Cultures were incubated in phosphate-free DMEM with 1 mCi [^{32}P]orthophosphate for 3 h. Fifty μM Lacta were present during the last 1 h of the labeling. One μM Bryo was added directly to the labeling medium, as indicated, and the incubation continued for 8 h. PKC-α proteins were extracted, immunoprecipitated with 2.5 μg antibody, separated by SDS-PAGE, and transferred to a PVDF membrane. The left and right panels show western analysis of PKC-α immunoprecipitated from 0.03 and 0.5 mg cell lysate, respectively. The middle panel is the ^{32}P autoradiogram of the right panel. The ^{32}P autoradiogram of the left panel (not shown) detected a similar increase in ^{32}P-labeled PKC-α, as in the middle panel. Filled and unfilled circles indicate 80- and 76-kDa PKC-α bands, respectively. Arrowheads indicate the position of PKC-α bands that have the same mobility as ubiquitinated PKC-α, as determined by immunostaining with ubiquitin antibody (See Fig. 25).

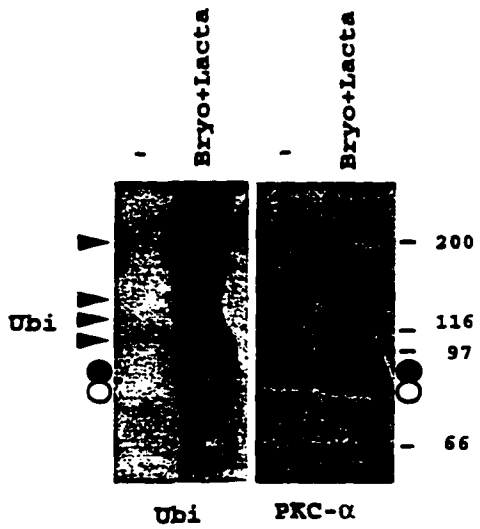

Figure 25. Demonstration of ubiquitinated PKC-α in renal epithelial cells treated with Bryo plus Lacta. The indicated cultures were incubated with 50 μM Lacta for 1 h before adding 1 μM Bryo. Twelve h later, the cultures were extracted, and PKC-α was immunoprecipitated from 2 mg lysate protein with 10 μg of antibody. Immunoprecipitates were fractionated by SDS-PAGE and transferred to a nitrocellulose membrane, and ubiquitin was detected with the 4F3 monoclonal antibody (Ubi). PKC-α bands were immunostained after detection of ubiquitinated proteins. Filled and unfilled circles indicate 80- and 76-kDa PKC-α bands, respectively. Arrowheads indicate the positions of ubiquitinated PKC-α bands.

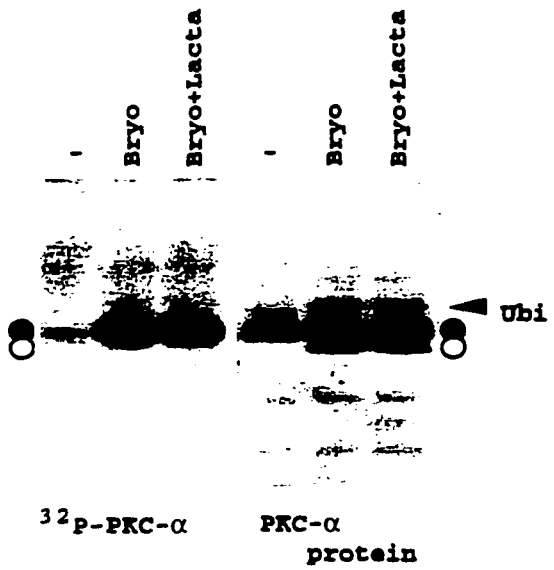

Figure 26. Lack of detectable ^{32}P in monoubiquitinated PKC-α in renal epithelial cells. Cultures were incubated in phosphate-free DMEM with 1 mCi [^{32}P]orthophosphate for 2 h before adding Lacta to 20 μM, as indicated. One h later, Bryo was added to the labeling medium to 1 μM, as indicated. After an additional 1 h, PKC-α was extracted with Triton X-100 and immunoprecipitated from 1 mg protein with 10 μg of antibody. Proteins were separated by SDS-PAGE and transferred to a PVDF membrane. After western analysis of PKC-α, the membrane was autoradiographed to detect ^{32}P. Filled and unfilled circles indicate 80- and 76-kDa PKC-α bands, respectively. Arrowhead indicates the position of PKC-α band that has the same mobility as ubiquitinated PKC-α, as determined by immunostaining with ubiquitin antibody (See Fig. 25).

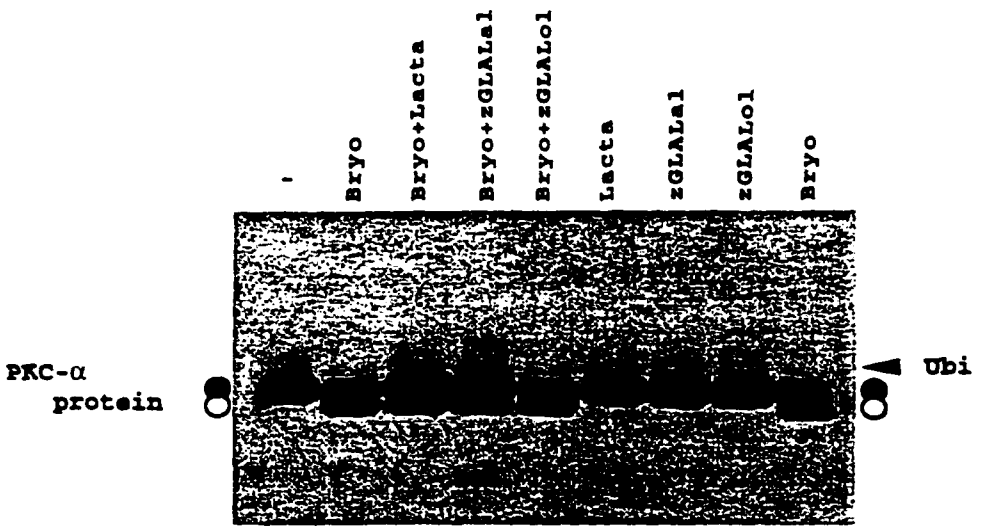

Figure 27. In vivo protection of PKC-α from degradation by proteasome inhibitors in renal epithelial cells. Cultures were incubated with 50 μM Lacta and 50 μM zGLALal or zGLALol, as indicated, for 1 h. One μM Bryo was added, as indicated, and the incubation continued for 8 h. PKC-α was extracted, immunoprecipitated, fractionated by SDS-PAGE, and visualized by western analysis. Blots are representative of at least three experiments. Filled and unfilled circles indicate 80- and 76-kDa PKC-α bands, respectively. Arrowhead indicates the position of PKC-α band that has the same mobility as ubiquitinated PKC-α, as determined by immunostaining with ubiquitin antibody (See Fig. 25).

Figure 28. Lacta preserves PKC activity and PKC-α protein in renal epithelial cells treated with Bryo or PMA. The indicated cultures were incubated with 20 μM Lacta for 1 h before adding Bryo or PMA, as indicated, for 4 or 20 h for panels A and B, respectively. Bryo was 1 or 0.1 μM in panels A and B, respectively, and PMA was 0.2 μM (panel B). PKC was extracted with Triton X-100 and purified by DEAE cellulose chromatography. Fractions were assayed for PKC activity and subjected to western analysis with a PKC-α specific antibody (insets).PKC activities are the total activity divided by total protein eluted from the DEAE cellulose column. None of the treatments significantly affected the amount of protein that was applied or eluted from the column. Values are mean ± SE, n = 4 (panel A), and n = 3 (panel B). Filled and unfilled circles indicate 80- and 76-kDa PKC-α bands, respectively.

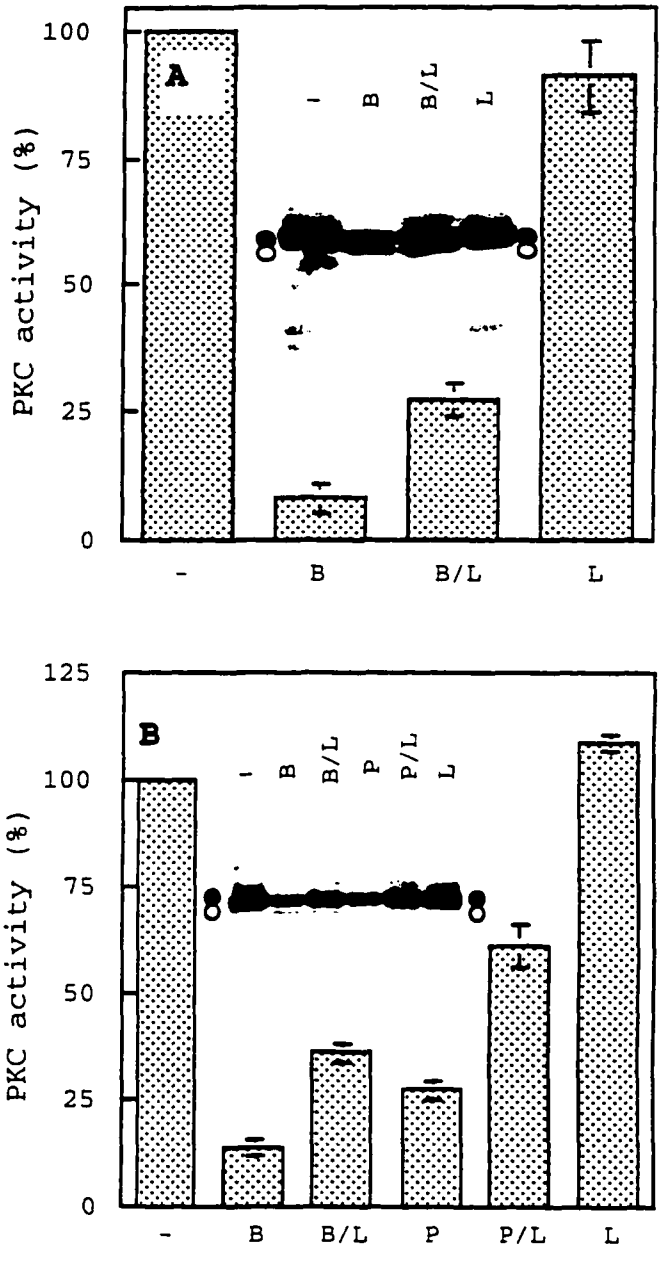

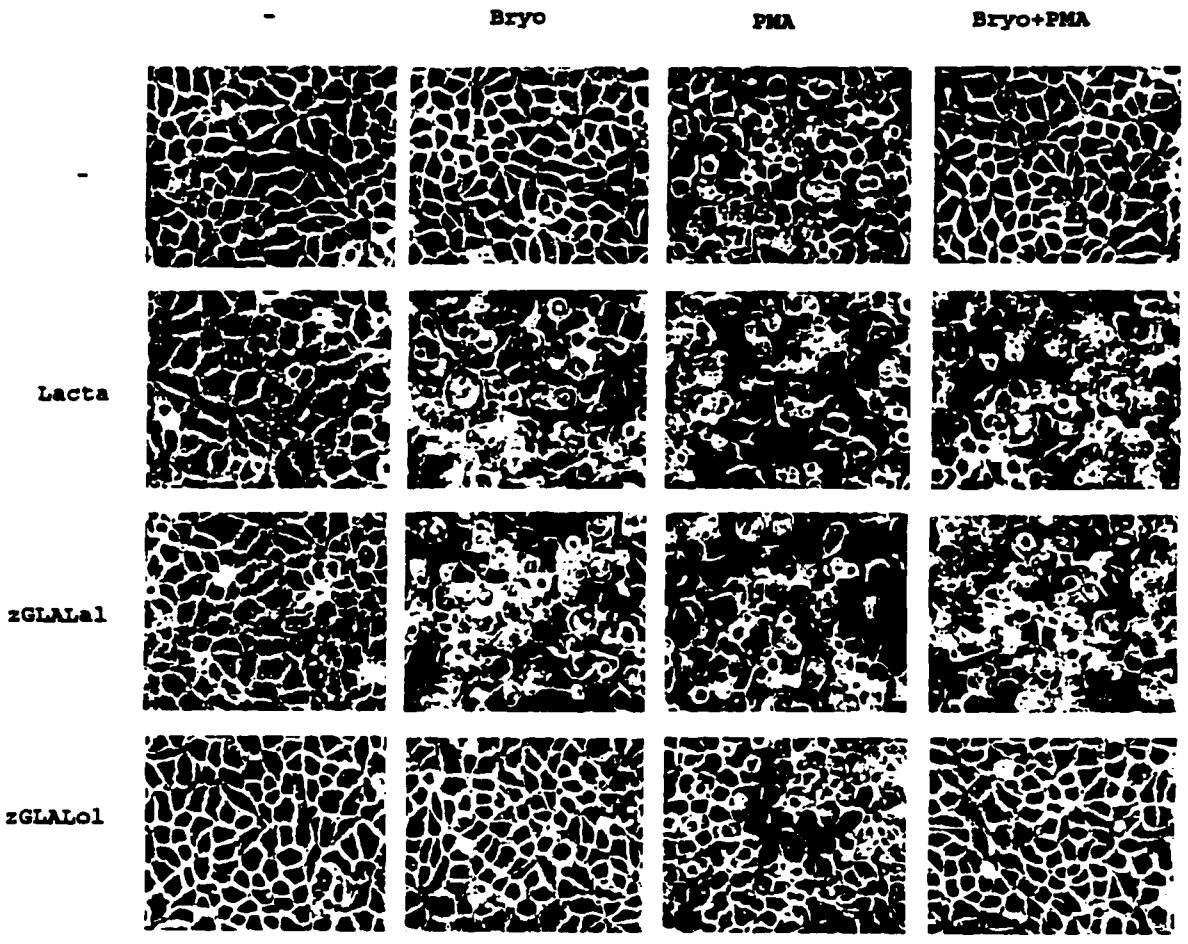

Figure 29. Effects of Bryo, PMA, Lacta, zGLAL-al, and zGLAL-ol on the morphology of renal epithelial cells. Confluent cultures were incubated for 1 h in plating medium with 10 μM Lacta or 50 μM zGLALal or zGLALol, as indicated. Bryo or PMA or both were added to 0.1 μM and the incubation continued for 23 h. Cells were photographed by phase-contrast microscopy.

LIST OF REFERENCES

Ahmed, Q., Marnyama, I. N., Kozma, R., Lee, J., Brenner, S., and Lim, L. (1992). The *Caenorhabditis elegans* unc-13 gene product is a phospholipid-dependent high affinity phorbol ester receptor. Biochem. J. *2870*, 955-999.

Areces, L. B., Kazanietz, M. G., and Blumberg, P. M. (1994). Close similarity of Baculovirus-expressed *n*-chimaerin and protein kinase Cα as phorbol ester receptors. J. Biol. Chem. *269*, 19553-19558.

Asaka, Y., Nakamura, S.-I., Yoshida, K., and Nishizuka, Y. (1992). Protein kinase C, calcium and phospholipid degradation. Trends Biochem. Sci. *17*, 414-417.

Bazzi, M. D., and Nelsestuen, G. L. (1989). Differences in the effects of phorbol esters and diacylglycerols on protein kinase C. Biochemistry *29*, 7624-97630.

Bell, R. M. (1986). Protein kinase C activation by diacylglycerol second messengers. Cell *45*, 631-632.

Bell, R. M., and Burns, D. J. (1991). Lipid activation of protein kinase C. J. Biol. Chem. *266*, 4661-4664.

Bell, R. M., Hannun, Y., and Loomis, C. (1986). Mixed micelle assay of protein kinase C. Methods in Enzymol. *124*, 353-359.

Borner, C., Filipuzzi, I., Wartmann, M., Effenberger, U., and Fabbro, D. (1989). Biosynthesis and posttranslational modifications of protein kinase C in human breast cancer cells. J. Biol. Chem. *264*, 13902-13909.

Boscá, L., and Morán, F. (1993). Circular dichroism analysis of ligand-induced conformational changes in protein kinase C. Biochem. J. *290*, 827-832.

Brown, K., Gerstberger, S., Carlson, L., Franzoso, G., and Siebenlist, U. (1995). Control of IκB-α proteolysis by site-specific, signal-induced phosphorylation. Science *267*, 1485-1488.

Cary, P. D., King, D. S., Crane-Robinson, C., Bradbury, E. M., and Rabbini, L. (1980). Structural studies on two high mobility-group proteins from calf thymus, HMG-14 and HMG-20 (ubiquitin), and their interaction with DNA. Eur. J. Biochem. *112*, 577-580.

Castagua, M., Takai, Y., Kabuchi, K., Sano, A., Kikkawa, U., and Nishizuka, Y. (1982). Direct activation of calcium-activated, phospholipid-dependent protein kinase by tumor-promoting phorbol esters. J. Biol. Chem. *257*, 7847-7851.

Cazaubon, S., Bornancin, F., and Parker, P. J. (1994). Threonine-497 is a critical site for permissive activation of protein kinase Cα. Biochem. J. *301*, 443-448.

Cazaubon, S. M., and Parker, P. J. (1993). Identification of the phosphorylated region responsible for the permissive activation of protein kinase C. J. Biol. Chem. *268*, 17559-17563.

Ciechanover, A. (1994). The ubiquitin-proteasome proteolytic pathway. Cell *79*, 13-21.

Cook, W. J., Jeffery, L. C., Kasperek, E., and Pickart, C. M. (1994). Structure of tetraubiquitin shows how multiubiquitin chains can be formed. J. Mol. Biol. *236*, 601-609.

Cook, W. J., Jeffery, L. C., Sullivan, M. L., and Viesta, R. D. (1992). Three-dimensional structure of a ubiquitin-conjugating enzyme (E2). J. Biol. Chem. *267*, 15116-15121.

Coris, D., Galluzzi, L., Crinelli, R., and Magnani, M. (1995). Ubiquitin is conjugated to the cytoskeletal protein α-spectrin in mature erythrocytes. J. Biol. Chem. *270*, 8928-8935.

Deverany, Q., Ustrell, V., Pickart, C., and Rechsteiner, M. (1994). A 26S protease subunit that binds ubiquitin conjugates. J. Biol. Chem. *269*, 7059-7061.

de Vries, D. J., Herald, C. L., Pettit, G. R., and Blumberg, P. M. (1988). Demonstration of sub-nanomolar affinity

of bryostatin 1 for the phorbol ester receptor in rat brain. Biochem. Pharmacol. *37*, 4069-4073.

Dunphy, W. G., Kochenburger, R. J., Castagna, M., and Blumberg, P. M. (1981). Kinetics and subcellular localization of specific [^{3}H]phorbol 12,13-dibutyrate binding in mouse brain. Cancer Res. *41*, 2640-2647.

Dutil, E., Keranen, M., DePaoli-Roach, A. A., and Newton, A. C. (1994). In vivo regulation of protein kinase C by trans-phosphorylation followed by autophosphorylation. J. Biol. Chem. *269*, 29359-29362.

Fenteany, G., Standaert, R. F., Lane, W. S., Choi, S., Corey, E. J., and Schreiber, S. L. (1995). Inhibition of proteasome activities and subunit specific-amino terminal threonine modification by lactacystin. Science *268*, 726-731.

Fenteany, G., Standaert, R. F., Reichard, G. A., Corey, E.J., and Schreiber, S.L. (1994). A β-lactone related to lactacystin induces neurite outgrowth in a neuroblastoma cell line and inhibits cell cycle progression in an osteosarcoma cell line. Proc. Natl. Acad. Sci. USA *91*, 3358-3362.

Flint, A. J., Paladini, R. D., and Koshland, Jr. D. E. (1990). Autophosphorylation of protein kinase C at three separated regions of its primary sequence. Science *294*, 408-411.

Goldberg, A. L. (1995). Functions of the proteasome: The lysis at the end of the tunnel. Science *268*, 522-523.

Goode, N. T., Nasser Hajibagheri, M. A., and Parker, P. J. (1995). Protein Kinase C (PKC)-induced PKC downregulation. Association with up-regulation of vesicle traffic. J. Biol. Chem. *270*, 2669-2673.

Gosink, M., and Vierstra, R. (1995). Redirecting the specificity of ubiquitination by modifying ubiquitin-conjugation enzymes. Proc. Natl. Acad. Sci. USA *92*, 9117-9121.

Guarino, L. A., Smith, G., and Dong, W. (1995). Ubiquitin is attached to membranes of baculovirus particles by a novel type of phospholipid anchor. Cell *80*, 301-309.

Hass, A. L., Bright, P. M., and Jackson, V. E. (1988). Functional diversity among putative E2 isozymes in the mechanism of ubiquitin-histone ligation. J. Biol. Chem. *263*, 13258-13267.

Hennings, H., Blumberg, P. M., Pettit, G. R., Herald, C. L., Shores, R., and Yupsa, S. H. (1987). Bryostatin 1, an activator of protein kinase C, inhibits tumor promotion by phorbol esters in SENCAR mouse skin. Carcinogenesis *8*, 1343-1346.

Hocevar, B. A., and Fields, A. P.(1991). Selective translocation of beta II-protein kinase C to the nucleus of human promyelocytic (HL60) leukemia cells. J. Biol. Chem. *266*, 28-33.

Hochstrasser, M. (1995). Ubiquitin, proteasomes, and regulation of intracellular protein degradation. Cur. Opin. Cell Biol. *7*, 215-223.

Hochstrasser, M., and Papa, F. R. (1993). The yeast DOA4 gene encodes a deubiquitinating enzyme related to a product of the human tre-2 oncogene. Nature *366*, 313-319.

House, C., and Kemp, B. E. (1987). Protein kinase C contains a pseudosubstrate prototype in its regulatory domain. Science *238*, 1726-1728.

House, C., Robinson, P. J., and Kemp, B. E. (1989). A synthetic peptide of the putative substrate-binding motif activates protein kinase C. FEBS Lett. *249*, 243-247.

Huang, K.-P., Chan, K. F., Singh, T. J., Nakabayashi, H., and Huang, F. L. (1986). Autophosphorylation of rat brain Ca^{2+}-activated and phospholipids-dependent protein kinase. J. Biol. Chem. 261, 12134-12140.

Hug, H., and Sarre, T. (1993). Protein Kinase C isoenzymes: divergence in signal transduction. Biochem. J. *291*, 329-343.

Huwiler, A. D., Fabbro, D., and Pfeilschifter, J. (1994). Comparison of different tumor promotors and bryostatin 1 on protein kinase C activation and down-regulation in rat renal mesangial cells. Biochem. Pharmacol. *48*, 689-700.

Inoue, M., Kishimoto, A., Takai, Y., and Nishizuka, Y. (1977). Studies on a cyclic nucleotide-independent protein kinase and its proenzyme in mammalian tissues II. J. Biol. Chem. *252*, 7610-7616.

Isakov, N., Galron, D., Mustelin, T., Pettit, G. R., and Altman, A. (1993). Inhibition of phorbol ester-induced

T-cell proliferation by bryostatin is associated with rapid degradation of protein kinase C. J. Immunol. *150*, 1195-1204.

Jalava, A., Lintunen, M., and Heikkila, J. (1993). Protein kinase C-α but not protein kinase C-ε is differentially down-regulated by bryostatin 1 and tetradecanoyl phorbol 13-acetate in SH-SY5Y human neuroblastoma cells. Biochem. Biophys. Res. Comm. *191*, 472-478.

Jentsch, S. (1992). The ubiquitin-conjugation system. Annu. Rev. Genet. *26*, 179-207.

Junco, M., Webster, C., Crawford, C., Bosca, L., and Parker, P. J. (1994). Protein kinase C V3 domain mutants with differential sensitivities to m-calpain are not resistant to phorbol-ester-induced down-regulation. Eur. J. Biochem. *223*, 259-263.

Kazanietz, M. G., Lewin, N. E., Gao, F.,Pettit, G. R., and Blumberg, P. M. (1994). Binding of [26-^{3}H]bryostatin 1 and analogs to calcium-dependent and calcium-independent protein kinase C isozymes. Mol. Pharm. *46*, 374-379.

Kishimoto, A., Mikawa, K., Hashimoto, K., Yasuda, I., Tanaka, S. -I., Tominaga, M., Kuroda, T., and Nishizuka, Y. (1989). Limited proteolysis of protein kinase C by calcium-dependent neutral protease (calpain). J. Biol. Chem. *204*, 4088-4092.

Kraft, A. S., Smith, J. B., and Berkow, R. L. (1986). Bryostatin, an activator of the calcium phospholipid-dependent protein kinase, blocks phorbol ester-induced differentiation of human promyelocytic leukemia cells. Proc. Natl. Acad. Sci. USA *83*, 1334-1338.

Laemmli, U. K. (1970). Cleavage of structural proteins during the assembly of the head group bacteriophage T4. Nature Lond. *227*, 680-685.

Lahav-Baratz, S., Sudakin, V., Ruderman, J. V., and Hershko, A. (1995). Reversible phosphorylation controls the activity of cyclosome-associated cyclin-ubiquitin ligase. Proc. Natl. Acad. Sci. USA *92*, 9303-9307.

Lester, D. S., Doll, L., Brumfeld, V., and Miller, I. R. (1990). Lipid-dependence of surface conformations of protein kinase C. Biochim. Biophys. Acta *1039*, 33-41.

Lewin, N. E., Dell'Aquila, M. L., Pettit, G. R., Blumberg, P. M., and Warren, B. S. (1992). Binding of

[^{3}H]bryostatin 4 to protein kinase C. Biochem. Pharmacol. *43*, 2007-2014.

Lin, W. -C., and Desiderio, S. (1993). Regulation of V(D)J recombination activator protein RAG-2 by phosphorylation. Science *260*, 953-959.

Löwe, J., Stock, D., Jap, B., Zwickl, P., Baumeister, W., and Huber, P. (1995). Crystal structure of the 20S proteasome from the archaeron *T. acidophilum* at 3.4 Å resolution. Science *268*, 533-539.

Lyu, R. -M., Smith, L., and Smith, J. B. (1987). Sodium-calcium exchange in renal epithelial cells: Dependence on cell sodium and competitive inhibition by magnesium. J. Membr. Biol. *124*, 73-83.

Ma, C. -P., Vu, J. H., Proske, R. J., Slaughter, C. A., and DeMartino, G. N. (1994). Identification, purification, and characterization of a high molecular weight, ATP-dependent activator (PA700) of the 20S proteasome. J. Biol. Chem. *269*, 3539-3547.

Mahoney, C. W., and Huang, K. -P. (1994). Molecular and catalytic properties of protein kinase C. In: Protein Kinase C, edited by Kuo, J. F. New York: Oxford University Press, pp16-63.

McGrath, J. P., Jentsch, S., and Varshavsky, A. (1991) UBA 1: an essential yeast gene encoding ubiquitinating-activating enzyme. EMBO J. 10, 227-236.

McPhail, L. C., Clyton, C. C., and Snyderman, R. (1984). A potential second messenger role for unsaturated fatty acids: Activation of Ca^{2+}-dependent protein kinase C. Science *224*, 622-625.

Mochly-Rosen, D., Khaner, H., Lopez, J., and Smith, B. L. (1991). Intracellular receptors for activated protein kinase C. Identification of a binding site for the enzyme. J. Biol. Chem. *266*, 14866-14868.

Murakami, K., Chan, S. Y., and Routtenberg, A. (1986). Protein kinase activation by *cis*-fatty acid in the absence of calcium and phospholipids. J. Biol. Chem. *261*, 15424-15429.

Murakami, Y., Matsufuji, S., Kameji, T., Hayashi, S.-I., Igarash, K., Tamura, T., Tanaka, K., and Ichihara, A. (1992). Ornithine decarboxylase is degraded by the 26S proteasome without ubiquitination. Nature *360*, 597-599.

Nelsestuen, G. L., and Bassi, M. D. (1991). Activation and regulation of protein kinase C enzymes. J. Bioenerget. Biomembr. *23*, 43-61.

Newton, A. C. (1993). Interaction of proteins with lipid headgroups: lessons from protein kinase C. Annu. Rev. Biophys. Biomol. Struct. *22*, 1-25.

Newton, A. C. (1995a). Protein kinase C: Structure, function, and regulation. J. Biol. Chem. *270*, 28495-28498.

Newton, A. C. (1995b). Protein kinase C. Seeing two domains. Curr. Biol. *5*, 973-976.

Nishizuka, Y. (1992). Intracellular signalling by hydrolysis of phospholipids and activation of protein kinase C. Science *258*, 607-614.

Nishizuka, Y. (1995). Protein kinase C and lipid signaling for sustained cellular responses. FASEB J. *9*, 484-496.

Nishizawa, M., Furuno, N., Okazaki, K., Tanaka, H., Ogawa, Y., and Segata, N. (1993). Degradation of Mos by the N-terminal proline (Pro^2)-dependent ubiquitin pathway on fertilization of *Xenopus* eggs: possible significance of natural selection for Pro^2 in Mos. EMBO J. *12*, 4021-4027.

Ohno, S., Konno, Y., Akita, Y., Yano, A., and Suzuki, K. (1990). A point mutation at the putative ATP-binding site of protein kinase Cα abolishes the kinase activity and renders it downregulation-insensitive. J. Biol. Chem. *265*, 6296-6230.

Omura, S., Matsuzaki, K., Fujimoto, T., Kosuge, K., Furuya, T., Fujita, S., and Nakagawa, A. J. (1991). Structure of lactacystin, a new microbial metabolite which induces differentiation of neuroblastoma cells. Antibiotics *44*, 117-118.

Orlowski, M. (1990). The multicatalytic proteinase complex, a major extralysosomal proteolytic system. Biochemistry *29*, 10289-10297.

Orlowski, M., Cardozo, C., and Michaud, C. (1993). Evidence for the presence of five distinct proteolytic components in the pituitary multicatalytic proteinase complex. Properties of two components cleaving bonds on the carboxyl side of branched chain and small neutral amino acids. Biochemistry *32*, 1563-1572.

Orr, J. W., and Newton, A. C. (1992). Interaction of Protein Kinase C with phosphatidylserine. 2. Specificity and regulation. Biochemistry *31*, 4667-4673.

Orr, J. W., and Newton, A. C. (1994). Requirement for negative charge in "activation loop" of protein kinase C. J. Biol. Chem. *269*, 27715-27718.

Pagano, M., Tom, S. W., Theodoras, A. M., Beer-Romero, P., Del Sal, G., Chau, V., Yew, P. R., Draetta, G. F., and Rolfe, M. (1995). Role of the ubiquitin-proteasome pathway in regulating abundance of the cyclin-dependent kinase inhibitor p27. Science 269. 682-685.

Papavassilion, A. G., Treier, M., Chavrier, C., and Bohmann, D. (1992). Targeted degradation of c-Fos, but not v-Fos, by phosphorylation-dependent signal on c-Jun. Science *258*, 1941-1944.

Pettit, G. R. (1991). The bryostatins. Prog. Chem. Org. Natl. Prod. 57, 153-195.

Pettit, G. R., Day, J. F., Hartwell, J. L., and Wood, H. B. (1970). Antineoplastic components of marine animals. Nature *227*, 962-963.

Pettit, G. R., Herald, C. L., Douber, D. L., Herald, L., Arnold, E., and Clardy, J. (1982). Isolation and structure of bryostatin 1. J. Am. Chem. Soc. *104*, 6846-6848.

Pears, C. J., Kour, G., House, C., Kemp, B. E., and Parker, P. J. (1990). Mutagenesis of the pseudosubstrate site of protein kinase C leads to activation. Eur. J. Biochem. *194*, 89-94.

Pears, C. S., Stabel, S., Cazaubon, S., and Parker, P. J. (1992). Studies on the phosphorylation of protein kinase C-α. Biochem. J. *283*, 515-518.

Peters, J. -M., Franke, W. W., and Kleinschmidt, J. A. (1994). Distinct 19S and 20S subcomplex of the 26S proteasome and their distribution in the nucleus and the cytosol. J. Biol. Chem. *269*, 7709-7718.

Philip, P. A. Rea, D., Thavasu, P., Carmichael, J., Stuart, N. S. A., Rockett, H., Talbot, D. C., Ganesan, T., Pettit, G. R., Balkwill, F., and Harris, A. L. (1993). Phase I study of bryostatin 1: Assessment of interleukin 6 and tumor necrosis factor α induction in vivo. J. Natl. Cancer Inst. *85*, 1812-1818.

Prendiville, J., Crowther, D., Thatcher, N., Woll, P. J., Fox, B. W., McGown, A., Testa, N., Stern, P., MacDermott, R., Potter, M., and Pettit, G. R. (1993). A phase I study of intravenous bryostatin 1 in patients with advanced cancer. Br. J. Cancer *68*, 418-424.

Quest, A. F. G., and Bell, R. M. (1994). The molecular mechanism of protein kinase C regulation by lipids. In Protein Kinase C, edited by Kuo, J. F. New York: Oxford University Press, pp64-95.

Rechsteiner, M. (1987). Ubiquitin-mediated pathway for intracellular proteolysis. Annu. Rev. Cell Biol. *3*, 1-30.

Rechsteiner, M., Hoffman, L., and Dubiel, N. (1993). The multicatalytic and 26S proteases. J. Biol. Chem. *268*, 6065-6068.

Ron, D., Chen, C. H., Caldwell, J., Jamieson, L., Orr, E., and Mochly-Rosen, D. (1995). Cloning of an intracellular receptor for protein kinase C: a homology of the beta subunit of G proteins. Proc. Natl. Acad. Sci. USA *91*, 839-843.

Sakane, F., Yamada, K., Kanoh, H., Yokoyama, C., Tanabe, T. (1990). Porcine diacylglycerol kinase sequence has zinc finger and E-F hand motifs. Nature *344*, 345-348.

Sako, T., Yupsa, S. H., Herald, C. L., Pettit, G. R., and Blumberg, P. M. (1987). Partial parallelism and partial blockage by bryostatin 1 of effects of phorbol ester tumor promoters on primary mouse epidermal cells. Cancer Res. *47*, 5445-5450.

Schuchter, I. M., Esa, A. H., May, W. S., Laulis, M. K., Pettit, G. R., and Hess, A. D. (1991). Successful treatment of murine melanoma with bryostatin 1. Cancer Res. *51*, 682-687.

Seemüller, E., Lupas, A., Stock, D., Löwe, J., Huber, P., and Baumeister, W.(1995). Proteasome from Thermoplasma acidophilum: a threonine protease. Science *268*, 579-582.

Senfert, W., Futcher, B., and Jentsch, S. (1995). Role of a ubiquitin-conjugating enzyme in degradation of S- and M-phase cyclins. Nature *373*, 78-81.

Sepp-Lorenzino, L., Ma, Z., Lebwohl, D. E., and Vinitsky, A. (1995). Herbimycin A induces the 20S proteasome- and

ubiquitin-dependent degradation of receptor tyrosine kinases. J Biol. Chem. *270*, 16580-16587.

Smith, J. B., Dwyer, S. D., and Smith, L. (1989). Decreasing extracellular Na+ concentration triggers inositol polyphosphate production and Ca2+ mobilization. J. Biol. Chem. *264*, 831-837.

Smith, L., Porzig, H., Lee, H. -W., and Smith, J. B. (1995). Phorbol esters downregulate expression of the sodium/calcium exchanger in renal epithelial cells. Am. J. Physiol. *269*, C457-463.

Smith, J. B., Smith, L., and Pettit, G. R. (1985). Bryostatin: Potent, new mitogens that mimic phorbol ester tumor promoters. Biochem. Biophys. Res. Commun. *132*, 939-945.

Sossin, D. R., and Schwartz, J. H. (1993). Ca2+-independent protein kinase Cs contain an amino-terminal domain similar to the C2 consensus sequence. Trends Biochem. Sci. *18*, 207-208.

Szallasi, Z., Denning M. F., Smith, C. B., Dlugosz, A. A., Yupsa, S. H., Pettit, G. R., and Blumberg, P.M. (1994). Bryostatin 1 protects protein kinase C-delta from down-regulation in mouse keratinocytes in parallel with its inhibition of phorbol ester-induced differentiation. Mol. Pharmacol. *46*, 840-850.

Takai, Y., Kishimoto, A., Iwasa, Y., Kawahara, Y., Mori, T., and Nishizuka, Y. (1979). Calcium-dependent activation of a multifunctional protein kinase by membrane phospholipids. J. Biol. Chem. *254*, 3692-3695.

Tallant, E. A., Smith, J. B., and Wallace, R. W. (1987). Bryostatins mimic the effects of phorbol esters in intact human platelet. Biochim. Biophys. Acta. *132*, 939-945.

Tamura, T., Shimbara, N., Aki, M., Ishida, N., Bey, F., Scherrer, K., and Tanaka, K. (1992). Molecular cloning of cDNAs for rat proteasomes: deduced primary structures of four other subunits. J. Biochem. (Tokyo) *112*, 530-534.

Tayer, S. S., and Radzio-Andzelm, E. (1994). Three protein kinase structures define a common motif. Structure *2*, 345-355.

Toullec, D., Pianetti, P., Coste, H., Bellevergue, P., Grand-Perret, T., Ajakane, M., Baudet, V., Boissin, P.,

Boursier, E., Loriolle, F., Duhame, L., Charon, D., and Kirilovsky, J. (1991). The bisindolylmaleimide GF 109203X is a potent and selective inhibitor of protein kinase C. J. Biol. Chem. *266*, 15771-15781.

Vijay-Kumar, S., Bugg, C. E., Wilkinson, K. D., and Cook, W. J. (1985). Three-dimensional structure of ubiquitin at 7.8 Å resolution. Proc. Natl. Acad. Sci. USA *82*, 3582-3585.

Vinitsky, A., Cardozo, C., Sepp-Lorenzino, L., Michaud, C., and Orlowski, M. (1994). Inhibition of the proteolytic activity of the multicatalytic proteinase complex (proteasome) by substrate-related peptidyl aldehydes. J. Biol. Chem. *269*, 29860-29866.

Wender, P. A., Cribbs, C. M., Kochler, K. F., Sharkey, N. A., Herald, C. L., Kamano, Y., Pettit, G. R., and Blumberg, P. M. (1988). Modeling of the bryostatins to the phorbol ester pharmacophore on protein kinase C. Proc. Natl. Acad. USA *85*, 7197-7201.

Young, S., Parker, P. J., Ullrich, A., and Stabel, S. (1987). Down-regulation of protein kinase C is due to an increased rate of degradation. Biochem. J. *244*, 775-779.

Zhang, J., Wang, L., Petrin, J., Bishop, W. R., and Bond, R. W. (1993). Characterization of site-specific mutants altered at protein kinase CβI isozyme autophosphorylation sites. Proc. Natl. Acad. Sci. USA *90*, 6130-6134.

Zhang, J., Wang, L., Schwartz, J., Bond, R. W. and Bishop, W. R. (1994). Phosphorylation of the Thr642 is an early event in the processing of newly synthesized protein kinase CβI and is essential for its activation. J. Biol. Chem. *269*, 19578-19584.

Zwickl, P., Grziwa, A., Puhler, G., Dahlmann, B., Lottspeich, F., and Baumeister, W. (1992). Primary structure of the Thermoplasma proteasome and its implications for the structure, function, and evolution of the multicatalytic proteinase. Biochemistry *31*, 964-972.

APPENDIX

ACTIVATION OF PROTEIN KINASES BY CADMIUM: ROLE OF A PUTATIVE ORPHAN RECEPTOR IN HUMAN DERMAL FIBROBLASTS

HYEON-WOO LEE, LUCINDA SMITH,
AND JEFFREY BINGHAM SMITH

Manuscript in preparation

ABSTRACT

Cadmium and certain other divalent metals evoke striking increases in inositol trisphosphate and cytosolic free Ca in human fibroblasts. An orphan receptor (unknown physiological stimulus) that is blocked by Zn and coupled to phospholipase C apparently mediates Ca release by Cd. Cd produced changes in ^{32}P-labeling of cellular proteins similarly to those induced by bradykinin (BK) in human fibroblasts, as determined by two dimensional gel electrophoresis. Changes in ^{32}P-labeling of proteins produced by Cd appear to be mediated by protein kinase C (PKC), protein kinase A (PKA), and Cal/CaM kinases. A 5 min incubation of the cells with 1.0 μM Cd increased ERK2 activity 3-fold. ERK2 activity of immunoprecipitates was assayed with [γ-^{32}P]ATP and myelin basic protein as substrates. Zn (2 μM) completely blocked the activation of ERK2 by Cd without affecting activation by BK. A 24 h incubation with phorbol myristate acetate (PMA) abolished ERK2 activation by Cd, BK, and PMA but had no effect on activation by epidermal growth factor (EGF). The PMA treatment downregulated PKC-α, as determined by western analysis. These findings indicate that a PMA-sensitive isoform of PKC is responsible for ERK2 activation by Cd. In vivo PKC activity was determined by immunoprecipitation of MARCKS from [^{32}P]orthophosphate labeled cells. A 2 min incubation with 1.0 μM Cd increased [^{32}P] MARCKS 3-fold, as did BK and PMA. Co, Ni, or ferrous iron (1, 10, and 10 μM, respectively), which trigger Ca release similarly to Cd, also

increased [^{32}P]MARCKS 3-fold. Zn (2 μM) abolished MARCKS [^{32}P] labeling evoked by Cd and the other metals without affecting the response to BK. Downregulation of PKC abolished PMA-evoked [^{32}P] labeling of MARCKS without affecting the response to Cd or BK. These findings indicate that Cd stimulates PKC, which in turn activates ERK2. A Ca-mobilizing orphan receptor that is blocked by Zn apparently mediates the activation of PKC by Cd in human fibroblasts.

INTRODUCTION

While investigating Ca^{2+} release from intracellular stores that was evoked by the replacement of extracellular Na^{2+}, Co^{2+} and Ni^{2+} were tested as potential inhibitors (1). Co^{2+} and Ni^{2+} alone immediately and markedly raised stored Ca^{2+} in human dermal fibroblasts (1). Subsequently, a variety of monovalent and divalent cations were tested to observe whether they trigger Ca^{2+} release from internal stores. Cd^{2+} was the most potent ($K_{0.5}$ ~40 nM) among the five "agonist" metals (Cd^{2+}, Co^{2+}, Ni^{2+}, Fe^{2+}, and Mn^{2+}) that mobilized stored Ca^{2+} (1-3). Ni^{2+}, Co^{2+}, Fe^{2+}, and Mn^{2+} are 6, 7, 17, and 380 times less potent than Cd^{2+}, respectively. Zn^{2+} and Cu^{2+} competitively inhibit Ca^{2+} release produced by Cd^{2+} (K_i ~ 80 and 100 nM, respectively). Zn^{2+} has the same apparent K_i value (80 to 90 nM) toward each of five metals. Many other divalent metals, including Ca^{2+}, Mg^{2+}, Ba^{2+}, Sr^{2+}, Be^{2+}, and Pd^{2+} neither release stored Ca^{2+} nor inhibit Ca^{2+} release evoked by Cd^{2+} (1-3). Additionally, several monovalent cations had no effect on Ca^{2+} release. Cd^{2+} and the other four metals also produced

Ca^{2+} release in human neuroblastoma cells and dog coronary endothelial cells (3,4). The potency order of the metals in the neuroblastoma and endothelial cells is the same as in human dermal fibroblasts (1-4). Additionally, Cd^{2+} produced the release of stored Ca^{2+} in human aortic and intestinal smooth muscle cells (4). Cd^{2+} failed to release stored Ca^{2+} in rat aortic myocytes, rat skin fibroblasts, and human A431 cells (4).

Cd^{2+} evokes a several fold increase in intracellular Ca^{2+} level in human dermal fibroblasts and coronary endothelial cells (2,3). Moreover, the $[Ca^{2+}]_i$ spike produced by Cd^{2+} is similar to that produced by bradykinin (BK). The Cd^{2+}-evoked $[Ca^{2+}]_i$ spike is caused by the release of stored Ca^{2+} because Cd^{2+} produced similar spikes in the presence and absence of extracellular Ca^{2+} (2,3). A preincubation with BK, which causes depletion of the inositol trisphosphate (IP_3)-sensitive Ca^{2+} store, abolished the $[Ca^{2+}]_i$ spike produced by Cd^{2+} (2). The addition of 5 or 10 μM Zn^{2+} prior to 1 μM Cd^{2+} inhibited the effect of Cd^{2+} on $[Ca^{2+}]_i$ without affecting the $[Ca^{2+}]_i$ response to BK (2,5). Rinsing the cells with a phosphate buffered solution (PBS) fully restored the $[Ca^{2+}]_i$ response to a subsequent addition of Cd^{2+} (2,5). The rapid reversibility of the inhibition by Zn^{2+} is consistent with the competitive mechanism of Zn^{2+} inhibition as described above.

Cd^{2+} and the other agonist metals produce a substantial decrease in total cell Ca^{2+} which is similar to that produced

by BK (6,7). The net Ca^{2+} efflux is probably caused by the plasma membrane Ca^{2+}-ATPase of human fibroblasts (6). The endoplasmic reticulum (ER) probably does not rapidly reaccumulate the released Ca^{2+} because of the prolonged active state of the IP_3-gated Ca^{2+} channel on the ER membrane. IP_3 probably causes the Ca^{2+} release evoked by Cd^{2+} and the other metals. Five μM of Cd^{2+} increased [^{3}H]IP_3 3 to 4 fold in 15 sec (2). A 1 min incubation with 20 μM Fe^{2+} or Co^{2+} increased [^{3}H]IP_3 3 to 5 fold, respectively (2). Additionally, Zn^{2+} abolished the increases in [^{3}H]IP_3 caused by Cd^{2+} or Fe^{2+}. The [^{3}H]IP_3 data agree well with the Ca^{2+} mobilization data. These data, as described so far, seem to be enough to propose that cadmium and the other active metals act like Ca^{2+}-mobilizing hormones by triggering a certain type of cell surface receptor. We have called this receptor an "orphan receptor" because there is no known endogenous stimulus. We suggest that these effects of the metals may promote cell growth, protooncogene expression, and tumor growth (8,9). Some of the oldest known carcinogens are metals such as Cd^{2+}, Ni^{2+}, As^{3+}, and Be^{2+} in human and animals (10-24).

A plausible hypothesis for the target of "agonist" and "antagonist" metals is an orphan receptor that has a site for a physiological important metal such as Zn^{2+}. We have proposed that the putative orphan receptor is a seven transmembrane domain receptor which is coupled to phospholipase C (PLC) via a G protein. The putative receptor presumably has a Zn^{2+} or

Cu^{2+} site that is on the external side of the plasma membrane. Cd^{2+}, which has no known biological function, fortuitously activates the putative receptor by binding to the metal site (1-4,6,7). The following observations suggest these metals act on an external site. First, no lag between the addition of 0.1 μM Cd^{2+} and the $[Ca^{2+}]_i$ increase was detected, as might be expected for an external rather than an intracellular site of action (2,3,25). Second, loading the cells with N,N,N',N'-tetrakis-(2-pyridylmethyl)-ethylenediamine, a heavy metal chelator, did not delay the onset or decrease the extent of $^{45}Ca^{2+}$-efflux evoked by Cd^{2+} (2,3). Third, neither intracellular Cd^{2+} nor Zn^{2+} was detected with fura-2, whose fluorescence is sensitive to these metals (2,26,27). Fourth, as described below, a cell surface sialoprotein appears to mediate metal responsiveness (27,28). It is unlikely that Cd^{2+} and the other active metals directly activate PLC. It has been known that Cd^{2+} potently inhibits one isoform of PLC and has no effect on the other isoforms (29).

We have hypothesized that Cd^{2+} activates an orphan receptor by binding to a site which is normally occupied by Zn^{2+}. Total Zn^{2+} in plasma ranges from 10 to 20 μM in adults (30). Free Zn^{2+} may be 0.2 to 1.0 μM because most of Zn^{2+} is loosely bound to plasma proteins. Because the apparent affinity of the metal site for Zn^{2+} is ~0.1 μM, based on its K_i for metals-evoked Ca^{2+} release, the site would be occupied by Zn^{2+} at the plasma level. As described previously, Zn^{2+} does not evoke hormone-like responses but competitively

inhibits those responses evoked by Cd^{2+} and the other agonist metals. Therefore, we speculate that Zn^{2+} plays a role in the binding of the physiological (unknown) stimulus or in receptor internalization or cycling.

Growth of human fibroblasts in culture medium containing 100 μM Zn^{2+} selectively and reversibly desensitizes them to Cd^{2+} (31). The desensitization produced by growth in high zinc is mechanistically distinct from competitive inhibition by zinc. A 10 h incubation in culture medium is required to restore Cd^{2+} responsiveness to the cells that have been grown in high Zn^{2+} (31). Growth in high zinc reversibly abolished Cd^{2+}-evoked $[Ca^{2+}]_i$ response, $^{45}Ca^{2+}$ efflux, and [^{3}H]inositol phosphates (IP) without affecting BK-evoked responses (31). The half-time for the abolishment of Cd^{2+}-responsiveness produced by the addition of 100 μM Zn^{2+} to the culture medium was 17 h (31). Inhibition of RNA or protein synthesis by actinomycin D or cycloheximide or of asparagine-linked glycosylation by tunicamycin (32) blocked the restoration of Cd^{2+} responsiveness. Brefeldin A, which reversibly and selectively disrupts Golgi stacks and thereby blocks post-translational processing of nascent peptides (33,34), also prevented the restoration of Cd^{2+} responsiveness (28). The subsequent removal of brefeldin A and incubation in culture medium for 8 or more hours fully restored Cd^{2+} responsiveness. Adding Zn^{2+} back to the medium at the time of brefeldin A removal prevented the restoration of Cd^{2+} responsiveness (28). These findings suggest that asparagine-linked glycosylation

is required to restore Cd^{2+} responsiveness to the cells that have been grown in high zinc. Additionally, studies with wheat germ agglutinin and neuraminidase have provided evidence that the orphan receptor is a cell surface sialoprotein (28, Chen and Smith, unpublished data).

Many external stimuli (such as peptide hormones, neurotransmitters, and growth factors which bind and activate cell surface receptors) initiate a cascade of intracellular events that culminate in a cellular response such as cell growth (8,35-38). One of the early responses produced by external stimuli is the formation of IP_3, which is the common intermediate for two major signaling pathways, one initiated by receptors coupled to heterotrimeric guanine nucleotide-binding proteins (G proteins) and the other by receptor tyrosine kinases (RTK) such as the epidermal growth factor (EGF) or platelet-derived growth factor (PDGF) receptor (39). Each of these receptor classes activates a different isoform of PLC, which hydrolyzes membrane phospholipid phosphatidylinositol 4,5-bisphosphate (a minor plasma membrane phospholipid) to IP_3 and diacylglycerol (DAG). IP_3 binds to and opens a Ca^{2+} channel of the ER membrane. DAG and Ca^{2+} in turn activate protein kinase C (PKC).

The signaling-transducing unit of G protein-coupled receptor has three main parts. The activated receptor transfers signal through a G protein to stimulate PLC (39, 40). Members of this receptor family are glycoproteins composed of an extracellular NH_2-terminal domain, a central

core composed of seven transmembrane helices and connecting loops, and an intracellular COOH-terminal domain. The ligand binding site is composed of the transmembrane helices, which interact with each other to form a pocket. The intracellular domain has several phosphorylation sites involved in receptor desensitization (41). Some of the intracellular loops connecting the transmembrane regions give the site for interacting with G protein (i.e., the next component of the signaling pathway). The G proteins are heterotrimeric GTP-binding proteins composed of α, β, and γ subunits. Upon receptor stimulation, the α subunit, which has intrinsic GTPase activity, dissociates from the membrane-attached $\beta\gamma$ complex to affect the next element of the signaling cascade such as PLC, adenylate cyclase, or ion channels. So far, more than 40 distinct G proteins have been identified, and their variability is mostly due to the presence of different α subunits, which are encoded by >15 different genes (40,42, 43). This structural variation gives the G proteins target and response specificity (43). The G_q class of G protein has been shown to regulate the β isoform of PLC (44).

RTK are the other receptor family that evoke IP_3 and DAG production by activating a phospholipase (40). Generation of IP_3 and DAG in response to RTK activation is slower than that produced by G protein-coupled receptors. The resulting calcium response is usually smaller, and there is a lag of several seconds between hormone addition and the rise in

$[Ca^{2+}]_i$. This receptor family is composed of a protein having a single transmembrane segment containing a COOH-terminal cytoplasmic segment responsible for phosphorylation of tyrosine residues and an extracellular NH_2-terminal segment that interacts with the stimulus. Stimuli induce receptor dimerization, which allows the two cytoplasmic tyrosine kinase domains to phosphorylate each other on specific tyrosine residues. This dimerization-induced tyrosine phosphorylation provides docking sites responsible for interacting with different members of SH2 domain-containing proteins such as PLC-γ and Grb 2 which are phosphorylated on specific tyrosine residues and evoke downstream events such as production of IP_3 and DAG in the case of PLC-γ.

As stated previously, we have proposed that activation of an orphan receptor by Cd^{2+} promotes tumor development and that this receptor appears to be coupled to PLC via a G protein. This hypothesis is partly supported by our previous studies showing that Cd^{2+} and the other agonist metals evoke early responses, including IP production and the mobilization of intracellular Ca^{2+}. The diagram illustrated on page 144 summarizes the key features of the orphan receptor hypothesis. The hormone-like early responses to the metals appear to be unprecedented and remarkable with respect to metal potency and specificity.

This study was designed to determine which protein kinases, if any, are activated by the metals and the role of orphan receptor in the protein kinase activation. Moreover,

recent studies implicate the role of the orphan receptor in protooncogene induction by metals. Elucidation of the signaling pathways between metal-induced early responses and protooncogene induction is critical for understanding the mechanisms by which divalent trace metals can affect cellular responses such as growth, differentiation, and apoptosis.

EXPERIMENTAL PROCEDURES

Cell culture. Human forearm skin fibroblasts were grown in Dulbecco's modified Eagle's medium (DMEM) containing 10% (v/v) fetal bovine serum (FBS) (2). Vascular smooth muscle cells from the tunica media of rat thoracic aorta were grown in Medium 199 containing 10% FBS and 10 mM HEPES (46).

Two-dimensional gel electrophoresis of ^{32}P-labeled proteins. Quiescent cultures were incubated with serum-free DMEM. After 24 h, the cells were rinsed with physiological salt solution (PSS) and incubated with 1 ml of PSS containing 10 mM glucose plus 0.5 mCi [^{32}P] orthophosphate for 2 h at 37°C. The cells were rinsed eight times with PSS and then incubated with 1 ml of PSS containing 10 mM glucose plus the indicated additions for 2 min. The incubation was stopped by rinsing three times with ice-cold PBS and adding cell lysis buffer (9.5 M urea, 3% [w/v] CHAPS, 2% ampholines, pH 4-8, and 0.1 M DTT). First dimensional isoelectric focusing gels (1 mm x 13 cm) contained a mixture of 1.1% ampholines, pH 4-8, and 4.4% ampholines, pH 3-10. About 5 µl of a cell extract containing 10 µg protein in the cell lysis buffer was electrophoresed with a constant voltage of 200 V for 2 h, 500

V for 5 h, and then 800 V for 16 h. Isoelectric focusing gels were extruded and embedded onto an SDS-polyacrylamide gel (stacking gel 5% acrylamide and separating gel 14.8% acrylamide). Electrophoresis was carried out with 0.1% SDS at 60 mA/gel constant current until the dye front reached the bottom of the gel. ^{32}P-labeled proteins were detected by autoradiography. ^{32}P-labeled spots on the X-ray film were analyzed by scanning densitometry.

In vivo phosphorylation of MARCKS (Myristorylated-Alanine-Rich-C-Kinase-Substrate). Quiescent plates of human skin fibroblasts were incubated with serum-free DMEM. After 24 h, the cells were rinsed with PSS and incubated with 1 ml of PSS containing 10 mM glucose plus 0.5 mCi [^{32}P] orthophosphate for 1 h at 37°C. The cells were rinsed eight times with PSS and incubated with 1 ml of PSS containing 10 mM glucose plus the indicated additions for 2 min. The incubation was stopped by rinsing three times with ice-cold 10 mM Tris-saline, pH 7.4, and adding ice-cold lysis buffer (10 mM Tris-HCl, pH 7.4, 5 mM Na EDTA, pH 7.4, 50 mM NaCl, 30 mM sodium pyrophosphate, pH 6.8, 50 mM NaF, 0.1 mM sodium vanadate, 1 mM PMSF, and 1% Triton X-100). The cells were scraped and passed three times through a 26 gauge needle to disperse large aggregates. The cell lysates were centrifuged for 30 min at 16,000 x g to remove particulate material. The supernatant was transferred to a new tube, and MARCKS was immunoprecipitated by incubating overnight at 4°C with 5 µl of rabbit polyclonal anti-MARCKS antibody and 20 µl of

Protein A/G-agarose. The pellets were washed eight times with the ice-cold lysis buffer at 4°C and resuspended in 30 µl of 2 x SDS sample buffer. All samples were boiled and centrifuged for 5 min, respectively. The supernatant was subjected to electrophoresis on a 10% SDS-polyacrylamide gel. The gel was stained, destained, dried, and exposed to X-ray film for autoradiography. The MARCKS signal was quantified by volume densitometry.

Immunoprecipitation of ERK2 (Extracellular Signal-Regulated Kinase) and in vitro kinase assay. Quiescent human skin fibroblasts were incubated with serum-free DMEM. After 24 h, the cells were rinsed with PSS and incubated with 1 ml of PSS containing 10 mM glucose plus the indicated additions for 5 min at 37°C. The culture medium was aspirated, and the cells were lysed with 0.5 ml of the ice-cold lysis buffer, maintaining constant agitation, for 30 min at 4°C. The cells were scraped and the lysates were passed three times through a 26 gauge needle. Particulate material was removed by centrifugation at 16,000 x g for 30 min at 4°C. ERK2 was immunoprecipitated by incubating for 3 h at 4°C with 5 µl of affinity purified rabbit polyclonal anti-ERK2 antibody (100 µg/ml, Santa Cruz Biotech.) and 20 µl of Protein A/G-agarose (Santa Cruz Biotech.). ERK2 activity was assayed as described (47). Immunocomplexes were washed eight times with kinase buffer (30 mM Tris-HCl, pH 7.4, 10 mM $MgCl_2$, 1 mM $MnCl_2$, and 0.5 mM DTT) and resuspended in 30 µl of kinase cocktail (kinase buffer containing 14 µg myelin basic

protein, 5 μM cold ATP, and 5 μCi [γ-^{32}P]ATP per sample). After 30 min at 30°C, kinase reactions were terminated by adding 10 μl of 4 x SDS sample buffer and boiling for 5 min. The reaction solution was centrifuged for 5 min. The supernatant was subjected to electrophoresis on a 15% SDS-polyacrylamide gel. The gel was stained, destained, dried, and exposed to X-ray film at -70°C. Stained MBP bands were cut and radioactivity was determined by scintillation counting.

PKC-α translocation. Quiescent plates of human skin fibroblasts were incubated with serum-free DMEM in the presence or absence 0.1 μM PMA. After 48 h, the cells were incubated with indicated conditions at 37°C. Each culture was washed twice with ice-cold PBS, and the cells were removed with 1 ml of homogenization buffer (20 mM Tris-HCl, pH 7.4, 0.5 mM EDTA, 0.5 mM EGTA, 10 μM leupeptin, 10 μM aprotinin, 1 mM benzamide, 1 mM DTT, 0.1 mM sodium vanadate) by scraping with a rubber policeman. The cells were homogenized by sonication. Soluble and particulate fractions were prepared by centrifugation at 100,000 x g for 1 h. The supernatant containing cytosolic proteins was concentrated with a Centricon tube. The pellets were resuspended into 100 μl of homogenization buffer containing 1% Triton X-100 and extracted by stirring with a round-tip glass rod and incubating on ice for 1 h. Triton-soluble and Triton-insoluble fractions were prepared by centrifugation at 100,000 x g for 20 min. The amount of protein of each

fraction was measured by the bicinchoninic acid (BCA) protein assay. The same amount of protein of each fraction was electrophoresed on a 10% SDS-polyacrylamide gel. Proteins were electrophoretically transferred to an Immobilon-P membrane. The membrane was incubated with the blocking buffer (2% [w/v] bovine serum albumin, 0.1 M NaCl, 10 mM Tris-HCl, pH 7.5, and 0.1% [w/v] Tween 20) for 1 h at 37°C and then incubated with the blocking buffer containing a 1:1,000 dilution of affinity purified rabbit polyclonal anti PKC-α antibody (Santa Cruz Biotech.) for 30 min at 37°C. The membrane was rinsed with washing buffer (50 mM NaCl, 10 mM Tris-HCl, pH 7.5, and 0.1% [w/v] Tween 20), which was changed every 5 min, for 30 min and then incubated with the blocking buffer containing 1:50,000 dilution of horseradish peroxidase conjugated donkey anti-rabbit IgG for 30 min at 37°C. The membrane was rinsed again with the washing buffer, changing the washing buffer every 5 min, for 30 min. PKC-α was detected by ECL detection protocol with X-ray film.

Materials. [^{32}P] orthophosphoric acid (25 mCi/ml in water) and [γ-^{32}P]ATP (3000 Ci/mmol) were from DuPont, NEN Research Products (Boston, MA). FBS was obtained from Hyclone Laboratories, Inc. (Logan, UT). Myelin basic protein was from GIBCO BRL (Gaithersberg, MD). A rabbit polyclonal IgG to an epitope corresponding to amino acids 651-672 of the carboxyl-terminus of rabbit PKC-α and a rabbit polyclonal IgG to an epitope corresponding to amino acids 345-358 of the carboxyl-

terminus of rat ERK2 were obtained from Santa Cruz Biotechnology, Inc. (Santa Cruz, CA).

Data are expressed as mean ± SE (n = number of experiments). Analysis of variance with the Scheffe F test was done with Statview II (Abacus Concepts, Inc., Berkeley, CA).

RESULTS

Activation of protein kinase C (PKC), protein kinase A (PKA) and Ca2+/calmodulin (Cal/CaM) protein kinases by Cd^{2+}. The addition of 1 μM Cd^{2+} to human fibroblasts prelabeled with [^{32}P] orthophosphate markedly and rapidly evoked changes in ^{32}P-labeling of several proteins. Two μM Fe^{2+}, another agonist metal, or 0.1 μM BK evoked similar change in ^{32}P-labeling of several proteins, as determined by two-dimensional (2D) gel electrophoresis (Fig. 1 and Table 1).

In order to determine which protein kinases were responsible for changes in ^{32}P protein labeling produced by Cd^{2+}, phorbol 12-myristate 13-acetate (PMA), forskolin, and ionomycin were used to activate PKC, PKA, and Cal/CaM kinases, respectively (Figs. 2 and 3 and Table 2). PMA increased ^{32}P labeling of protein spot 1 corresponding to pI 4.7 and M.W. 87 kDa, which is probably MARCKS. The increase in ^{32}P-labeling of protein spot 4 (approximately pI 5.7 and M.W. 21 kDa) is due to the activation of PKA because forskolin increased the labeling of this protein. Dideoxy (dd)-forskolin, the inactive form of forskolin, had no effect

on ^{32}P-labeling of cellular proteins. Activation of Cal/CaM kinases appears to be responsible for changes in ^{32}P-labeling of the other proteins (spots 2, 3, 5, and 6) because ionomycin changed ^{32}P-labeling of these spots (Fig. 3 and Table 2).

It is noteworthy that either forskolin or ionomycin increased the ^{32}P-labeling of one protein (spot 4) (Fig. 3 and Table 2), and the Cd^{2+} or ionomycin-induced change in the spot 4 may be due to the activation of type I adenylyl cyclase, which is the Cal/CaM activated isoform of the cyclase (48-50). This possibility is supported by the study in which Cd^{2+} and ionomycin increased cAMP production (51). In contrast to human fibroblasts, Cd^{2+} had no effect on ^{32}P-labeling of proteins in rat aortic myocytes (Fig. 4). Cd^{2+} and the other agonist metals fail to release stored Ca^{2+} in the myocyte, apparently because they lack the putative orphan receptor (1,4). In contrast to Cd^{2+}, angiotensin II changed the ^{32}P-labeling of several proteins in the myocytes (Fig. 4). The data on the myocytes suggest that Cd^{2+} does not directly activate protein kinases in human fibroblasts.

Cd^{2+} activates ERK2 by PKC activation. ERK2 was immunoprecipitated from human skin fibroblasts that were treated with Cd^{2+} and assayed with [γ-^{32}P]ATP and myelin basic protein. Western analysis using an affinity purified rabbit polyclonal ERK2 antibody indicated that there was a similar amount of ERK2 protein in each immunoprecipitate (Lee et al., unpublished data). The ERK2 peptide, used to produce the

antibody, completely abolished ERK2 immunoprecipitation. A 5 min incubation with Cd^{2+} (0.01, 0.1, 1, and 10 μM) increased ERK2 activity to 182 ± 25, 330 ± 50, 319 ± 42, and 235 ± 44% control (mean ± S.E., n = 4), respectively (Fig. 5). BK (0.1 μM), PMA (0.1 μM), or EGF (100 ng/ml) increased ERK2 activity to 238 ± 1, 333 ± 36, and 289 ± 16% control (n = 4) (Fig. 6). Zn^{2+} is known to antagonize the release of stored Ca^{2+} by the agonist metals (4). We tested the effect of Zn^{2+} on Cd^{2+} evoked ERK2 activation. Zn^{2+} (2 μM) by itself had no effect (86 ± 10% control, n = 3), but blocked Cd^{2+} evoked ERK2 activation (122 ± 21% control, n =3) without affecting the activation by BK (250 ± 17% control, n = 3) (Fig. 7). These data suggest that ERK2 activation by Cd^{2+} may be due to stimulating orphan receptor.

The effects of PMA, forskolin, and ionomycin were tested to determine which protein kinase is responsible for Cd^{2+}-induced ERK2 activation. PMA but not forskolin or ionomycin activated ERK2 (Fig. 8).

In order to further clarify the role of PKC in ERK2 activation by Cd^{2+}, we used PKC downregulated cells. Figure 9 shows that a 48 h incubation of human skin fibroblasts with 0.1 μM PMA completely eliminated PKC-α from both cytosol and particulate fractions. PKC downregulation abolished ERK2 activation by Cd^{2+}, BK, or PMA (90 ± 19, 118 ± 27, and 82± 15% control, n = 4, respectively) but had no effect on the response to EGF (250 ± 36% control, n = 4) (Fig. 10).

Orphan receptor-mediated PKC activation by agonist metals. It is known that triggering PLC and a G protein-coupled receptor activates ERK (52). It has been reported that PKC directly phosphorylates and activates Raf-1, which stimulates a MAPK kinase called MEK (53,54). To assess the role of PKC in ERK2 activation by Cd^{2+} and determine if the orphan receptor is involved in metal-evoked PKC activation, we assayed in vivo PKC activity by immunoprecitating MARCKS from ^{32}P-labeled human skin fibroblasts. In vivo ^{32}P-labeling of MARCKS is a specific marker for PKC activation (55-57). The pharmacologic specificity of agonist and antagonist metals was used to determine whether activation of orphan receptor correlated with PKC activation. A 2 min incubation with Cd^{2+} (0.01, 0.1, 1, and 10 μM) increased MARCKS phosphorylation to 195 ± 255, 225 ± 235, 332 ± 75, and 226 ± 44% control (n = 4), respectively (Fig. 11 A). Co^{2+}, Ni^{2+}, and Fe^{2+} (1, 10, and 10 μM, respectively) also increased MARCKS phosphorylation to 413 ± 55, 463 ± 96, and 445 ± 105% control (n = 4), respectively (Figs. 12 A and 12 B). Zn^{2+} (2 μM) by itself had no effect on MARCKS phosphorylation but abolished MARCKS phosphorylation evoked by 1 μM Cd^{2+}, 1 μM Co^{2+}, 10 μM Ni^{2+}, or 10 μM Fe^{2+} (95 ± 7, 83 ± 35, 149 ± 43, and 48 ± 33% control, n = 3, respectively) without affecting the response to BK (232 ± 17% control, n = 3) (Figs. 11 B and 13). These data support the idea that the putative orphan receptor is responsible for PKC activation by the metals.

Downregulation of PKC abolished PMA-induced MARCKS phosphorylation but had no effect on Cd^{2+} or BK-evoked MARCKS phosphorylation. A 48 h incubation with 0.1 μM PMA blocked PMA-evoked MARCKS phosphorylation (125 ± 17% control, n = 3) without affecting the response to Cd^{2+} or BK (282 ± 57 and 200 ± 23% control, n = 3, respectively) (Fig. 14). However, Cd^{2+}-, BK-, or PMA-induced ERK2 activation was almost completely prevented by PKC downregulation. Several possibilities could account for these results. First, it has been shown that Cd^{2+} and BK activate other kinases besides PKC such as PKA and Cal/CaM kinases in human fibroblasts. These protein kinases may be able to phosphorylate MARCKS. However, our previous data (Figs. 2 and 3 and Table 2) using 2D gel electrophoresis showed that the activation of PKA and Cal/CaM kinases did not increase MARCKS phosphorylation. Another possibility is that Cd^{2+} and BK may activate a PKC isoform(s) which is not activated or downregulated by PMA, in contrast to the α isoform, which was completely downregulated by a 48 h incubation with PMA (Fig. 9). This possibility implies that there is a functional diversity among PKC isoforms such that one or several PKC isoform(s) activated commonly by PMA and Cd^{2+} or BK may be responsible for ERK2 activation but not MARCKS phosphorylation.

Effects of herbimycin A (HA) on PKC and ERK2 activation by Cd2+. Our previous studies showed that HA, a potent and specific inhibitor of tyrosine kinases, had no effect on Cd^{2+}

or BK-evoked Ca^{2+} mobilization but blocked Ca^{2+} release by PDGF (58,59). Genistein, another selective inhibitor of tyrosine kinases, has been shown to abolish IP production and Ca^{2+} mobilization evoked by PDGF but only slightly affect these responses to Cd^{2+} or BK, suggesting that second messenger production by Cd^{2+} does not depend on tyrosine phosphorylation (60-62). However, it has been shown that Cd^{2+}-induced protooncogene expression was prevented by HA (Pijuan and Smith, unpublished data). These findings suggest that tyrosine kinase(s) may be involved in Cd^{2+}-induced signaling cascade but not in second messenger production by Cd^{2+}.

An experiment was carried out to test the effects of HA on Cd^{2+}-induced PKC and ERK2 activation. Figure 15 shows that incubating human fibroblasts with 1 μM HA for 24 h had no effect on Cd^{2+}-, or PMA-induced MARCKS phosphorylation, indicating that HA has no effect on activation of PKC, a Ser/Thr kinase. However, 1 μM HA almost completely abolished Cd^{2+}-, PMA-, or EGF-induced activation of ERK2 (Fig. 16), which is known to be phosphorylated on threonine and tyrosine residues by the dual specificity protein kinase of MEK (63,64). These results indicate that preventing Cd^{2+}-induced protooncogene expression by HA may result from the inhibition of Cd^{2+}-induced ERK2 activation.

DISCUSSION

Present studies have shown that Cd^{2+} produced changes in ^{32}P-labeling of cellular proteins which are remarkably similar to those evoked by BK, as determined by 2D gel

electrophoresis (Fig. 1 and Chen and Smith, unpublished data). Changes in ^{32}P-labeled proteins induced by Cd^{2+} or BK appear to be mediated by Cal/CaM kinases, PKA, and PKC in human dermal fibroblasts (Figs. 2 and 3 and Table 2). This idea was tested by comparing Cd^{2+}-, or BK-induced changes in ^{32}P-protein labeling with those produced by ionomycin, forskolin, or PMA, which increase cytoplasmic Ca^{2+}, increase cyclic AMP, or activate PKC, respectively. Zn^{2+} inhibited Cd^{2+}-induced changes in ^{32}P-labeled proteins without affecting those evoked by BK (Chen and Smith, unpublished data). Growth of the cells in high zinc abolished Cd^{2+}-induced changes in ^{32}P-labeled proteins but not those induced by BK (Chen and Smith, unpublished data). Additionally, by contrast to human fibroblasts, Cd^{2+} had no effect on ^{32}P-labeling of cellular proteins in rat aortic smooth muscle cells, which are known to lack second messenger responses to the agonist metals (Fig. 4). Angiotensin II, which activates a Ca^{2+}-mobilizing seven transmembrane receptor in rat aortic myocytes (65), produced changes in the ^{32}P-labeling of several proteins (Fig. 4). These results support the view that, in human fibroblasts, Cd^{2+}-induced changes in ^{32}P-labeling of cellular proteins are mediated by triggering the putative orphan receptor.

As a second messenger, Ca^{2+} plays a critical role in many aspects of cellular signaling. Although a variety of proteins mediate intracellular responses to Ca^{2+}, calmodulin is the predominant intracellular "Ca^{2+}-receptor" that activates

enzymes in response to a rise in free Ca^{2+} (66). Protein kinases are prominent among the enzymes activated by Ca^{2+}/calmodulin. Several protein kinases, including myosin light chain kinase, phosphorylase kinase, CaM kinase III (an elongation factor-2 kinase), and multifunctional Ca^{2+}-/CaM-dependent protein kinase (type II CaM kinase), have been identified as Ca^{2+}/calmodulin-dependent (66). Type I adenylyl cyclase is also known to be activated by Ca^{2+}/calmodulin (48-50). Although the expression of the type I adenylyl cyclase has not yet been directly demonstrated in human fibroblasts, it is likely that Cd^{2+} activates PKA via type I adenylyl cyclase in human fibroblasts (Fig. 2). Cd^{2+} or BK increased the ^{32}P-labeling of a protein (pI 5.7 and M.W. 21 kDa) similarly to forskolin (Figs. 1 and 2). Ionomycin, which raises cytosolic Ca^{2+} level, also increased that protein (Fig. 3). The view that Cd^{2+} activates type I adenylyl cyclase and, thus, PKA by activating an orphan receptor is also supported by previous data indicating that raising cytoplasmic Ca^{2+} markedly increases cyclic AMP production in human fibroblasts (51).

Cd^{2+} increased the ^{32}P incorporation by MARCKS in human skin fibroblasts (Figs. 11A,11B,14, and 15), which was also increased by PMA, as determined by 2D gel electrophoresis (Fig. 2). Phosphorylation of MARCKS, an acidic actin cross-linking protein, is known to increase rapidly upon PKC stimulation and is a sensitive indicator of PKC activation in vivo (55-57). The increase in ^{32}P-MARCKS labeling induced by

Cd^{2+} was similar to that produced by BK or PMA (Figs. 11B,14, and 15). Cd^{2+}-induced ^{32}P-MARCKS labeling was prevented by Zn^{2+}, which had no effect on ^{32}P-MARCKS labeling evoked by BK (Figs. 11A and 11B). In addition, divalent metals such as Fe^{2+}, Co^{2+}, and Ni^{2+}, which are agonists of the putative orphan receptor, increased MARCKs phosphorylation similarly to Cd^{2+} (Fig. 12A,12B, and 13). Zn^{2+} strongly decreased MARCKS phosphorylation evoked by Fe^{2+}, Co^{2+}, or Ni^{2+} (Fig. 13). These findings suggest that Cd^{2+} activates PKC by triggering the putative orphan receptor.

PKA, Ca^{2+}/CaM kinases, and PKC are integral components of kinase cascades that link a number of extracellular signals to a variety of cellular functions. PKC has been shown to phosphorylate and activate Raf and thereby activate MEK, which in turn activates ERK (53,67,68). The Raf-MEK-ERK pathway was the signaling pathway and a key component for cellular responses induced by growth factors. This is one possible pathway by which PKC activation regulates gene expression.

Changes in gene expression caused by extracellular stimuli result in cell proliferation or differentiation in many cell types (8,36). Proliferative stimuli in a variety of cell types, including human diploid fibroblasts, rapidly induce protooncogenes such as c-myc, c-jun, and c-fos (69-71). Ca^{2+} mobilizing hormones also rapidly induce protooncogenes (8,37,72), many of which are regarded as "immediate-early genes" because induction occurs within

minutes and is independent of protein synthesis (73). Cd^{2+} has been shown to increase c-jun and c-myc transcripts in L6 myoblasts (74), TIS genes in Swiss 3T3 cells (75), c-myc in NRK cells (76), and c-myc, c-fos, and egr-1 in human fibroblasts (5).

Recently, some studies were done to determine whether orphan receptor stimulation mediates protooncogene induction by Cd^{2+} in human fibroblasts. Metals such as Cd^{2+}, Co^{2+}, Ni^{2+}, and Fe^{2+}, which stimulate the putative orphan receptor (1,3,59), increased c-myc and egr-1 expression (5,59). Zn^{2+} by itself had no effect on c-myc expression but prevented c-myc induction by Cd^{2+} and Ni^{2+}. Zn^{2+} had no effect on FBS-evoked c-myc expression. Moreover, growth of the cells in high zinc almost abolished Cd^{2+}-induced c-myc and egr-1 expression. Incubating the cells for 24 h in the usual culture medium completely restored induction of c-myc and egr-1 by Cd^{2+}. These studies provide correlative data which support the view that Cd^{2+} induces protooncogene expression, at least in part, by activating the calcium-mobilizing orphan receptor (Pijuan and Smith, unpublished data).

Protein phosphorylation represents a major mechanism of signal transduction that couples signals initiated at the cell surface to the regulation of nuclear events. For example, activated PKA translocates from the cytosol to the nucleus (77,78) and phosphorylates CREB at Ser^{133}, which in turn causes transactivation of gene expression (79). It has been proposed that ERKs have an important role in the

regulation of gene expression (80,81). ERKs appear to be an integral component of signal transduction initiated by a variety of extracellular signals (63). Transcriptional factor proteins such as c-Myc and c-Fos have been identified as substrates phosphorylated by ERKs (80-82), which are known to be present in the nucleus and the cytoplasm (80,83). c-Fos complexes with c-Jun to form stable heterodimers known as transcription factor AP1 (81,84). c-Myc also interacts with a partner protein, called Max, to form a transcription factor (85,86). These transcription factors bind to specific genes and regulate their expression. It is known that phosphorylation of c-Myc and c-Fos by ERKs regulates their function (82).

Our data using an in vitro kinase assay of ERK2 immunoprecipitated from Cd^{2+}-treated human skin fibroblasts indicate that Cd^{2+} activated the kinase (Figs. 6-8 and 10). The activation of ERK2 by Cd^{2+} was dose dependent and similar in extent to that induced by BK or PMA (Figs. 5 and 6). Zn^{2+} prevented ERK2 activation by Cd^{2+} without affecting the response to BK (Figs. 5 and 7). Cd^{2+} had no effect on ERK2 in cells that had been treated for 48 h with PMA to downregulate PKC (Fig. 10). Cd^{2+} activates PKC, Cal/CaM kinases, and PKA, as shown in Figures 2 and 3. Figure 8 indicates that activation of PKC but not Cal/CaM kinases or PKA contributes to ERK2 activation by Cd^{2+}. These results suggest that activation of PKC mediates ERK2 activation by Cd^{2+}. Orphan

receptor stimulation would be expected to increase production of DAG, which activates PKC (59).

ERKs (pp44, ERK1, and pp42, ERK2) are a subgroup of mitogen-activated protein kinases (MAPK), which includes p38 and Jun kinase (JNK). ERKs are stimulated by growth factors via RTK or receptors that are coupled to G protein (64,87,88). Phosphorylation of both a tyrosine and a threonine residue by MEK (MAPK kinase) is required for maximal activation of ERK (63,64). The activation of ERKs has at least two consequences which may be critical for DNA synthesis and cell differentiation: the direct phosphorylation of substrates such as transcription factors and the activation of other protein kinases such as $p90^{rsk}$ and MAPKAP kinase 2 (89).

A signaling pathway initiated from RTK to ERK has been elucidated (90): RTK activation leads to autophosphorylation on tyrosine residues, causing the receptor to interact with SH2 domain-containing proteins such as Grb2. Grb2 binds to Sos, an adaptor protein. These interactions cause the accumulation of Ras containing bound GTP instead of GDP and thereby activate the protein kinase cascade comprising Raf, MEK, and ERK. The first evidence with respect to upstream activation of MEK-ERK came from Raf- or Ras-transfected cells, in which ERKs are constitutively active (90). It turned out that this constitutive activation was due to the ability of Raf to phosphorylate and activate MEK directly. Recent studies have shown that activated Ras may not activate

Raf directly but may induce the recruitment of Raf to the plasma membrane from the cytoplasm. However, the exact mechanism of Raf activation is still unclear, although regulatory proteins such as the 14-3-3 protein seems to be involved in activation of membrane-bound Raf (91). Another protein called MEK kinase (MEKK) has been cloned (52,92,93). MEKK activity is increased in response to EGF in a Ras-dependent manner and is weakly responsive to phorbol ester (93). Recent studies suggested that both MEKK and Raf are activated by Ras, but the downstream kinases are different. Raf increases ERK activity by activating MEK1 and MEK2, whereas MEKK stimulates JNK by activating an isoform of MEK (47). That is different from MEK1 and 2.

The relationship between G protein coupled receptors and ERK activation has been investigated by several laboratories. The activation of PKC in response to the stimulation of a G protein coupled receptor appears to be responsible for ERK activation (51,53,92). Carroll and Muy (54) and Kolch et al. (53) have proposed that Raf-1 is directly phosphorylated by PKC independently of Ras. Cook et al. (94) and Howe and Marshall (95) showed that lysophosphatidic acid, which is presumed to interact with a G protein coupled receptor, activated ERK via Ras and Raf. Therefore, it is critical to elucidate whether cadmium activates Raf and MEK in a Ras-dependent manner and whether triggering the putative orphan receptor is responsible for Cd^{2+}-induced activation of Raf and MEK in human fibroblasts. These future experiments may

provide the link between the early second messenger responses to the metals and protooncogene induction.

HA is a potent and specific inhibitor of tyrosine kinases. It was originally found as an agent that could reverse the transformed morphology of Rous Sarcoma virus-infected rat kidney cells (58,96). It has been suggested that HA binds irreversibly to thiol groups of tyrosine kinases (97,98). HA has been used to implicate tyrosine kinases in the regulation of the cell cycle (99).

Our recent studies have shown that HA has no effect on Cd^{2+} or BK-induced Ca^{2+} mobilization but prevents Ca^{2+} release by PDGF in human fibroblasts. Additionally, the isoflavone genistein, another selective inhibitor of tyrosine kinases (60), was shown to abolish IP production (Lee and Smith, unpublished data) and Ca^{2+} mobilization evoked by PDGF, but to affect only slightly these responses to Cd^{2+} or BK (61), suggesting that a G protein coupled receptor, rather than RTKs, mediates IP production and Ca^{2+} mobilization evoked by Cd^{2+}.

Cd^{2+}-induced c-myc and egr-1 expression are prevented by HA, indicating that tyrosine kinase may be involved in Cd^{2+}-induced signaling cascade (Pijuan and Smith, unpublished data). Here, we observed that HA had no effect on Cd^{2+}-induced PKC activation (Fig. 15) but almost completely abolished Cd^{2+}-induced ERK2 activation (Fig. 16). The inhibition of Cd^{2+}-induced ERK activation by HA may be responsible for inhibition of Cd^{2+}-induced c-myc and egr-1

expression. These results support the view that ERK plays a critical role in induction of protooncogenes by Cd^{2+}. Taken together, the present findings support the view that Cd^{2+}-induced ERK2 activation is due to the stimulation of PKC, presumably by triggering orphan receptor, independently of receptor tyrosine kinase-Ras-Raf pathway, and ERK2 activation by Cd^{2+}, at least in part, may be responsible for protooncogene induction.

REFERENCES

1. Dwyer, S. D. (1990) *Cadmium increases [3H] inositol phosphate production and releases stored Ca2+: Evidence for a novel Ca2+-mobilizing receptor antagonized by zinc*. Dissertation, University of Alabama at Birmingham, Birmingham, AL

2. Smith, J. B., Dewyer, S. D., and Smith, L. (1989) *J. Biol. Chem.* 264, 7115-7118

3. Dewyer, S. D., Zhuang, Y., and Smith, J. B. (1991) *Exp. Cell Res.* 192, 22-31

4. Smith, J. B., Dewyer, S. D., and Smith, L. (1989) *J. Biol. Chem.* 264, 8723-8728

5. Lyu, R.-M., Zhuang, Y., Pijuan, V., and Smith, J. B. (1992) *Toxicologist* 12, 363

6. Smith, J. B., Dewyer, S. D., and Smith, L. (1989) *J. Biol. Chem.* 264, 831-837

7. Smith, J. B., and Smith, L. (1987) *J. Biol. Chem.* 262, 17455-17460

8. Rozengurt, R. (1986) *Science* 234, 161-166

9. Berridge, M. J. (1993) *Nature* 361, 315-325

10. Goyer, R. A. (1984) in Cassarett and Doull's Toxicology: *The Basic Science of Poisons* (Amdur, M. O., Doull, J., and Klaassen, C. D. eds) pp 623-680, Macmillan, New York

11. Leonard, A., Gerber, G. B., Jacquet, P., and Lauwerys, R. R. (1984) in *Mutagenicity, Carcinogenicity, and*

Teratogenicity of Industrial Pollutants (Kirsch-Volder, M. ed) pp. 59-125, Plenum, New York

12. Sunderman Jr, F. W. (1978) *Fed. Proc.* 37, 40-46

13. Waalkes, M. P., and Rehm, S. (1992) *Fundam. Appl. Toxicol.* 19, 512-520

14. Hadley, J. G., Conklin, A. W., and Sanders, C. L. (1979) *Toxicol. Lett.* 4, 107-111

15. Takenaka, S., Oldiges, H., König, H., Hochrainer, D., and Oberdörster, G. (1983) *J. Natl. Cancer Inst.* 70, 367-371

16. Ottolenghi, A. D., Hasman, J. K., Payne, W. W., Salk, H. L., and MacFarland, H. M. (1977) *J. Natl. Cancer Inst.* 54, 1165-1172

17. Sunderman, F. W., and Donnelly, A. J. (1965) *Am. J. Pathol.* 46, 1027-1041

18. Gunn, S. A., Gould, T. C., and Anderson, W. A. D. (1963) *J. Natl. Cancer Inst.* 31, 745-759

19. Terracio, L., and Nachtigal, M. (1986) *Arch. Toxicol.* 58, 141-151

20. Terracio, L., and Nachtigal, M. (1988) *Arch. Toxicol.* 61, 450-456

21. Bouttler, S. D., and Ord, M. J. (1988) *J. Cell Sci.* 91, 423-429

22. Gunn, S. A., Gould, T. C., and Anderson, W. A. D. (1964) *Proc. Soc. Exp. Biol. Med.* 115, 653-657

23. Waalkes, M. P., Rehm, S., Riggs, C. W., Bare, R. M., Devor, D. E., Poirier, L. A., Wenk, M. L., and Henneman, J. R. (1989) *Cancer Res.* 49, 4282-4288

24. Bremner, I. (1974) *Q. Rev. Biophys.* 7, 75-124

25. Chen, Y.-C., and Smith, J. B. (1992) *Toxicol. Appl. Pharmacol.* 117, 249-256

26. Hinkle, P., Shanshala, E. D., and Nelson, E. J. (1992) *J. Biol. Chem.* 267, 25553-25559

27. Grynkiewicz, G., Poenie, M., and Tsien, R. Y. (1985) *J. Biol. Chem.* 260, 3440-3450

28. Chen, Y.-C., and Smith, J. B. (1992) *Mol. Biol. Cell* 3, 239a

29. Ryu, S. H., Cho, K. S., Lee, K.-Y., Suh, P.-G., and Rhee, G.(1987) *J. Biol. Chem.* 262, 12511-12528

30. Sandstead, H. H. (1981) in *Disorders of Mineral Metabolism* (Bronner, F., and Coburn, J. W. eds) pp. 93-157, Academic Press, New York

31. Smith, L., Pijuan, V., Zhuang, Y., and Smith, J. B. (1992) *Exp. Cell Res.* 202, 174-182

32. Duksin, D., and Mahoney, W. C. (1982) *J. Biol. Chem.* 257, 3105-3109

33. Fujiwara, T., Oda, K., Yokota, S., Takatsuki, A., and Ikehara, Y. (1988) *J. Biol. Chem.* 263, 18545-18552

34. Ulmer, J. B., and Palade, G. (1989) *Proc. Natl. Acad. Sci. USA* 86, 6992-6996

35. Berridge, M. J. (1987) *Annu. Rev. Biochem.* 56, 159-193

36. Aaronson, S. A. (1991) *Science* 254, 1146-1153

37. Villereal, M. L., and Byron, K. L. (1992) *Rev. Physiol. Biochem. Pharmacol.* 119, 68-121

38. Nishizuka, Y. (1992) *Science* 258, 607-614

39. Dohlman, H. G., Thorner, J., Caron, M. G., and Lefkowitz, R. J. (1991) *Annu. Rev. Biochem.* 60, 653-688

40. Karin, M. (1992) *FASEB J.* 6, 2581-2590

41. Lefkowitz, R. J., Hansdorff, W. P., and Caron, M. G. (1990) *Trends Pharm. Sci.* 11, 190-194

42. Gilman, A. G. (1987) *Annu. Rev. Biochem.* 56, 615-649

43. Simon, M. I., Strathman, M. P., and Gautman, N. (1991) *Science* 252, 802-808

44. Sternweis, P. C., and Smrcka, A. V. (1992) *Trends Biochem. Sci.* 17, 502-506

45. Kim, H. K., Kim, J. W., Zilberstein, A., Margolis, B., Kim, J. G., Schlessinger, J., and Rhee, S. G. (1991) *Cell* 65, 435-442

46. Smith, J. B., Cragoe, E. J., and Smith, L. (1987) *J. Biol. Chem.* 262, 11988-11994

47. Minden, A., Lin, A., McMahon, M., Langer-Cater, C. A., Derijard, B., Davis, R. J., Johnson, G. L., and Karin, M. (1994) *Science* 266, 1719-1723

48. Krupinski, J., Coussen, F., Bakalyar, H. A., Tang, W.-J., Feinstein, P. G., Orth, K., Slanghter, C., Reed, R. R., and Gilman, A. G. (1989) *Science* 244, 1558-1564

49. Minocherhomjee, A. E. V., Shattuck, R. L., and Storm, D. R. (1988) in *Calmodulin* (Klee, C. B. ed) pp. 249-263, Elsevier, New York

50. Choi, E.-J., Wong, S. T., Hinds, T. R., and Storm, D. R. (1992) *J. Biol. Chem.* 267, 12440-12442

51. Pijuan, V., Smith, L., and Smith, J. B. (1992) *Toxicologist* 12, 363

52. Lange-Carter, C. A., Pleiman, C. M., Gardner, A. M., Blumer, K. J., and Johnson, G. L. (1993) *Science* 260, 315-319

53. Kolch, W., Heidecker, G., Kolchs, G., Hummel, R., Vahidi, H., Mischak, H., Finkenzeller, G., Marmë, D., and Rapp, U. R. (1993) *Nature* 364, 249-252

54. Carroll, M. P., and Muy, W. S. (1994) *J. Biol. Chem.* 269, 1249-1256

55. Rozengurt, E., Rodriguez-Pena, M., and Smith, K. A. (1983) *Proc. Natl. Acad. Sci. USA* 80, 7244-7248

56. Li, J., and Aderem, A. (1992) *Cell* 70, 791-801

57. Hartuig, J. H., Thelen, M., Rosen, A., Janmey, P. A., Nairn, A. C., and Aderem, A. (1992) *Nature* 356, 618-622

58. Uehara, Y., Hori, M., Takeuchi, T., and Umezawa, H. (1985) *Jpn J. Cancer Res.* 76, 672-675

59. Smith, J. B., Smith, L., Pijuan, V., Zhuang, Y., and Chen, Y. -C. (1994) *Environ. Health Perspect.* 102, 181-189

60. Akiyama, T., Ishida, J., Nakagawa, S., Ogawara, H., Watanabe, S.-I., Shibuya, M., and Fukami, Y. (1987) *J. Biol. Chem.* 262, 5592-5595

61. Lyu, R.-M., and Smith, J. B. (1993) *Cell. Biol. Toxicol.* 9, 141-148

62. Lyu, R. M., Barens, S., and Smith, B. J. (1991) *FASEB J.* 5, A482

63. Cobb, M. H., Boulton, T. G., and Robbins, D. J. (1991) *Cell Regul.* 2, 965-978

64. Ray, L. B., and Sturgill, T. W. (1988) *Proc. Natl. Acad. Sci. USA* 85, 3753-3758

65. Smith, J. B. (1986) *Am. J. Physiol.* 250, F759-769

66. Haason, P. I., and Sculman, H. (1992) *Annu. Rev. Biochem.* 61, 559-601

67. Rapp, U. R. (1991) *Oncogene* 6, 495-500

68. Dent, P., Haser, W., Haystead, T. A. J., Vincent, L. A., Roberts, T. M., and Sturgill, T. W. (1992) *Science* 257, 1404-1407

69. Cao, X., Guy, G. R., Sukhatme, V. P., and Tan, Y. H. (1992) *J. Biol. Chem.* 267, 1345-1349

70. Jamieson, G. A. Jr, Mayforth, R. D., Villereal, M. L., and Sukhatme, V. P. (1989) *J. Cell. Physiol.* 139, 262-268

71. Owen, T. A., Losenza, S. C., Soprano, D. R., and Soprano, K. J. (1987) *J. Biol. Chem.* 262, 15111-15117

72. Greenberg, M. E., Ziff, E. B., and Greene, L. A. (1986) *Science* 234, 80-83

73. Lau, L. F., and Nathans, D. (1985) *EMBO J.* 4, 3145-3151

74. Jin, P., and Ringertz, N. R. (1990) *J. Biol. Chem.* 265, 14061-14064

75. Epner, D. E., and Herschman, H. R. (1991) *J. Cell. Physiol.* 148, 68-74

76. Tang, N., and Enger, M. D. (1992) *Toxicology* 71, 161-171

77. Meinkoth, J. L., Ji, Y., Taylor, S. S., and Feramisco, J. R. (1990) *Proc. Natl. Acad. Sci. USA* 87, 9595-9599

78. Adams, S. R., Harootunian, A. T., Buechler, Y. J., Taylor, S. S., and Tsien, R. Y. (1991) *Nature* 349, 694-697

79. Gonzalez, G. A., and Montminy, M. R. (1989) *Cell* 59, 675-680

80. Alvarez, E., Northwood, I. C., Gonzalez, F. A., Latour, D. A., Seth, A., Abate, C., Curran, T., and Davis, R. J. (1991) *J. Biol. Chem.* 266, 15277-15285

81. Pulverer, B. J., Kyriakis, J. M., Avruch, J., Nikolakaki, E., and Woodgett, J. R. (1991) *Nature* 353, 670-674

82. Seth, A., Gonzalez, F. A., Gupta, S., Raden, D. L., and Davis, R. J. (1992) *J. Biol. Chem.* 267, 24796-24804

83. Chen, R.-H., Sarnecki, C., and Blenis, J. (1992) *Mol. Cell. Biol.* 12, 915-927

84. Karin, M. (1990) in *Molecular Aspects of Cellular Regulation, Vol. 6, The Hormonal Control of Gene Transcription* (Cohen, P., and Poulkes, J. G. eds). pp. 235-253, Elsevier,Amsterdam

85. Blackwood, E. M., and Eiseman, R. N. (1991) *Science* 251, 1211-1217

86. Mäkelä, T. P., Koskinen, P. J., Västrik, I., and Alitalo, K. (1992) *Science* 256, 373-377

87. Crews, C. M., Alessandrini, A., and Erikson, R. L. (1992) *Science* 258, 478-480

88. Boulton, T. G., Nye, S. H., Robbins, D. J., Ip, N. Y., Radziejewska, E., Morgenbesser, S. D., DePinho, R. A., Panayotos, N., Cobb, M. H., and Yancopoulos, G. D. (1991) *Cell* 65, 663-675

89. Howe, L. R., Leevers, S. J., Gómez, N., Nakielny, S., Cohen, P., and Marshall, C. J. (1992) *Cell* 7, 335-342

90. Avruch, J., Zhang, X. F., and Kyriakis, J. M. (1994) *Trends Biochem. Sci.* 19, 279-283

91. Hopkin, K. (1994) *J.NIH Res.* 6, 62-65

92. Crews, C. M., and Erikson, R. L. (1993) *Cell* 74, 215-217

93. Lange-Carter, C. A., and Johnson, G. L. (1994) *Science* 265, 1458-1461

94. Cook, S. J., Rubinfeld, B., Albert, I., and McCormick, F. (1993) *EMBO J.* 12, 3475-3485

95. Howe, L. R., and Marshall, C. J. (1992) *J. Biol. Chem.* 268, 20717-20720

96. Uehara, Y., Hori, M., Takeuchi, T., and Umezawa, H. (1986) *Mol. Cell. Biol.* 6, 2198-2206

97. Uehara, Y., Fukazawa, H., Murakami, Y., and Mizuno, S. (1989) *Biochem. Biophys. Res. Commun.* 163, 803-809

98. Fukazawa, H., Mizuno, S., and Uehara, Y. (1990) *Biochem. Biophys. Res. Commun.* 173, 276-282

99. Satoh, T., Uehara, Y., and Kaziro, Y. (1992) *J. Biol. Chem.* 267, 2537-2541

Diagram of transmembrane-signaling events and protooncogene induction via the orphan receptor triggered by cadmium. The key features of hypothesis are: a) a seven transmembrane domain receptor (upper left) is coupled to phospholipase C (PLC) via a heterotrimeric GTP-binding protein composed of subunits $\alpha, \beta,$ and γ; b) two second messengers, inositol trisphosphate (IP_3) and diacylglycerol (DAG), are produced simultaneously by the hydrolysis of phosphatidylinositol bisphosphate (PIP_2) when Cd^{2+} binds to a Zn^{2+} site in the external domain of the receptor; c) IP_3 opens an intracellular Ca^{2+} channel which releases Ca^{2+} from the endoplasmic reticulum; and d) DAG activates protein kinase C (PKC), which phosphorylates an actin crosslinking protein called myristorylated alanine-rich C-kinase substrate (MARCKS). The diagram depicts the activation of Ca2+/calmodulin (CaM) kinase and mitogen-activated protein kinase or extracellular signal regulated kinase (MAPK or ERK) in response to bradykinin or epidermal growth factor. Cd^{2+} induces "immediate/early" protooncogenes (egr-1 and c-myc). The diagram shows the activation of Ca^{2+}/calmodulin-activated adenylyl cyclase (Type I adenylyl cyclase), which apparently causes the cAMP increases produced by Cd^{2+}, calcium ionophores, or bradykinin in human dermal fibroblasts.

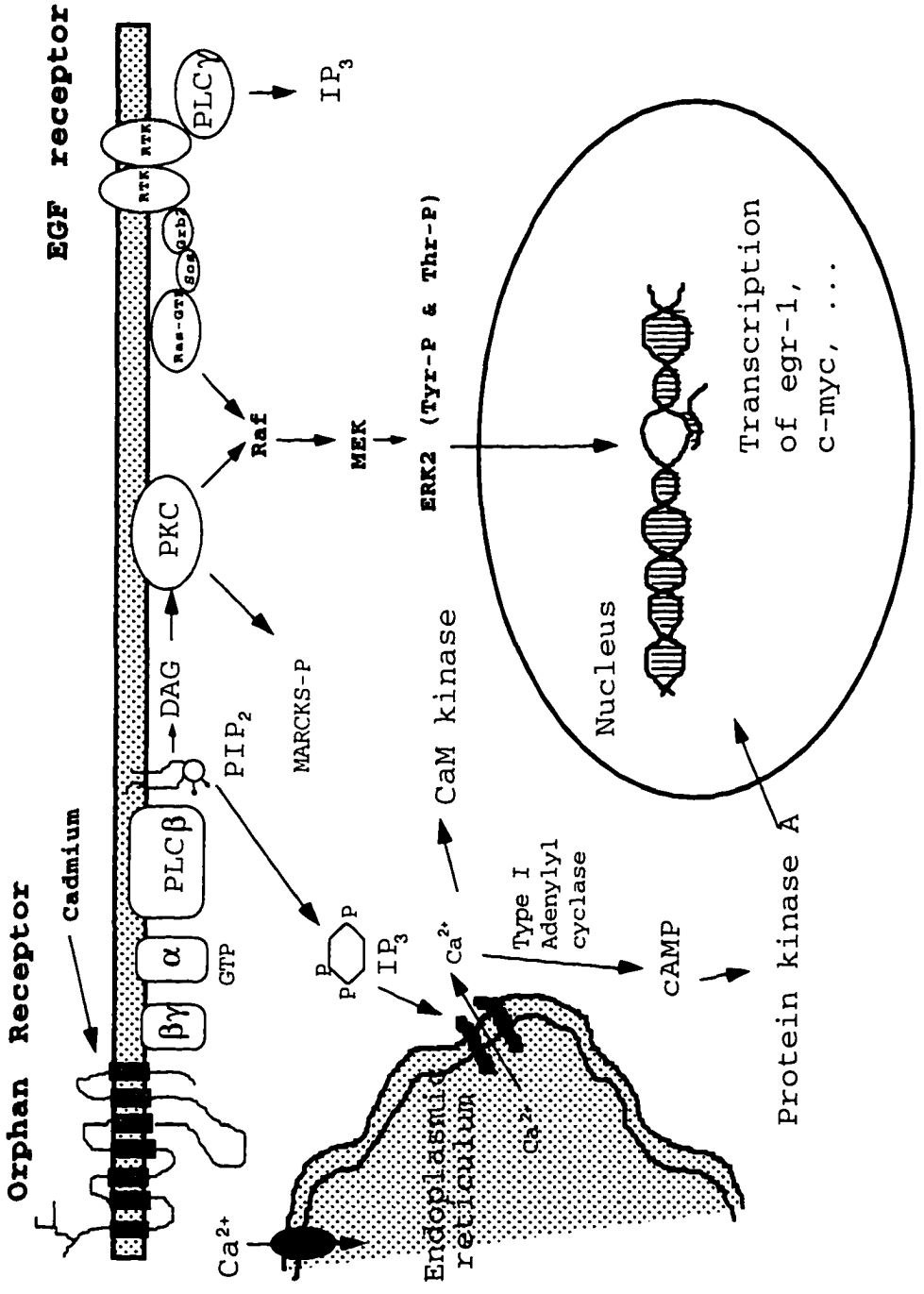

Table 1. Densitometric analysis of ^{32}P-labeled proteins from Figure 1

	Cd^{2+}	Fe^{2+}	BK
spot 1	235 ± 14*	214 ± 27*	223 ± 23*
spot 2	290 ± 89*	219 ± 41	379 ± 115*
spot 3	244 ± 39*	196 ± 43*	231 ± 45*
spot 4	785 ± 134*	575 ± 113*	782 ± 75*
spot 5	768 ± 139*	467 ± 99*	668 ± 146*
spot 6	849	900	1531

Values are % mean control ± SE of 2-5 experiments.
The asterisks indicate a significant difference from control at 95% confidence, as determined by ANOVA.
^{32}P-labeled protein spots are defined in Figure 1.

Table 2. Densitometric analysis of ^{32}P-labeled proteins from Figures 2 and 3

	Cd2+	PMA	forskolin	dd-forskolin	ionomycin
spot 1	384 ± 76*	437 ± 78*	118 ± 10	91 ± 16	127 ± 18
spot 2	331 ± 93*	177 ± 37	116 ± 15	106 ± 11	242 ± 51*
spot 3	222 ± 32*	117 ± 19	121 ± 21	136 ± 21	261 ± 86*
spot 4	428 ± 66*	176 ± 46	465 ± 78*	158 ± 54	575 ± 208*
spot 5	416 ± 96*	154 ± 17	132 ± 17	195 ± 50	636 ± 247*
spot 6	774 ± 254*	95 ± 18	100 ± 12	110 ± 20	1114 ± 502*

Values are means ± SE of 2-5 experiments.
The asterisks indicate a significant difference from control at 95% confidence, as determined by ANOVA.
^{32}P-labeled protein spots are defined in Figures 2 and 3.

Figure 1. Effect of Cd^{2+}, Fe^{2+}, and bradykinin on in vivo phosphorylation of fibroblast proteins. Human skin fibroblasts were rinsed three times with PSS and labeled for 2 h in 1 ml of PSS containing 0.5 mCi [^{32}P] orthophosphate and 10 mM glucose at 37°C. The cells were challenged with 1 μM Cd^{2+}, 2 μM Fe^{2+}, or 0.1 μM BK during last 2 min labeling. The reaction was terminated by rinsing eight times with ice-cold PBS. The cell monolayer was scraped into 100 μl of IEF sample solution and sonicated for 2 min. The cell lysates were centrifuged at 14,000 rpm for 20 min and supernatant was collected. About 5 x 10^5 cpm of TCA-precipitable proteins were applied on the IEF gel. The SDS-polyacrylamide gels were fixed, stained, destained, dried, and autoradiographed with one intensifying screen. Autoradiograms were scanned and analyzed with densitometer.

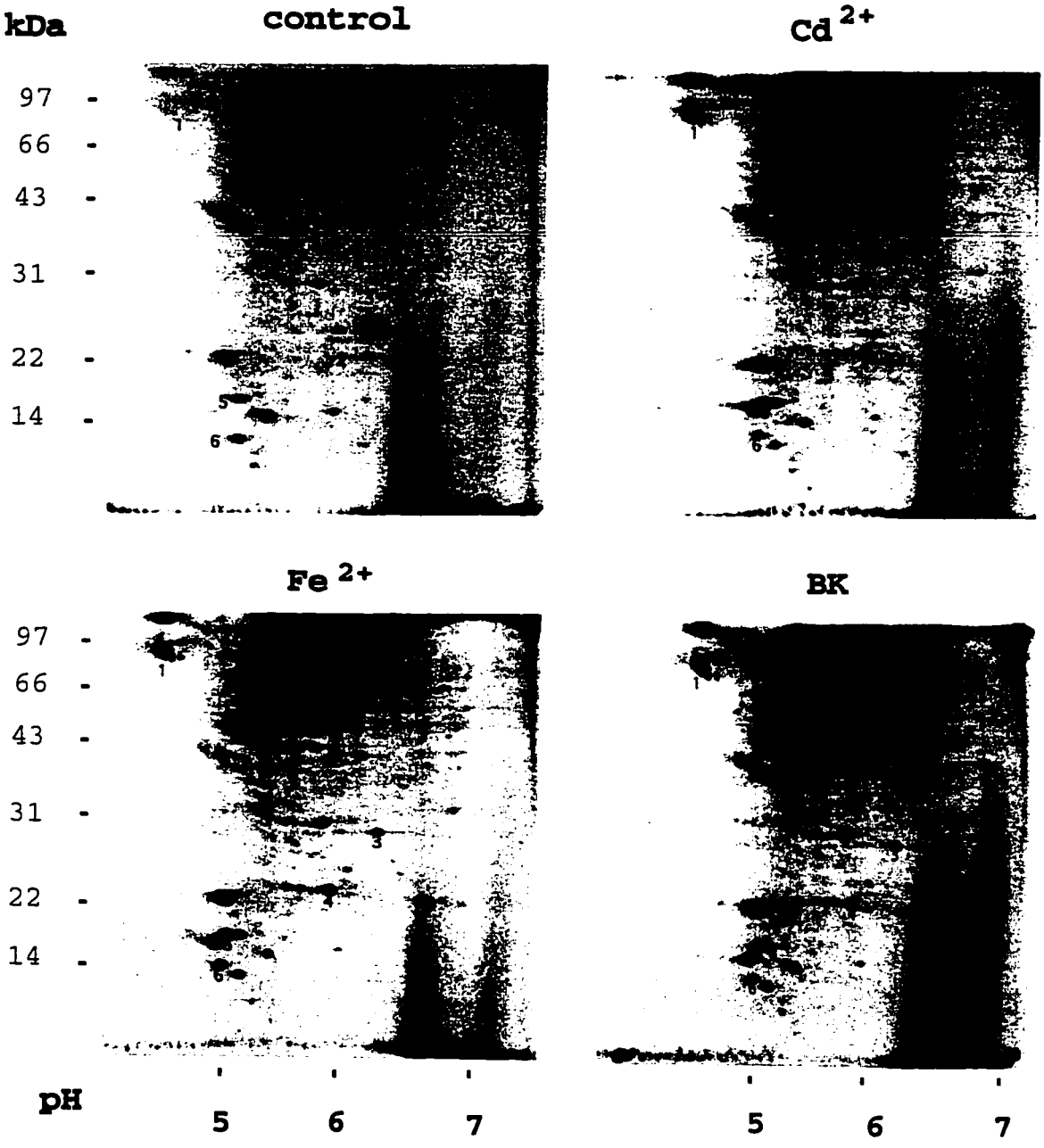

Figure 2. Effect of Cd^{2+}, forskolin, and PMA on in vivo phosphorylation of fibroblast proteins. Human skin fibroblasts were rinsed three times with PSS and labeled for 2 h in 1 ml of PSS containing 0.5 mCi [^{32}P] orthophosphate and 10 mM glucose at 37°C. The cells were challenged with 1 µM Cd^{2+}, 100 µM forskolin, or 0.1 µM PMA during last 2 min labeling. The reaction was terminated by rinsing eight times with ice-cold PBS. The cell monolayer was scraped into 100 µl of IEF sample solution and sonicated for 2 min. The cell lysates were centrifuged at 14,000 rpm for 20 min and supernatant was collected. About 5 x 10^5 cpm of TCA-precipitable proteins were applied on the IEF gel. The SDS-polyacrylamide gels were fixed, stained, destained, dried, and autoradiographed with one intensifying screen. Autoradiograms were scanned and analyzed with densitometer.

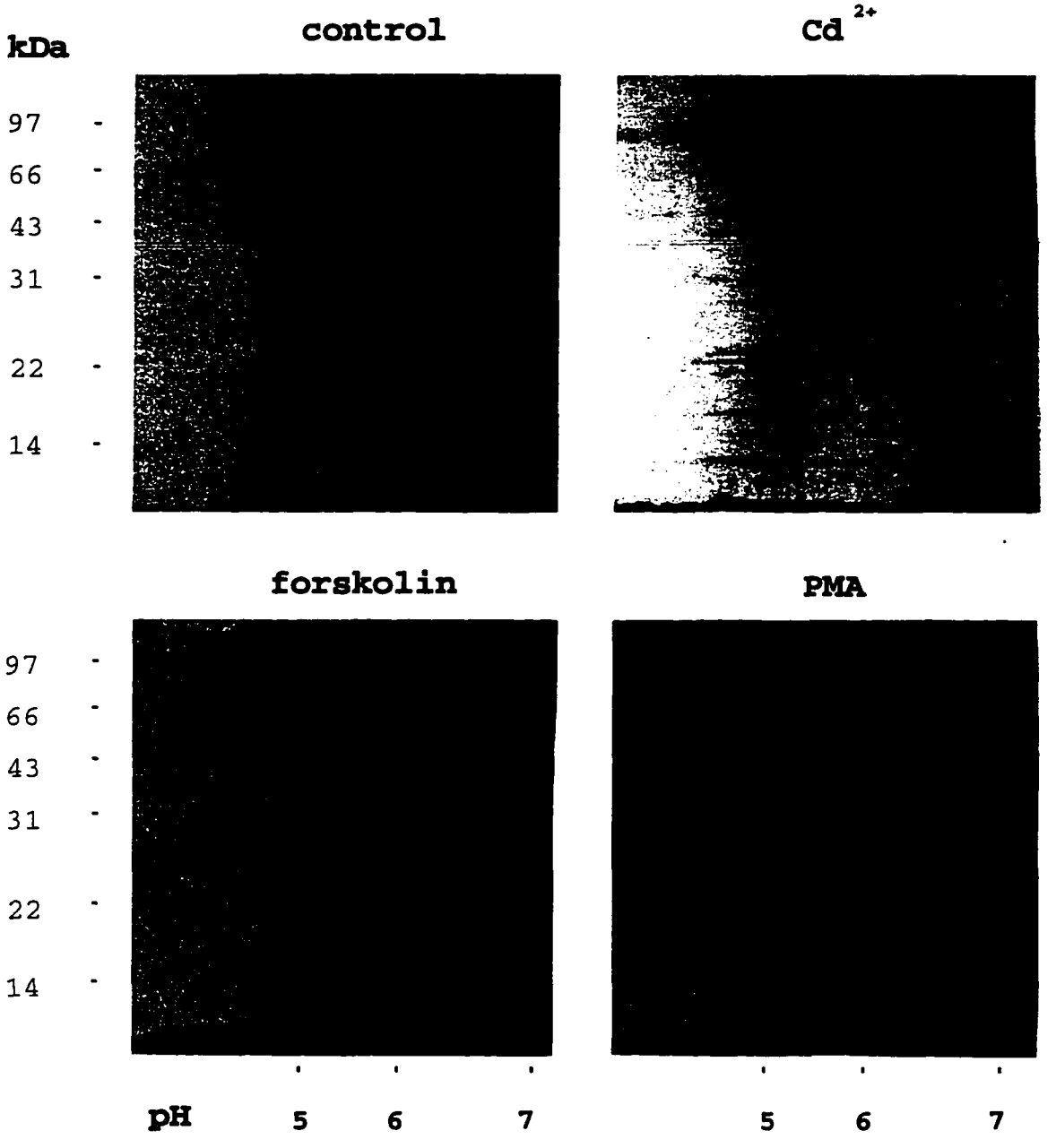

Figure 3. Effect of forskolin, dd-forskolin, and ionomycin on in vivo phosphorylation of fibroblast proteins. Human skin fibroblasts were rinsed three times with PSS and labeled for 2 h in 1 ml of PSS containing 0.5 mCi [^{32}P] orthophosphate and 10 mM glucose at 37°C. The cells were challenged with 100 μM dd-forskolin, 100 μM forskolin, or 5 μM ionomycin during last 2 min labeling. The reaction was terminated by rinsing eight times with ice-cold PBS. The cell monolayer was scraped into 100 μl of IEF sample solution and sonicated for 2 min. The cell lysates were centrifuged at 14,000 rpm for 20 min and supernatant was collected. About 5 x 10^5 cpm of TCA-precipitable proteins were applied on the IEF gel. The SDS-polyacrylamide gels were fixed, stained, destained, dried, and autoradiographed with one intensifying screen. Autoradiograms were scanned and analyzed with densitometer.

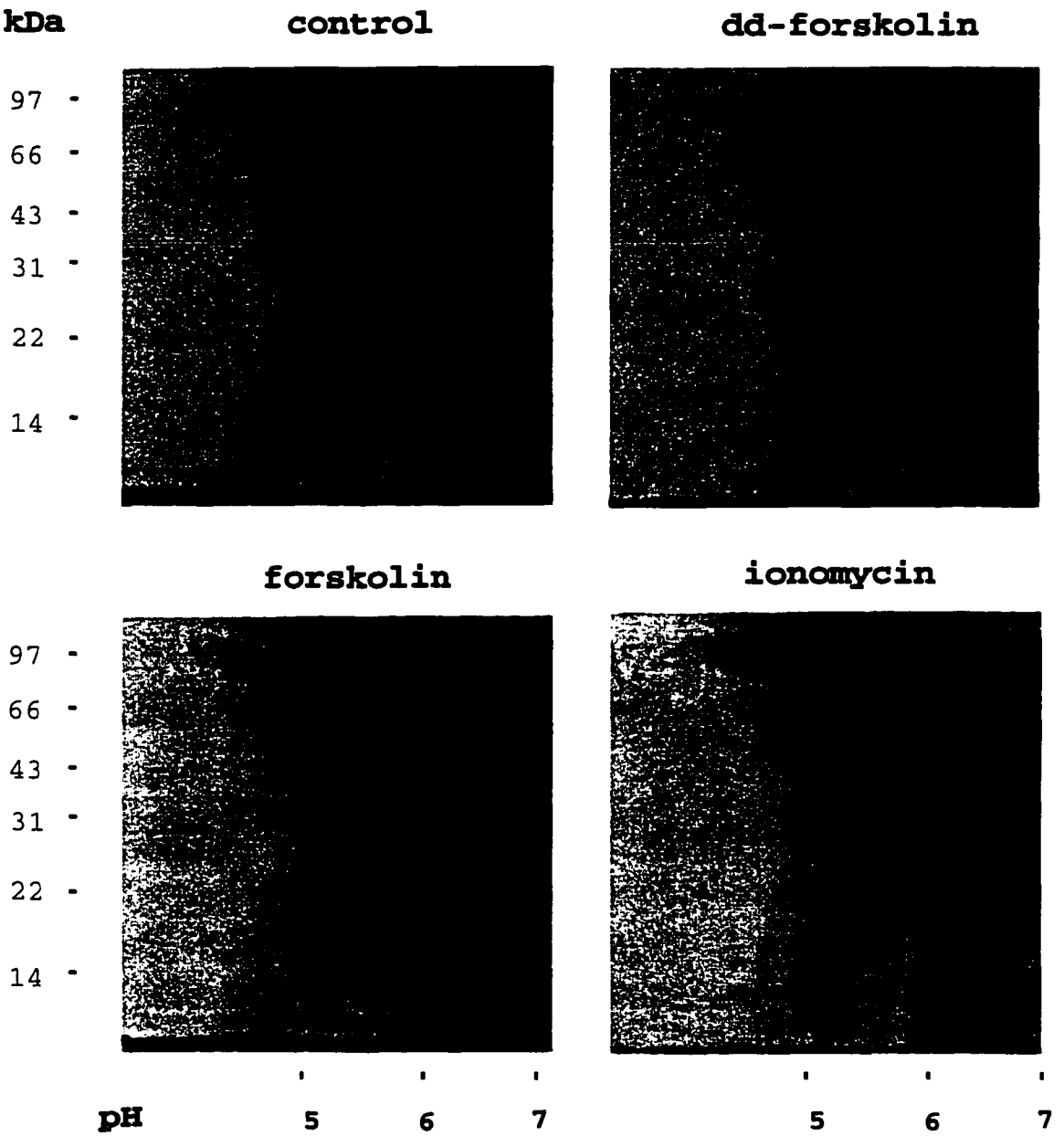

Figure 4. Effect of Cd^{2+}, angiotensin II, and ionomycin on in vivo protein phosphorylation in rat aortic myocytes. Rat aorta smooth muscle cells were rinsed three times with PSS and labeled for 2 h in 1 ml of PSS containing 0.5 mCi [^{32}P] orthophosphate and 10 mM glucose at 37°C. The cells were challenged with 1 μM Cd^{2+}, 0.1 μM angiotensin II or 2 μM ionomycin during last 2 min labeling. The reaction was terminated by rinsing eight times with ice-cold PBS. The cell monolayer was scraped into 100 μl of IEF sample solution and sonicated for 2 min. The cell lysates were centrifuged at 14,000 rpm for 20 min and supernatant was collected. About 5 x 10^5 cpm of TCA-precipitable proteins were applied on the IEF gel. The SDS-polyacrylamide gels were fixed, stained, destained, dried, and autoradiographed with one intensifying screen. Autoradiograms were scanned and analyzed with densitometer.

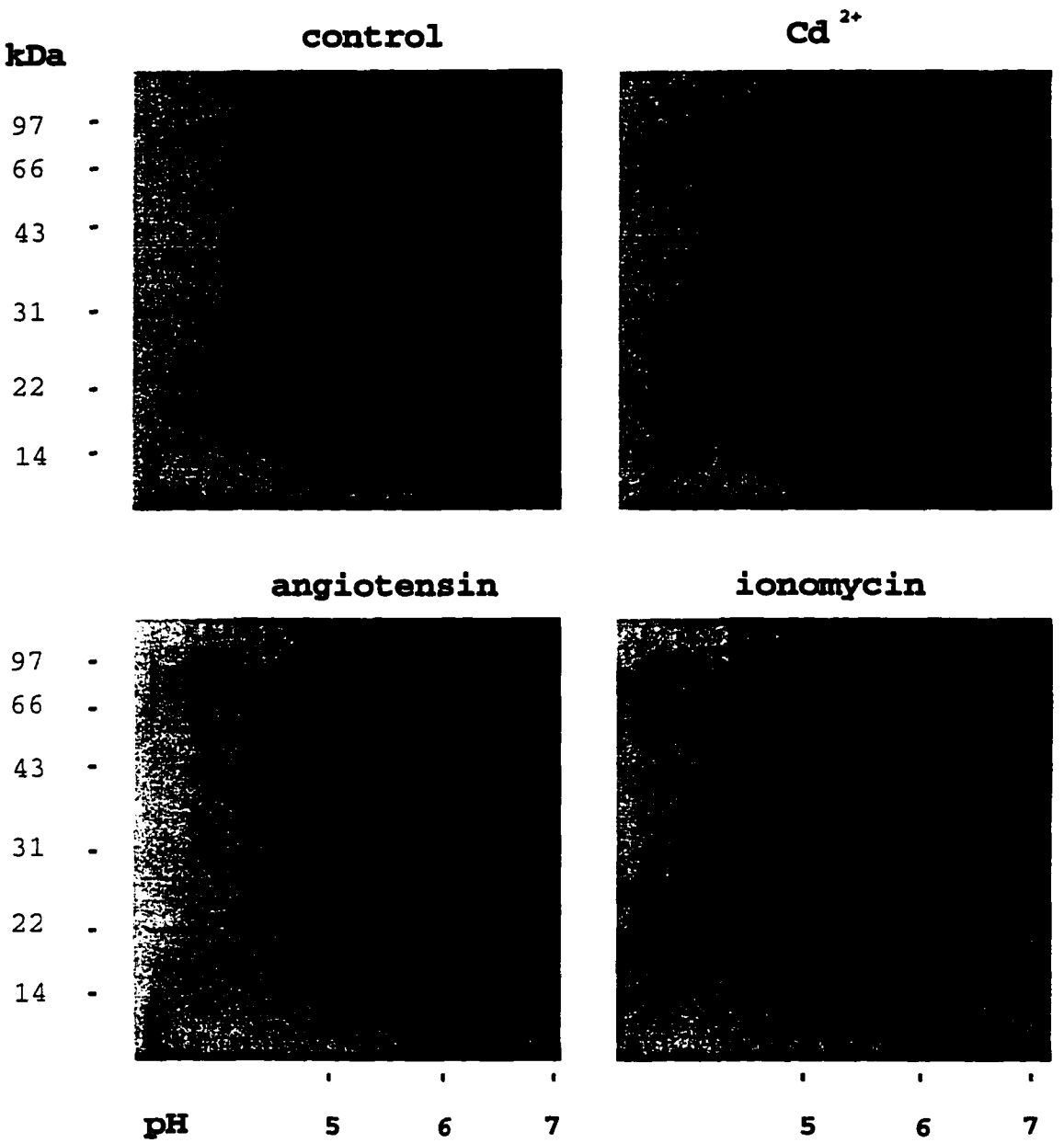

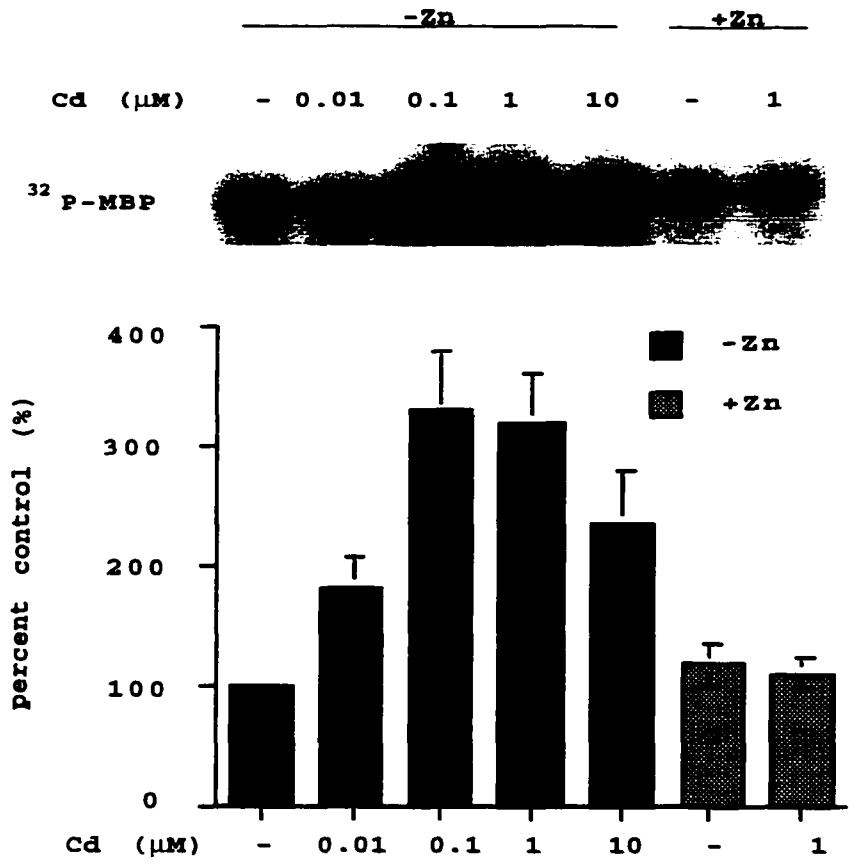

Figure 5. Activation of ERK2 by Cd^{2+} and antagonism by Zn^{2+}. Human skin fibroblasts were incubated in PSS containing glucose plus indicated concentrations of $CdCl_2$, 2 μM $ZnCl_2$ or 2 μM $ZnCl_2$ + 1 μM $CdCl_2$ for 5 min. Immunoprecipitation of ERK2 and in vitro kinase assay were done as described in "Experimental Procedures." After autoradiography, MBP bands were cut from the gel and radioactivity associated with M3P was determined by liquid scintillation counting. Results are expressed as % control (mean ± SE of 4 experiments).

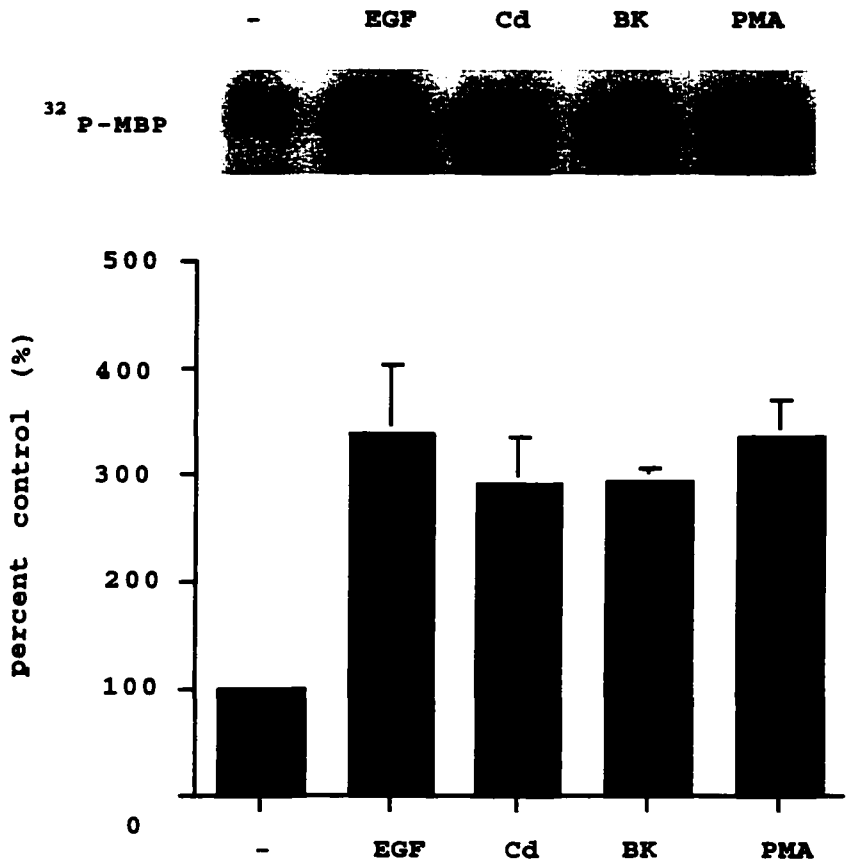

Figure 6. Activation of ERK2 by EGF, Cd^{2+}, bradykinin, and PMA. Human skin fibroblasts were incubated in PSS containing glucose plus 100 ng/ml EGF, 1 μM $CdCl_2$, 0.1 μM bradykinin or 0.1 μM PMA for 5 min. Immunoprecipitation of ERK2 and in vitro kinase assay were done as described in "Experimental Procedures." After autoradiography, MBP bands were cut from the gel and radioactivity associated with MBP was determined by liquid scintillation counting. Results are expressed as % control (mean ± SE of 4 experiments).

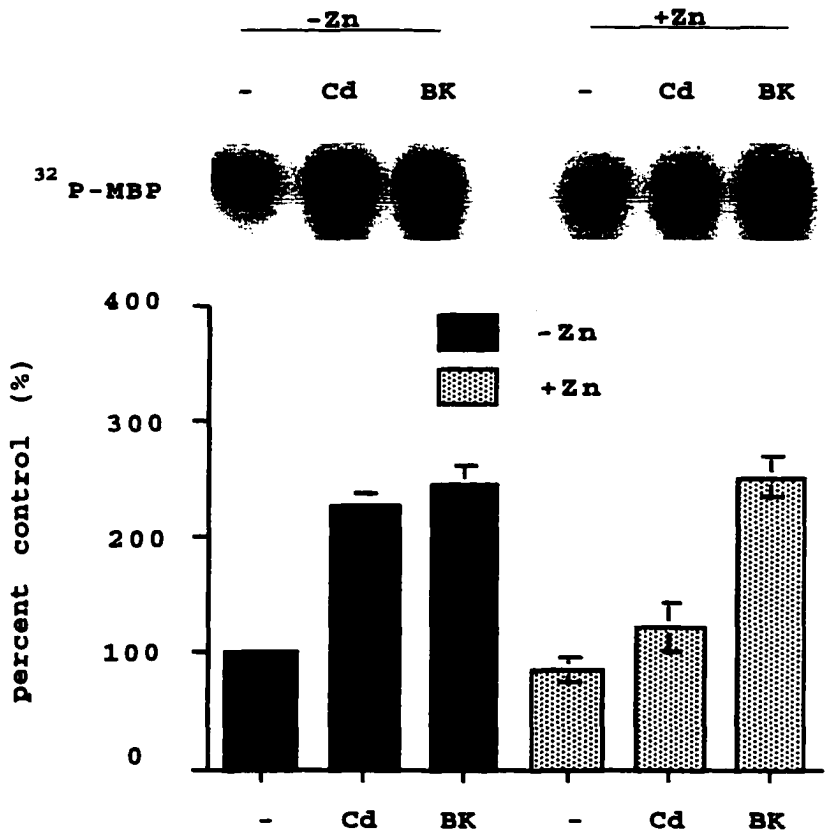

Figure 7. Zn^{2+} blocks Cd^{2+}-evoked ERK2 activation without affecting the response to bradykinin. Human skin fibroblasts were incubated in PSS containing glucose plus 1 μM $CdCl_2$ or 0.1 μM bradykinin in the presence or absence of 2 μM $ZnCl_2$ for 5 min. Immunoprecipitation of ERK2 and in vitro kinase assay were done as described in "Experimental Procedures." After autoradiography, MBP bands were cut from the gel and radioactivity associated with MBP was determined by liquid scintillation counting. Results are expressed as % control (mean ± SE of 4 experiments).

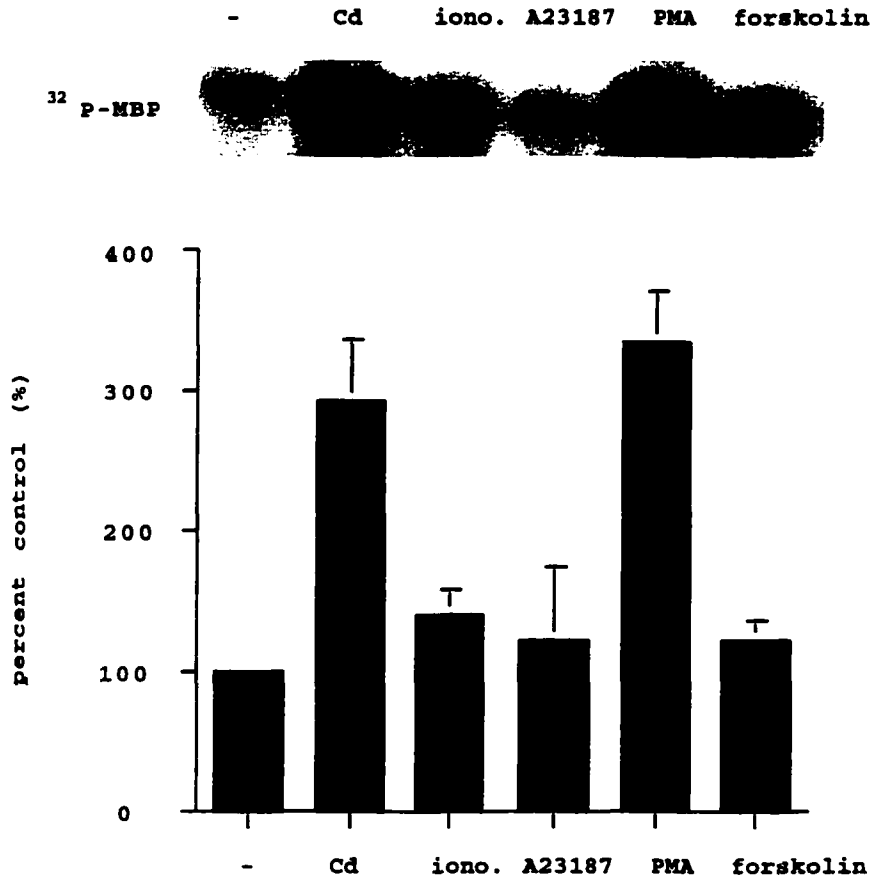

Figure 8. Activation of ERK2 by Cd^{2+} and PMA but not by calcium ionophores or forskolin. Human skin fibroblasts were incubated in PSS containing glucose plus 1 μM $CdCl_2$, 2 μM ionomycin, 5 μM A23187, 0.1 μM PMA, or 100 μM forskolin for 5 min. Immunoprecipitation of ERK2 and in vitro kinase assay were done as described in "Experimental Procedures." After autoradiography, MBP bands were cut from the gel and radioactivity associated with MBP was determined by liquid scintillation counting. Results are expressed as % control (mean ± SE of 3 experiments).

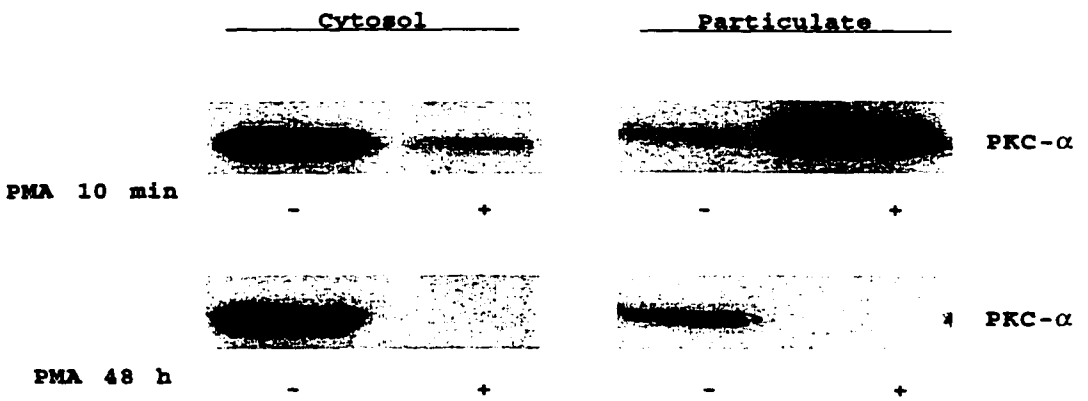

Figure 9. PKC-α translocation and downregulation. Quiescent human skin fibroblasts per condition were incubated with serum-free DMEM ± 0.1 μM PMA for 48 h. The cells were incubated with ± 0.1 μM PMA for 10 min. The membrane and cytosol fractions were prepared as described under "Experimental Procedures." Equivalent amounts of each fraction (25 μg) were applied to a 10% SDS-polyacrylamide gel. PKC-α was detected by immunoblotting with affinity purified rabbit anti PKC-α antibody and HRP-conjugated donkey anti-rabbit IgG. This represents one of two independent experiments that gave similar results.

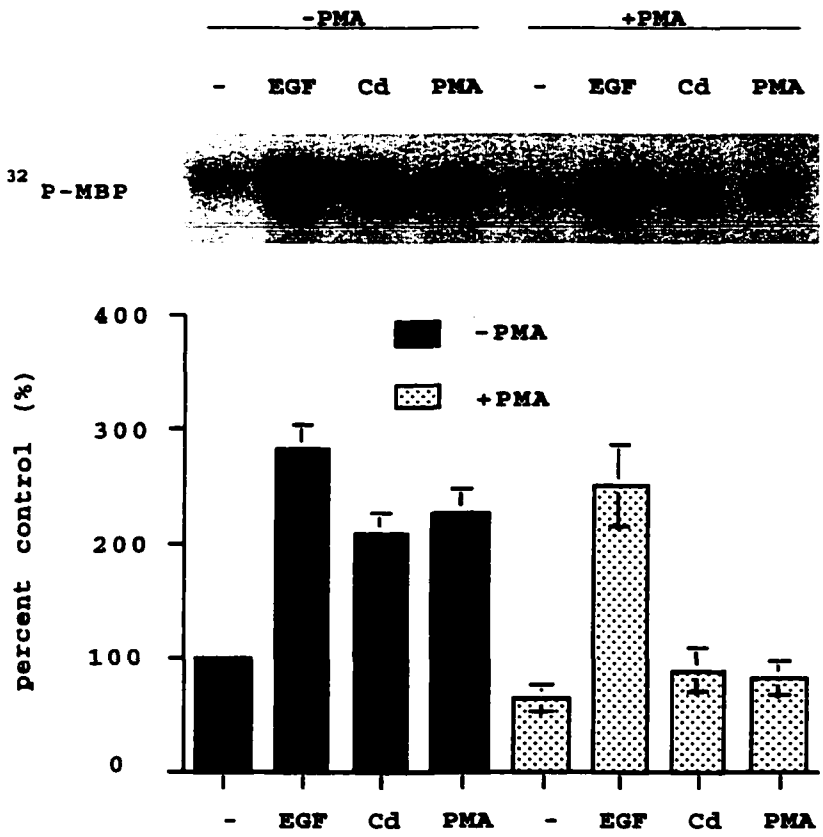

Figure 10. Downregulation of PKC abolishes ERK2 activation by Cd^{2+} and PMA but not EGF. Quiescent human skin fibroblasts were incubated with serum-free DMEM ± 0.1 μM PMA for 48 h. The cells were incubated in PSS containing glucose plus 100 ng/ml EGF, 1 μM $CdCl_2$ and 0.1 μM PMA for 5 min. Immunoprecipitation of ERK2 and in vitro kinase assay were done as described in "Experimental Procedures." After autoradiography, MBP bands were cut from the gel and radioactivity associated with MBP was determined by liquid scintillation counting. Results are given as % control (mean ± SE of 4 experiments).

Figure 11. Cd^{2+} increases MARCKS phosphorylation and Zn^{2+} blocks Cd^{2+}-evoked MARCKS phosphorylation without affecting the response to bradykinin. Quiescent human skin fibroblasts were incubated in PSS containing glucose plus 0.5 mCi [^{32}P] orthophosphate per dish at 37°C for 1 h and rinsed with PSS. The cells were then incubated with indicated concentrations of $CdCl_2$ ± 2 μM $ZnCl_2$ (A) and 1 μM $CdCl_2$ or 0.1 μM bradykinin ± 2 μM $ZnCl_2$ (B) for 2 min. MARCKS was extracted and immunoprecipitated as described in "Experimental Procedures." Results are expressed as % control (mean ± SE of 3-4 experiments).

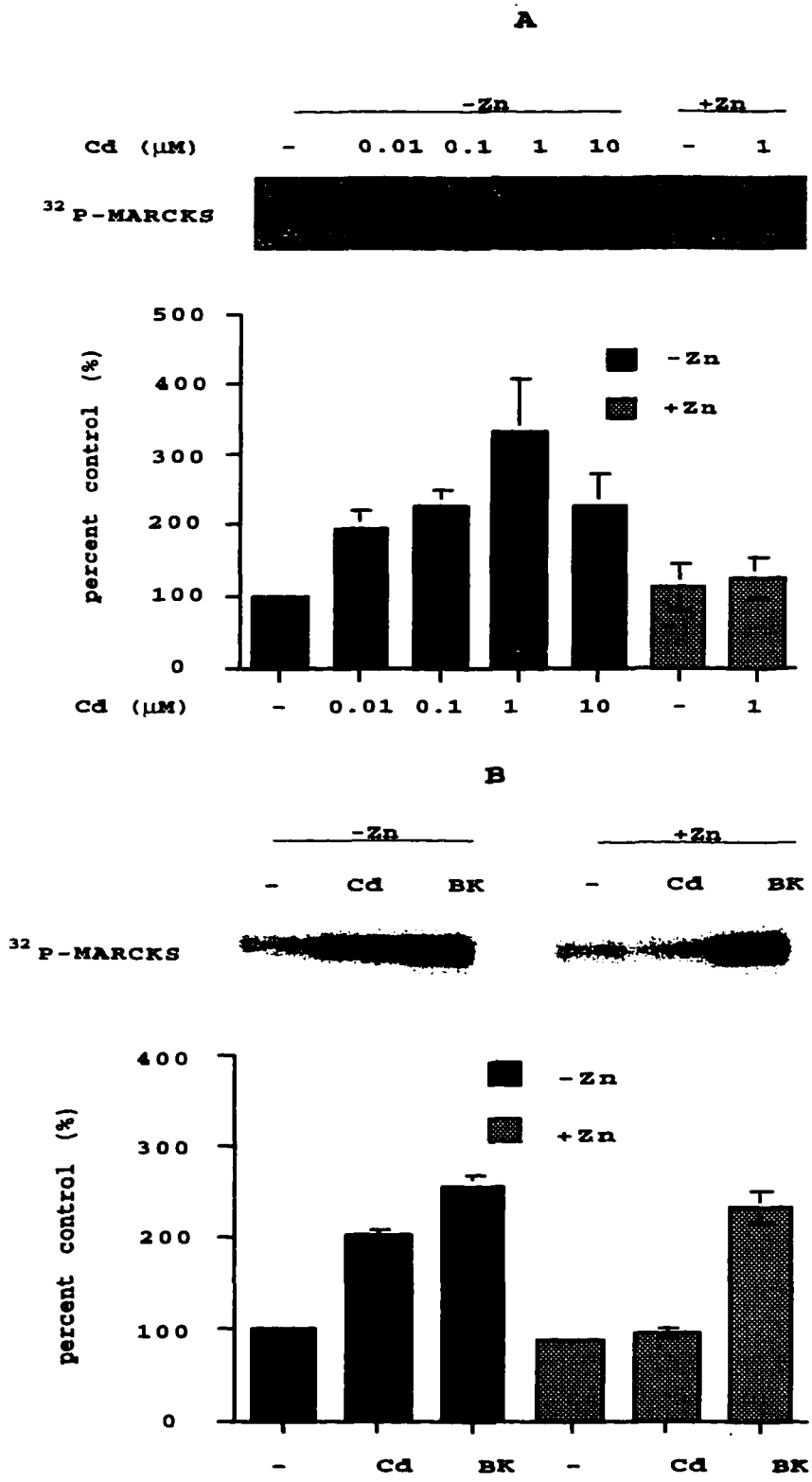

Figure 12. In vivo phosphorylation of MARCKS by Ni^{2+}, Co^{2+} (A), and Fe^{2+} (B). Quiescent human skin fibroblasts were incubated in PSS containing glucose plus 0.5 mCi [^{32}P] orthophosphate per dish at 37°C for 1 h and rinsed with PSS. The cells were then incubated with indicated concentrations of $CoCl_2$, $NiCl_2$ (A), or $FeSO_4$ (B) for 2 min. MARCKS was extracted and immunoprecipitated as described in "Experimental Procedures." Results are expressed as % control (mean ± SE of 4 experiments).

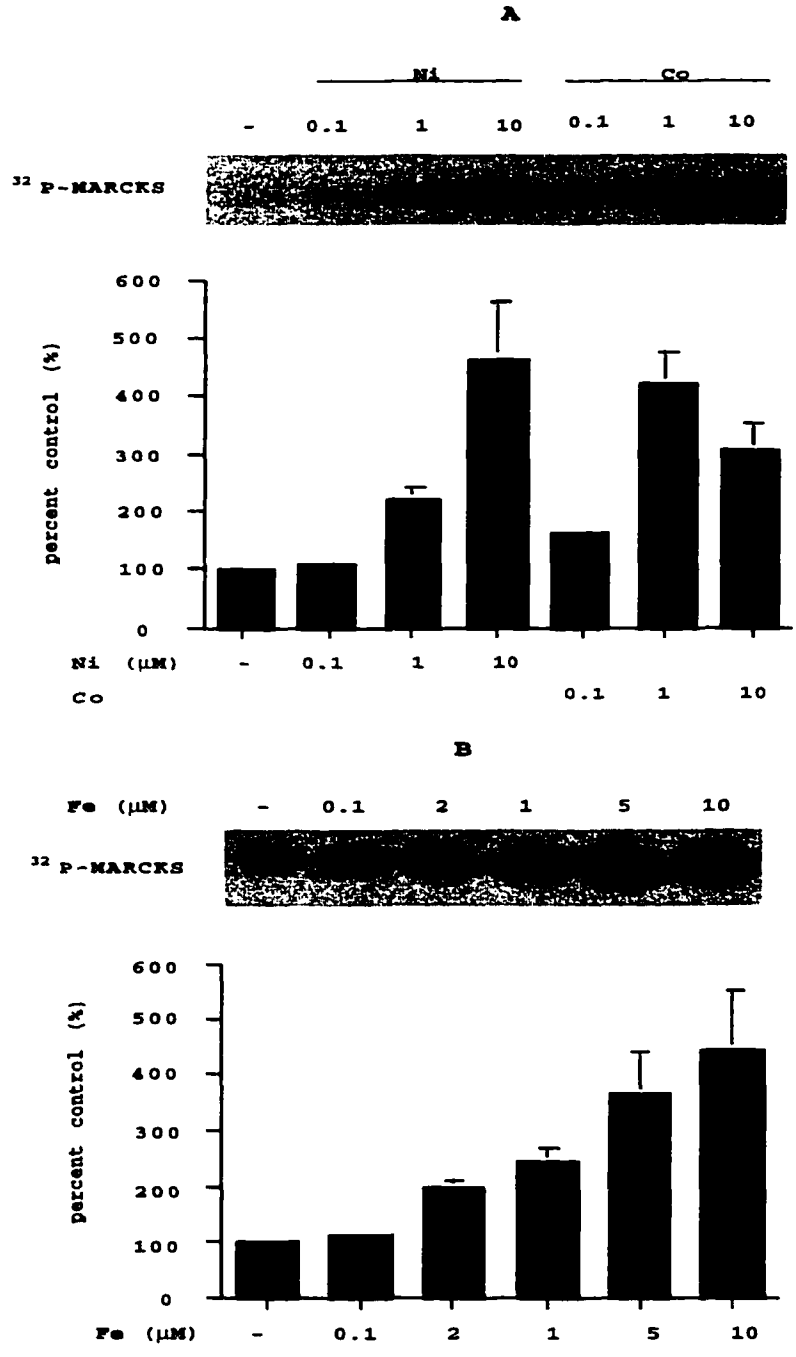

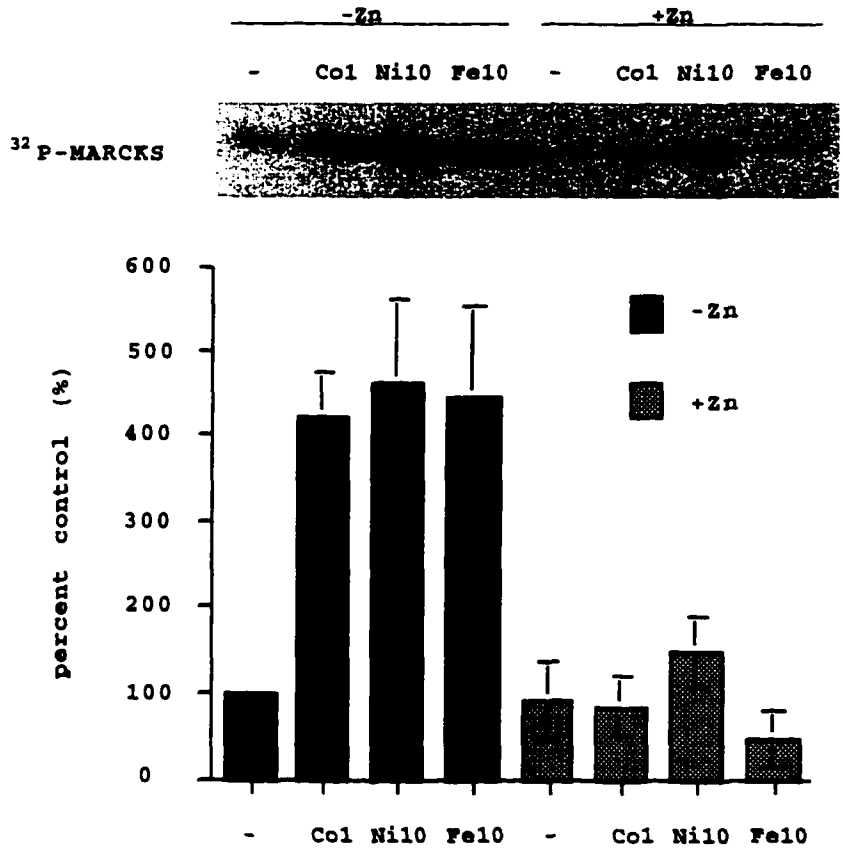

Figure 13. In vivo phosphorylation of MARCKS by metals and antagonism of Zn^{2+}. Quiescent human skin fibroblasts were incubated in PSS containing glucose plus 0.5 mCi [^{32}P] orthophosphate per dish at 37°C for 1 h and rinsed with PSS. The cells were then incubated with the indicated concentrations of $CoCl_2$, $NiCl_2$, or $FeSO_4$ in the presence or absence of 2 μM $ZnCl_2$ for 2 min. MARCKS was extracted and immunoprecipitated as described in "Experimental Procedures." Results are expressed as % control (mean ± SE of 3 experiments).

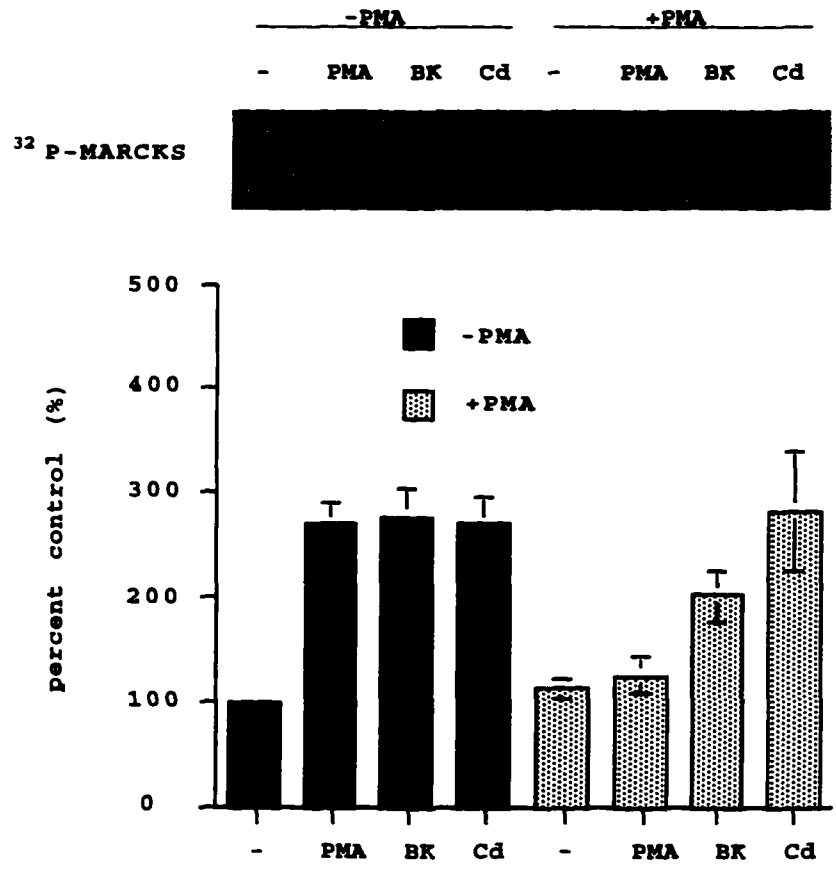

Figure 14. Downregulation of PKC has no effect on MARCKS phosphorylation evoked by Cd^{2+} or bradykinin in vivo. Quiescent human skin fibroblasts were incubated with serum-free DMEM ± 0.1 µM PMA for 48 h. The cells were incubated with PSS containing glucose plus 0.5 mCi [^{32}P] orthophosphate ± 0.1 µM PMA per dish at 37°C for 1 h and rinsed with PSS. The cells were then incubated with 0.1 µM PMA, 0.1 µM bradykynin, or 1.0 µM $CdCl_2$ for 2 min. MARCKS was extracted and immunoprecipitated as described in "Experimental Procedures." Results are expressed as % control (mean ± SE of 3 experiments).

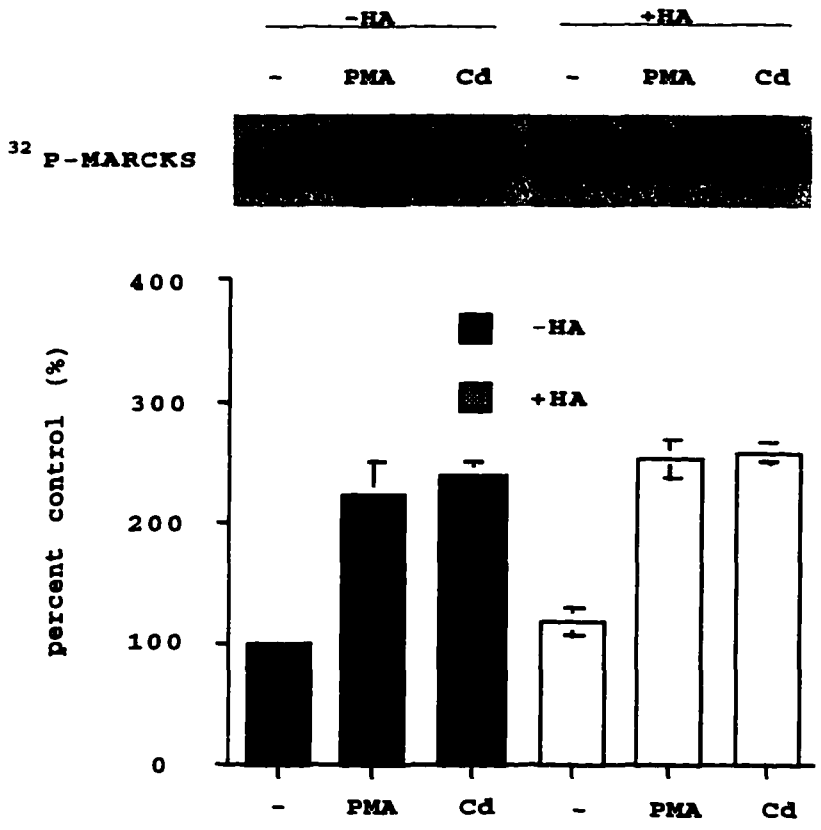

Figure 15. Herbimycin A has no effect on MARCKS phosphorylation evoked by Cd^{2+} and PMA. Quiescent human skin fibroblasts were incubated with serum-free DMEM ± 1 μM herbimycin A for 24 h. The cells were incubated with PSS containing glucose plus 0.5 mCi [^{32}P] orthophosphate ± 1 μM herbimycin A per dish at 37°C for 1 h and rinsed with PSS. The cells were then incubated with 0.1 μM PMA or 1 μM $CdCl_2$ for 2 min. MARCKS was extracted and immunoprecipitated as described in "Experimental Procedures." Results are expressed as % control (mean ± SE of 3 experiments).

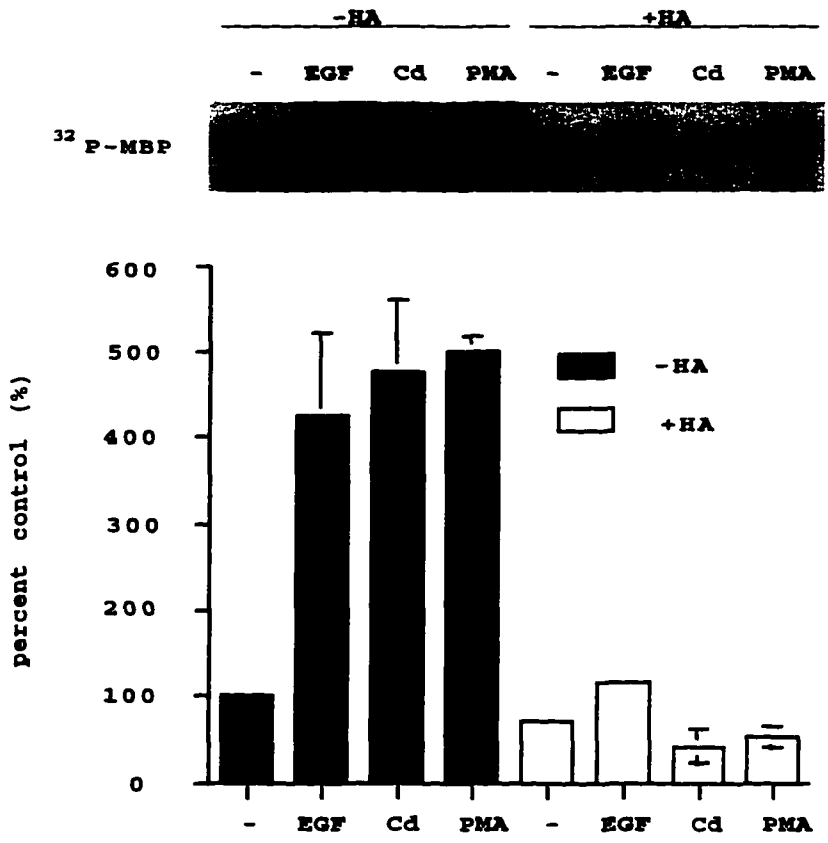

Figure 16. Herbimycin A abolishes ERK2 activation evoked by EGF, Cd^{2+}, and PMA in vivo. Quiescent human skin fibroblasts were incubated with serum-free DMEM ± 1 μM herbimycin A for 24 h. The cells were incubated with PSS containing glucose plus 100 ng/ml EGF, 0.1 μM PMA, or 1 μM $CdCl_2$ for 5 min. Immunoprecipitation of ERK2 and in vitro kinase assay were done as described in "Experimental Procedures." After autoradiography, MBP bands were cut from the gel and radioactivity associated with MBP was determined by liquid scintillation counting. Results are expressed as % control (mean ± SE of 3 experiments).

GRADUATE SCHOOL
UNIVERSITY OF ALABAMA AT BIRMINGHAM
DISSERTATION APPROVAL FORM

Name of Candidate Hyeon-Woo Lee

Major Subject Pharmacology

Title of Dissertation Bryostatin Downregulates Protein Kinase C by Production of Incompetent Enzyme and Degradation by the Ubiquitin-Proteasome Pathway

Dissertation Committee:

Stephen Bcme., Chairman

Director of Graduate Program

Dean, UAB Graduate School

Date May 20, 1996

PS-1428